Deutsches Institut für Ernährungsforschung
Abteilung Molekulare Genetik

Arc Expression in the Parabrachial Nucleus Following Taste Stimulation

Dissertation

zur Erlangung des akademischen Grades
„Doctor of Philosophy“
(Ph.D.)

eingereicht an der
Humanwissenschaftlichen Fakultät
der Universität Potsdam

von

Susan Margot Tyree

Potsdam, den 16 September 2016

Published online at the
Institutional Repository of the University of Potsdam:
URN urn:nbn:de:kobv:517-opus4-396600
http://nbn-resolving.de/urn:nbn:de:kobv:517-opus4-396600

"We are not interested in the fact that the brain has the consistency of cold porridge."

- Alan Turing

Abstract

Researchers have made many approaches to study the complexities of the mammalian taste system; however molecular mechanisms of taste processing in the early structures of the central taste pathway remain unclear. More recently the *Arc* catFISH (cellular compartment analysis of temporal activity by fluorescent *in situ* hybridisation) method has been used in our lab to study neural activation following taste stimulation in the first central structure in the taste pathway, the nucleus of the solitary tract. This method uses the immediate early gene *Arc* as a neural activity marker to identify taste-responsive neurons. *Arc* plays a critical role in memory formation and is necessary for conditioned taste aversion memory formation. In the nucleus of the solitary tract only bitter taste stimulation resulted in increased *Arc* expression, however this did not occur following stimulation with tastants of any other taste quality. The primary target for gustatory NTS neurons is the parabrachial nucleus (PbN) and, like *Arc*, the PbN plays an important role in conditioned taste aversion learning.

The aim of this thesis is to investigate *Arc* expression in the PbN following taste stimulation to elucidate the molecular identity and function of *Arc* expressing, taste-responsive neurons. Naïve and taste-conditioned mice were stimulated with tastants from each of the five basic taste qualities (sweet, salty, sour, umami, and bitter), with additional bitter compounds included for comparison. The expression patterns of *Arc* and marker genes were analysed using *in situ* hybridisation (ISH). The *Arc* catFISH method was used to observe taste-responsive neurons following each taste stimulation. A double fluorescent *in situ* hybridisation protocol was then established to investigate possible neuropeptide genes involved in neural responses to taste stimulation.

The results showed that bitter taste stimulation induces increased *Arc* expression in the PbN in naïve mice. This was not true for other taste qualities. In mice conditioned to find an umami tastant aversive, subsequent umami taste stimulation resulted in an increase in *Arc* expression similar to that seen in bitter-stimulated mice. Taste-responsive *Arc* expression was denser in the lateral PbN than the medial PbN. In mice that received two temporally separated taste stimulations, each stimulation time-point showed a distinct population of *Arc*-expressing neurons, with only a small population (10 – 18 %) of neurons responding to both stimulations. This suggests that either each stimulation event activates a different population of neurons, or that *Arc* is marking something other than simple cellular activation, such as long-term cellular changes that do not occur twice within a 25 minute time frame. Investigation using the newly established double-FISH protocol revealed that, of the bitter-responsive *Arc* expressing neuron population: 16 % co-expressed calcitonin RNA; 17 % co-expressed glucagon-like peptide 1 receptor RNA; 17 % co-expressed hypocretin receptor 1 RNA; 9 % co-expressed gastrin-releasing peptide RNA; and 20 % co-expressed neurotensin RNA. This co-expression with multiple different neuropeptides suggests that bitter-activated *Arc* expression mediates multiple neural responses to the taste event, such as taste aversion learning, suppression of food intake, increased heart rate, and involves multiple brain structures such as the lateral hypothalamus, amygdala, bed nucleus of the stria terminalis, and the thalamus.

The increase in *Arc*-expression suggests that bitter taste stimulation, and umami taste stimulation in umami-averse animals, may result in an enhanced state of *Arc*-dependent synaptic plasticity in the PbN, allowing animals to form taste-relevant memories to these aversive compounds more readily. The results investigating neuropeptide RNA co-expression suggest the amygdala, bed nucleus of the stria terminalis, and thalamus as possible targets for bitter-responsive *Arc*-expressing PbN neurons.

Zusammenfassung

Trotz vielfältiger experimenteller Ansätze, die Komplexität des Geschmackssystems der Säugetiere zu erforschen, bleiben viele molekulare Mechanismen der Geschmacksverarbeitung in den frühen Strukturen der zentralen Geschmacksbahn unklar. Kürzlich wurde in unserem Labor die *Arc* catFISH-Methode (cellular compartment analysis of temporal activity by fluorescent *in situ* hybridisation) angewandt, um die neuronale Aktivierung nach Geschmacksstimulation in der ersten zentralnervösen Struktur der Geschmacksbahn, dem *Nucleus tractus solitarii* (NTS) zu untersuchen. Diese Methode nutzt das Immediate-early-Gen *Arc* als neuronalen Aktivitätsmarker, um geschmacksverarbeitende Neurone zu identifizieren. *Arc* spielt eine wichtige Rolle bei der Gedächtnisbildung und ist notwendig für die Ausprägung konditionierter Geschmacksaversionen. Im NTS führten nur Bitterstimuli zu einer erhöhten *Arc*-Expression, jedoch nicht Stimuli der anderen Geschmacksqualitäten. Das primäre Projektionsziel für geschmacksverarbeitende NTS-Neurone ist der Nucleus parabrachialis (PbN). Wie *Arc*, spielt dieser eine wichtige Rolle bei der Ausbildung konditionierter Geschmacksaversionen.

Das Ziel dieser Arbeit ist, die Expression von *Arc* im PbN nach Geschmacksstimulation zu untersuchen, um die molekulare Identität der *Arc*-exprimierenden, geschmacksverarbeitenden Neurone aufzuklären. Naive und konditionierte Mäuse wurden mit Geschmacksstoffen der fünf Geschmacksqualitäten (süß, salzig, sauer, umami und bitter) stimuliert, wobei zum Vergleich mehrere Bitterstoffe verwendet wurden. Die Expression von *Arc* und ausgewählter Markergene wurde per *In-situ*-Hybridisierung (ISH) analysiert. Die *Arc* catFISH-Methode wurde eingesetzt, um geschmacksverarbeitende Neuronen zu untersuchen, die durch den jeweiligen Geschmacksstimulus aktiviert wurden. Ein Fluoreszenz-*in-situ*-Hybridisierungs-Protokoll (FISH) mit zwei RNA-Sonden wurde etabliert, um den Einfluss von Neuropeptiden in der neuronalen Verarbeitung von Geschmacksinformation zu untersuchen.

Die Ergebnisse zeigen, dass in unkonditionierten Mäusen nur Bitterstimuli zu einer erhöhten *Arc*-Expression im PbN führen, nicht jedoch Stimuli anderer Geschmacksqualitäten. Bei Mäusen, die konditioniert wurden, einen Umami-Stimulus zu vermeiden, führt die nachfolgende Stimulation mit diesem Geschmacksstoff zu einer erhöhten *Arc*-Expression, die der in bitterstimulierten Mäusen vergleichbar ist. Die geschmacksinduzierte *Arc*-Expression ist im lateralen PbN stärker konzentriert als im medialen PbN. Bei Mäusen, die im Abstand von 25 min zwei Geschmackstimulationen erhielten, führt jede der Stimulationen zu einer Erregung eigenen Population von *Arc*-exprimierenden Neuronen. Nur ein geringer Anteil (10 - 18 %) reagiert auf beide Stimuli. Dies deutet darauf hin, dass entweder jeder Stimulationsvorgang eine eigene Neuronenpopulation aktiviert oder dass *Arc* nicht als einfacher Aktivitätsmarker zu verstehen ist, sondern vielmehr als Marker für längerfristige neuronale Veränderungen, die nicht zweimal innerhalb des 25-minütigen Zeitrahmens des Experiments auftreten. Die Ergebnisse des neu etablierten Doppel-FISH-Protokolls zeigen, dass von den Neuronen mit *Arc*-Expression nach Bitterstimulation: 16 % Calcitonin-RNA koexprimieren; 17 % Glucagon-like-peptide-1-receptor-RNA koexprimieren; 17 % Hypocretin-receptor-1-RNA koexprimieren; 9 % Gastrin-releasing-peptide-RNA koexprimieren; und 20 % Neurotensin-RNA koexprimieren. Diese Koexpression mit verschiedenen Neuropeptiden deutet darauf hin, dass die bitterinduzierte *Arc*-Expression an verschiedenen neuralen Prozessen beteiligt ist, die durch Geschmacksstimulation hervorgerufen werden. Darunter sind das Erlernen von Geschmacksaversion, reduzierte Nahrungsaufnahme und gesteigerte Herzfrequenz. Außerdem deutet dies darauf hin, dass an diesen Prozessen mehrere

Hirnstrukturen, wie lateraler Hypothalamus, Amygdala, Nucleus interstitialis striae terminalis und Thalamus beteiligt sind.

Die erhöhte *Arc*-Expression deutet darauf hin, dass Stimulation mit Bitterstoffen und die Stimulation mit einem Umami-Stimulus bei umami vermeidenden Tieren zu einer erhöhten *Arc*-abhängigen neuronalen Plastizität führt. Dies könnte den Tieren ermöglichen, geschmacksbezogene Erinnerungen bezüglich aversiver Stimuli zu formen. Die Ergebnisse der Koexpression von *Arc* und Neuropeptiden legen die Amygdala, den *Nucleus interstitialis striae terminalis* und den Thalamus als mögliche Projektionsziele der *Arc*-exprimierenden PbN-Neurone nahe.

Table of Contents

List of Figures

List of Tables

List of Abbreviations

2/3 CL	Lobules 2 and 3 of the cerebellar vermis
4V	Fourth ventricle
VII	Facial nerve
IX	Glossopharyngeal nerve
X	Vagus nerve
AMPA	α-amino-3-hydroxy-5-methyl-4-isoxazolepropionic acid
ANOVA	Analysis of variance
Arc	activity-regulated cytoskeleton-associated protein
Arg3.1	activity-regulated gene 3.1
as	antisense
BCIP	5-Bromo-4-chloro-3-indolyl phosphate
BdNST	Bed nucleus of the Stria Terminalis
bp	base pairs
BR	Blocking reagent
Calca	Calcitonin
catFISH	cellular compartment analysis of temporal activity by fluorescent *in situ* hybridisation
cDNA	complementary DNA
CGRP	Calcitonin gene-related peptide
CT	Chorda tympani (lat.)
CTA	Conditioned taste aversion
Cuc	Cucurbitacin I
Cy3	Avidin-Cy3
Cyx	Cycloheximide
DAPI	4',6-Diamidinie-2'-phenylindole dyhydrochloride
DEPC	Diethylpyrocarbonate
Dig	Digoxigenin
DLL	Dorsal nucleus of the lateral lemniscus
DMSO	Dimethylsulfoxide
DNA	Deoxyribonucleic acid
DNase	Deoxyribonuclease
dNTPs	Deoxynucleotide triphosphates
DR	Dorsal raphe nucleus
DTT	Dithiothreitol
E. coli	Escherichia coli
EDTA	Ethylenediaminetetraacetic acid
ENaC	Epithelial sodium channel
et al.	*et alii* (lat. And others)
etc.	*et cetera* (lat. and so forth)
EW	Edinger-Westphal nucleus
EtOH	Ethanol
FAM	Fluorescein
FISH	Fluorescent *in situ* hybridisation
GABA	γ-aminobutyric acid
GC	Gustatory cortex
GG	Geniculate ganglion
GI	gastrointestinal
Glp1r	Glucagon-like 1 peptide receptor
GN	Nodose ganglion
GP	Petrosal ganglion
Grp	Gastrin-releasing peptide
H_2O_2	Hydrogen peroxide
HCl	Hydrochloric acid
Hcrtr1	Hypocretin receptor 1
IEG	Immediate early gene
IHC	Immunohistochemistry
ISH	*In situ* hybridisation
IVT	*in vitro* transcription
KCl	Potassium chloride
LB	Lysogeny broth
LiCl	Lithium chloride
lPbN	lateral PbN
M	molar, Mol per litre
MeOH	Methanol
mM	millimolar, Millimol per litre
µM	micromolar, Micromol per litre
MOPS	3-(N-Morpholino)propanesulfonic acid
mPbN	medial PbN
mRNA	messenger RNA
MWB	Maleate wash buffer
NaCl	Sodium chloride
$NaHCO_3$	Sodium bicarbonate
NBT	4-Nitro blue tetrazolium chloride
NMDA	N-methyl-D-aspartate
NPM	Nervus petrosus major (lat.)
NTE	Sodium chloride-Tris-EDTA buffer
NTP	Nucleoside triphosphate
NTS	Nucleus tractus solitarii (lat.)
Nts	Neurotensin
OD	Optical density
PbN	Parabrachial nucleus
PBS	Phosphate-buffered saline
pBS	pBluescript KS+
PCR	Polymerase chain reaction
PFA	Paraformaldehyde
Pfu	Pyrococcus furiosus
PK	Proteinase K
Pkd2l1	Polycystic kidney disease 2-like 1
POD	Horseradish peroxidase
Qui	Quinine HCl
RNA	Ribonucleic acid
RNase	Ribonuclease
RT-PCR	Reverse-transcription polymerase chain reaction
s	sense
SCP	Superior cerebellar peduncle (also brachium conjunctivum)
SE	Standard error
SI	Substantia innominata
SN	Substantia nigra
SOA	Sucrose octaacetate

SSC	Saline-sodium citrate
TAE	Tris-acetate-EDTA-buffer
Tas1r	Taste receptor type 1
Tas2r	Taste receptor type 2
TB	Terrific broth
TEA	Triethanolamine
Th	Thalamus
TN	Tris-sodium chloride buffer
TNB	TN with blocking reagent
TRC	Taste receptor cell
TSA	tyramide signal amplification
UV	Ultra violet
VN	Vestibular nucleus
VPMpc	Ventral posterior medial nucleus of the thalamus, parvicellular part
ZI	Zona incerta

Taste stimulation tastants

No Stim	No stimulation
Control	25 mM potassium chloride and 2.5 mM sodium bicarbonate
Sweet	0.5 M saccharose
Salty	0.8 M sodium chloride
Sour	30 mM citric acid
Umami	1 mM monosodium glutamate
Cyx	0.5 mM cycloheximide
Qui	10 mM quinine hydrochloride
Cuc	1 mM cucurbitacin I

Lickometre and CTA session tastants

Cyx	1 µM Cycloheximide
Umami	20 mM Monosodium glutamate

Intracellular distribution of *Arc*

N	Nuclear *Arc* expression
C	Cytoplasmic *Arc* distribution
N+C	Both nuclear and cytoplasmic *Arc* distribution

Introduction

This chapter gives an introduction into the topic of this thesis. The chapter opens with a summary of the current understanding of perception and neural processing of taste information, with a particular focus on the role of the parabrachial nucleus (PbN); this is followed by the introduction of the *Arc* catFISH method and finally an outline of the main research questions and methods.

1.1 Functional and anatomical bases of taste

In order to successfully navigate through our environment, we must be able to generate an internal representation of our surroundings using our senses. This is possible using our various sensory systems such as vision, hearing, olfaction, touch, taste, and others. Our sense of taste is particularly important for helping us to evaluate possible food sources within our environment by determining nutritive value, or warning us of potentially harmful substances; thus guiding our food choices. This discrimination is critical to survival. Along with our other senses, we use our ability to distinguish between sweet, sour, salty, bitter, and umami tastes to categorise food choices into appetitive or aversive foods; these distinctions are based on previous pairings of these tastes with positive or negative post-ingestive effects and are largely considered innate.

1.1.1 Detection of flavours in the periphery

Taste perception begins with taste stimulation: a substance is placed in the mouth where it comes into contact with the taste buds. Taste buds are onion-shaped clusters of 50-150 taste receptor cells located in the epithelium of the tongue, soft palate, pharynx, larynx, epiglottis, and oesophagus (Breslin & Spector, 2008).

Taste buds are found distributed over the tongue in three different types of papillae: circumvallate papillae contain hundreds of taste buds in mice (Voigt et al., 2012) and thousands of taste buds in humans and are located toward the back of the tongue; foliate papillae contain around a dozen taste buds in mice and hundreds of taste buds in humans, and are located at the posterior lateral edge of the tongue (Miller & Smith, 1984; Miller & Spangler, 1982). Lastly, fungiform papillae contain one taste bud in rodents or three to five taste buds in humans, and are located in the anterior two-thirds of the tongue (Miller & Smith, 1984; Miller & Spangler, 1982). There are also some notable species differences, for example, the number of circumvallate papillae; mice have only one, whereas humans

have around a dozen (Frank, 1991; Whiteside, 1927). Rodents have an additional set of taste buds called the incisive papillae located behind the incisors (Travers et al., 1986).

At the apical pole of these taste buds is a taste pore, where taste receptor cells extend microvilli which contain taste receptors (see **Figure 1.1**). These microvilli come into contact with tasting compounds in foods dissolved in saliva and the relevant taste receptor cells are then activated (Farbman, 1965; Paran et al., 1975). Each taste bud contains taste receptors for multiple taste qualities (Kinnamon, 1987).

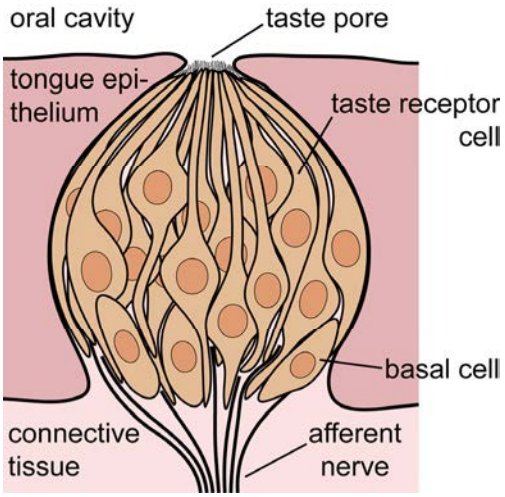

Figure 1.1 Physiology of the taste buds.
Image from Dr. Jonas Töle (DIfE, Nuthetal).

At present, scientific consensus recognises five taste qualities: sweet, salty, sour, umami, and bitter. Sweet and umami compounds are detected by heterodimers from the taste receptor 1 (Tas1r) family, and identify foods that are rich in nutrients and energy by detecting carbohydrates and proteins, leading the animal to seek out these foods (Li et al., 2002). The perception of salt taste is crucial for maintaining electrolyte balance; an animal accepts or rejects salty foods depending on their present electrolyte status and the intensity or concentration of the stimulus. At present there are two known mechanisms underlying salt taste perception: epithelial sodium channels, which are blocked by the diuretic amiloride, and an amiloride-insensitive pathway, which is less well understood (Chandrashekar et al., 2010; Lewandowski et al., 2016; Ninomiya, 1998). Sour and bitter compounds detect immature, spoiled, or poisonous food, and can trigger the animal to reject the food. Though the identity of the sour taste receptor is not yet known, it is believed that polycystic kidney disease 2-like 1 (PKD2L1)-expressing receptor cells (Huang et al., 2006) are involved in detecting acids and allow animals to accept or reject sour foods depending on the intensity or concentration of the stimulus. Bitter compounds are detected by the largest known family of taste receptors called the taste receptor 2

(Tas2r) family, which comprises around 25 genes in humans and around 35 genes in mice (Adler et al., 2000; Conte et al., 2003; Go et al., 2005; Shi et al., 2003).

Other potential tastes have also been suggested, however at present they are not widely accepted as additional taste qualities: fatty (Cartoni et al., 2010; Galindo et al., 2012; Voigt et al., 2014), metallic (Lawless et al., 2004; Lawless et al., 2005), starchy (Sclafani, 2004), and even watery (Rosen et al., 2010). In addition to taste perception we have other food-relevant senses which also interact with taste information and modulate food behaviour, such as olfactory and trigeminal cues (Zeigler et al., 1984). Our sense of smell can aid us in finding food sources and determining if they may be edible (Dalton et al., 2000). Trigeminal cues are understood to sense irritants that come into contact with mucous membranes, described as either pain- or temperature-sensations, such as those caused by capsaicin or menthol (Caterina et al., 1997; McKemy et al., 2002). Information from these sensory systems also contribute to our cognitive perception of a food source and modulate future food choices.

Although taste stimulation is predominantly thought to occur in the mouth, taste receptor cells can also be found in non-gustatory tissue, and the taste receptors in our mouths are not the only taste receptors that modulate feeding behaviour. Taste receptors have been found in the upper respiratory tract (Tizzano et al., 2010), lungs (Deshpande et al., 2010; Shah et al., 2009), heart (Foster et al., 2014; Foster et al., 2013), colon (Prandi et al., 2013), testes (Li & Zhou, 2012; Voigt et al., 2012; Xu et al., 2013), sperm (Li, 2013), and brain (Singh et al., 2011; Stolzenburg, 2016; Voigt, Bojahr, et al., 2015; Voigt, Hübner, et al., 2015), suggesting additional possible functions for these taste receptor cells. Administration of bitter taste stimulus denatonium directly into the gastrointestinal (GI) tract generates both behavioural (conditioned aversions), and physiological (delayed gastric emptying) responses; Glendinning et al. (2008) hypothesised that these responses are triggered by activation of Tas2r cells and other chemosensory cells in the GI tract. This would suggest a possible taste-function of taste receptors located in non-gustatory tissues.

1.1.2 Forwarding and central processing of taste information

Taste receptor cells in the oral cavity are innervated by sensory neurons located in the geniculate, petrosal, and nodose ganglia that reach the taste buds via branches of three cranial nerves: the fungiform papillae located on the anterior tongue are innervated by the chorda tympani, a branch of the facial nerve (VII); the circumvallate papillae of the posterior tongue are innervated by the lingual-tonsillar branch of the glossopharyngeal

nerve (IX); the foliate papillae along the lateral tongue are innervated by the chorda tympani (anterior-most ridges) and the glossopharyngeal nerve (posterior ridges); the incisive papillae and soft palate are innervated by the greater superficial petrosal nerve (VII); and lastly, the vagus nerve (X) innervates the pharynx, the larynx, and the epiglottis (Mistretta, 1984; Roper, 2013).

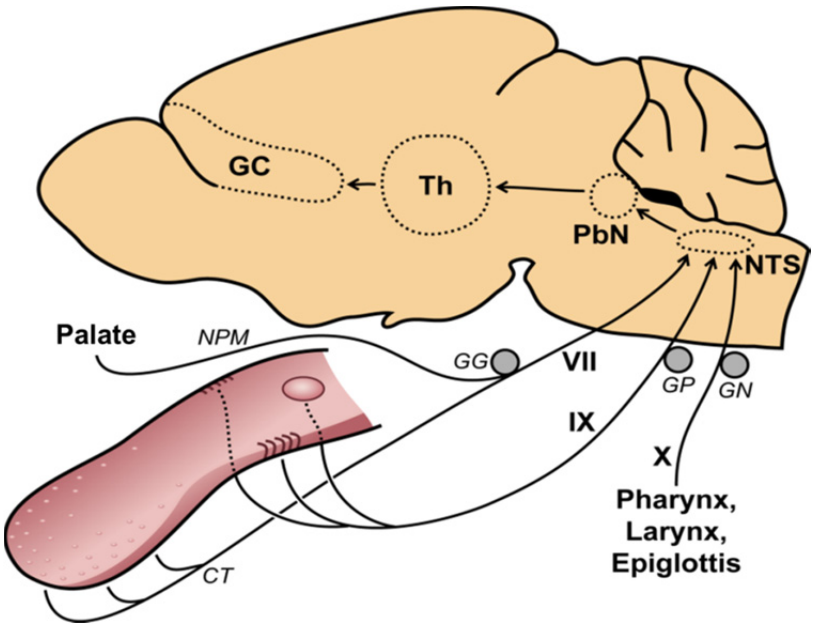

Figure 1.2 The taste pathway in the mouse.
VII: facial nerve; IX: glossopharyngeal nerve; X: vagus nerve; CT: chorda tympani; GC: gustatory cortex; GG: geniculate ganglion; GN: nodose ganglion; GP: petrosal ganglion; NPM: greater petrosal nerve (nervus petrosus major); NTS: nucleus of the solitary tract; PbN: parabrachial nucleus; Th: thalamus. Image from Dr. Jonas Töle (DIfE, Nuthetal).

Each fungiform taste bud is innervated by ~4-6 ganglion cells in mice (Zaidi & Whitehead, 2006), ~2-16 in rats (Krimm & Hill, 1998), and ~5-35 in hamsters (Whitehead et al., 1999). The ganglion cells then convey the taste information to the nucleus of the solitary tract (NTS; from the Latin **n**ucleus **t**ractus **s**olitarii) in an overlapping rostro-caudal distribution with the VII nerve terminating most rostrally (Contreras et al., 1982; Hamilton & Norgren, 1984; Hanamori & Smith, 1989).

Though there are multiple pathways originating from each taste relay, the ascending gustatory pathway has been well established (see **Figure 1.2**). Gustatory NTS neurons send taste information to the parabrachial nuclei (PbN) of the pons (Norgren & Leonard, 1973), which then projects to the thalamus. Interestingly, taste information from the PbN is projected to the ventral posterior medial nucleus of the thalamus, parvicellular part (VPMpc), directly adjacent to a population of neurons that receive input from the tongue-somatosensory projections (Emmers et al., 1962). Tracing studies showed that taste

information the travels from the VPMpc to the dysgranular and agranular insular cortex, also referred to as the gustatory cortex (Kosar et al., 1986a, 1986b). Then taste information is integrated with other sensory information in the gustatory cortex, where there are distinct populations of neurons for each taste quality (Chen et al., 2011). Though these studies have confirmed the structures involved in the taste pathway, they do not provide insight into the neural encoding of taste information in these structures.

1.2 The processing of taste information

One of the goals of taste research is to understand how taste information is processed along the structures of the taste pathway, from the tongue to the gustatory cortex. To help understand the neural coding patterns of taste information, two main theories were developed: the labelled line theory and the across fibre pattern theory (Pfaffmann, 1959). The labelled line theory suggests that taste information from each taste quality travels on parallel pathways through taste quality-specific cells and do not cross over (Pfaffmann, 1941; Smith & St John, 1999). The across fibre pattern theory suggests that all neurons along the taste pathway contribute to the coding of each taste quality and therefore there is no cell-taste-specificity (Smith & Frank, 1972; Smith et al., 1979). Although these theories were proposed over half a century ago, there is still no consensus regarding which theory is more likely to be true due to the wealth of supporting evidence for both theories throughout the taste pathway (for in-depth review, see Erickson, 2008).

Much of the support for the labelled-line theory has come from the field of electrophysiology. Researchers recording gustatory nerves in non-human primates observed finely-tuned taste responses in tastant-specific chorda tympani and glossopharyngeal fibres (Danilova et al., 2002; Hellekant et al., 1998). Subsequent stimulation of these tastant-specific fibres was sufficient to produce responses normally elicited by taste stimulation with the tastant the fibres were tuned to (Danilova et al., 2002; Danilova & Hellekant, 2004). This suggests that these fibres are already connected to taste-specific pathways.

Using electrophysiology to observe taste activation in the ganglia, Barretto et al. (2015) showed that most (~75 % of the neurons they recorded) ganglion neurons were singly tuned to one taste quality, the rest were predominantly (~24 %) responsive to two taste qualities (the biggest group, ~12 %, being a population of bitter-sour responsive neurons), and only ~1 % of the neurons recorded responded to more than two taste qualities. Suggesting that the majority of taste-responsive ganglia cells respond to only one

taste quality, and that 12% may be tuned to “aversive” stimuli and thus respond to both bitter and sour tastants. However, another study using confocal calcium imaging to record taste responses from ganglion neurons showed that up to 69 % of the ganglion neurons recorded responded to multiple tastants (Wu et al., 2015). These two studies show contradictory results; the former supports the labelled line theory of information processing, and the latter supports the across fibre pattern theory.

Further along the taste pathway, further support for the across-fibre pattern theory has been observed in the NTS. Primate and rat electrophysiology studies have shown that though there does appear to be some specificity to certain tastants, it seems as though most NTS taste-responsive cells are somewhat broadly tuned (Lemon & Smith, 2005; Scott et al., 1986). Additionally, Boucher et al. (2003) and Van Buskirk and Erickson (1977) showed that the firing-activity of taste-responsive neurons in the NTS and PbN can be modulated by trigeminal stimulation. This provides evidence that – even as early as the first central taste relay – neural responses to taste information are already converging with other sensory cues that are relevant to the taste event.

Researchers have also used neural-activity markers to observe taste responses in the brain – using this method Chen et al. (2011) observed topographically distinct populations of neurons for each taste quality in the insula in the mouse brain. Further exploration of these taste-specific neuron populations showed that activating them triggered characteristic taste-specific responses in naïve mice, and trained taste-responses in trained mice (Peng et al., 2015). This suggests that activating these taste-specific populations of neurons triggers a cognitive percept of the tastant, and not just a behavioural or physiological response.

Further support for the across-fibre theory comes from a study by Di Lorenzo et al. (2003) reported distinct temporal patterns of neural activation in the NTS corresponding with sweet and bitter taste stimulation. Subsequent artificial stimulation of NTS neurons with a “sweet” temporal pattern resulted in characteristic sweet behavioural responses. Additionally, when pairing “sweet” neuronal firing patterns with administration of malaise-inducing lithium chloride, the animals would develop an aversion to sweet taste stimuli. This study agrees with the across-fibre theory because it suggests that instead of taste quality specific neurons these earlier taste pathway structures use temporal firing patterns to transmit messages regarding taste quality.

1.2.1 Discrimination of bitter substances

The theories of taste perception focus on the distinction between taste qualities, however it is also worth considering the ability to distinguish between different tastants within taste qualities. Considering the structural diversity of the thousands of known bitter tastants (Meyerhof et al., 2010; Wiener et al., 2012) and the large family of bitter taste receptors (Adler et al., 2000; Conte et al., 2003; Go et al., 2005; Shi et al., 2003), this suggests that there is some ability for animals to distinguish between different bitter compounds.

Bitter is a unique taste quality, even in comparison to other aversive tastants, it is consistently considered to be aversive upon first presentation – even at low concentrations (Glendinning, 1993) – whereas sour and salty can be preferred to water at low concentrations (Tordoff et al., 2008). Since many toxic compounds are bitter to humans, inherent reception of bitter tastants could be considered an evolutionary advantage (Glendinning, Davis, et al., 2002); however, some bitter compounds can be beneficial, and preferences for bitter compounds can be learned if the bitter compound is paired with beneficial post-ingestive effects (Myers & Sclafani, 2003). This suggests a possible biological purpose for possessing an ability to discriminate between different bitter compounds.

Due to the inherent aversive responses to bitter taste stimulation as well as the negative post-ingestive effects that occur following administration of many bitter tastants, behavioural studies investigating bitter taste discrimination require additional complexity in order to overcome these negative effects. Some methods of overcoming these problems include 22 – 23 hour water deprivation or extensive taste-training with positive post-ingestive effects after bitter taste perception to encourage animals to drink bitter taste solutions or even conditioning taste preferences.. So far, results have been mixed in studies using standard taste-discrimination paradigms: evidence for bitter discrimination has been shown in hamsters (Frank et al., 2004), but not in rats (Spector & Kopka, 2002). Therefore, based on behavioural evidence, it is not yet clear whether the multitude of bitter taste receptors allows for bitter taste discrimination beyond the tongue.

1.3 Anatomical and structural function of the PbN

The parabrachial nucleus (PbN) is named for its location around the brachium conjunctivum (alternatively referred to as the superior cerebellar peduncle, SCP) in the

rostral pons (Franklin & Paxinos, 2007). Afferent inputs to the PbN originate from the hypothalamus (Saper et al., 1976, 1979), amygdala (Hopkins & Holstege, 1978), and the NTS (Loewy & Burton, 1978).

The efferent connections of the PbN are wide-ranging, it is connected with various subnuclei in the thalamus, hypothalamus, and amygdala, as well as the bed nucleus of the stria terminalis (BdNST), NTS, dorsal raphe, substantia nigra, substantia innominata, zona incerta, superior central raphe nucleus, Edinger-Westphal nucleus, nucleus of the diagonal band of Broca, cerebellum, as well as more far-reaching connections in the frontal, infralimbic, and granular insular cortices (Saper & Loewy, 1980), see **Figure 1.3**. Along with these projection targets, tracing studies have also revealed many intra-structural projections within the PbN, suggesting communications occurring within the structure itself (Saper & Loewy, 1980).

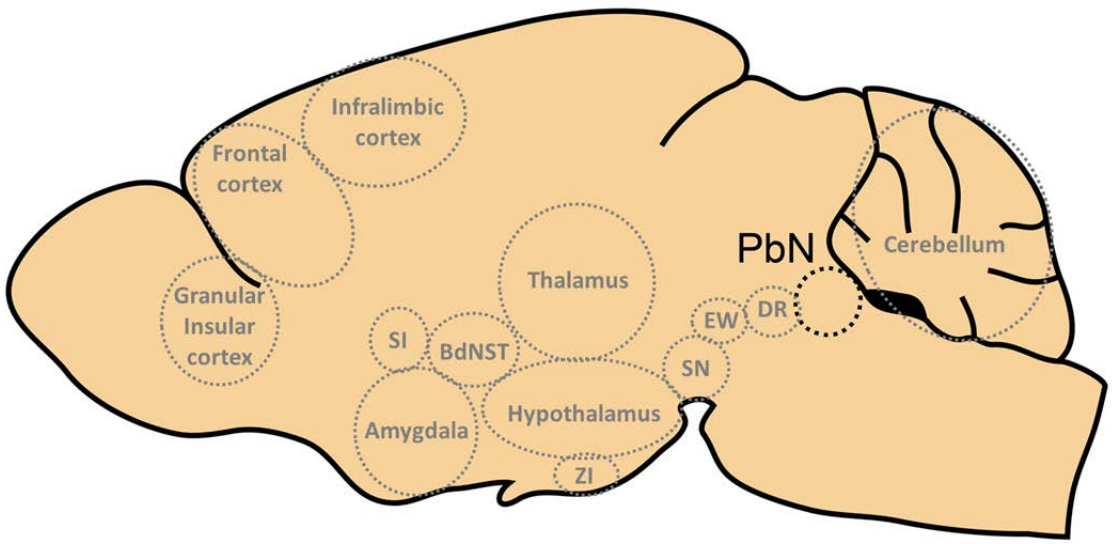

Figure 1.3 Efferent projections from the parabrachial nucleus.
BdNST: bed nucleus of the stria terminalis; DR: dorsal raphe nucleus; EW: Edinger-Westphal nucleus; PbN: parabrachial nucleus; SI: substantia innominata; SN: substantia nigra; ZI: zona incerta. Adapted from Dr. Jonas Töle (DIfE, Nuthetal) with results from Saper and Loewy (1980).

Possessing connections with a vast array of brain structures, the PbN is involved in mediating numerous autonomic functions, including taste processing (Yamamoto, 2006; Yamamoto, Shimura, Sakai, et al., 1994), modulation of food intake (DiPatrizio & Simansky, 2008; Richard et al., 2014; Wilson et al., 2003), thermoregulation (Geerling, Kim, Agostinelli, et al., 2015; Geerling, Kim, Mahoney, et al., 2015), pain circuitry (Han et al., 2015), cardiovascular and respiratory responses to stress (Chamberlin & Saper, 1994;

Davern, 2014), immune responses (Paues et al., 2001; Paues et al., 2006; Richard et al., 2005), and even controlling bladder functions (Liu et al., 2007).

In accordance with the complexity of its connections and functions, the PbN also has an intricate internal structure made up of several sub-nuclei which are characterised by the molecular identity, efferent connections, size, and shape of their neurons (Fulwiler & Saper, 1984). The subnuclei of the PbN are organised into two main groups, separated by the brachium conjunctivum, a bundle of fibres dividing the lateral and medial subnuclei of the PbN. Due to early findings showing the most intense taste responses occurring in the medial PbN (Norgren & Pfaffmann, 1975) and evidence of somatosensory and visceral responses occurring in the lateral subnuclei of the PbN (Chamberlin & Saper, 1994; Yamamoto et al., 1992), the medial and lateral groups of nuclei have often been referred to as the gustatory and non-gustatory nuclei, respectively.

1.3.1 Parabrachial subnuclei: known distinctions and functions

Though the lateral PbN is made up of seven different subnuclei (Fulwiler & Saper, 1984), attempts to characterise the functions for each of these subnuclei have only uncovered distinct functions for some of them. The dorsal lateral PbN is involved in thermoregulatory signals that innervate the preoptic area (Geerling, Kim, Agostinelli, et al., 2015; Geerling, Kim, Mahoney, et al., 2015). The superior lateral PbN contains a population of neurons that respond to leptin administration (Elias et al., 2000), which implies a functional role for the PbN in satiety. It also contains a population of glucose-sensing neurons, with a counter-regulatory capacity, that act via the ventromedial hypothalamus (Garfield et al., 2014).

The extreme lateral PbN houses the majority of PbN neurons that innervate the BdNST (Fulwiler & Saper, 1984). Subsequent research showed that optogenetic activation of this pathway resulted in an augmented startle response, suggesting that this pathway may be involved in the regulation of anxiety-like states (Sink et al., 2011).

The external lateral PbN is perhaps the most complex of the PbN subnuclei, it houses the densest population of neurons that project to the amygdala (Fulwiler & Saper, 1984), and its neurons contain a range of different neuropeptides including corticotropin-releasing factor, cholecystokinin (Herbert & Saper, 1990), neurotensin (Saleh et al., 1997; Yamano et al., 1988), gastrin releasing peptide (Grp) (Wada et al., 1990), and calcitonin gene-related peptide (CGRP) (Schwaber et al., 1988). Functionally, the external lateral PbN is involved in various autonomic regulatory functions such as thermoregulation (Geerling,

Kim, Agostinelli, et al., 2015; Geerling, Kim, Mahoney, et al., 2015), immune response (Paues et al., 2001; Tkacs & Li, 1999), and appetite suppression (Carter et al., 2013).

Some studies have been able to draw conclusions regarding the functional role of specific populations of neurons in the external lateral PbN. For example, neurotensin neurons in the external lateral PbN that project to the central nucleus of the amygdala are believed to trigger cardiovascular responses to stress (Davern, 2014; Yamano et al., 1988). Additionally, CGRP neurons in the PbN are somehow involved in processing aversions; activation of CGRP neurons in the parabrachial nucleus is sufficient to induce a conditioned taste aversion (Carter et al., 2015). This CGRP function is also carried further along the taste pathway, as both inherently aversive bitter tastants and salty or sweet tastants that have been conditioned aversive result in increased CGRP immunoreactivity in the gustatory insular cortex (Yamamoto et al., 1990). Suggesting that CGRP activation along the taste pathway may play a role in processing both inherent and conditioned aversions.

1.3.2 The role of the parabrachial nucleus in taste processing

The parabrachial nucleus is the second relay nucleus in the ascending taste processing pathway; its role in processing taste information has been studied using various standard neuroscience tools. The two predominant methods used to study neural taste responses are electrophysiological recordings of single neurons after taste stimulation, and neural activity markers to compare neural populations that respond to different tastants.

Single-unit electrophysiology is a useful tool which allows researchers to observe individual neurons with a high temporal resolution, giving a clear picture of how an individual neuron responds to taste stimulation across numerous trials. Electrophysiological recordings can be analysed based on their response magnitude or the temporal characteristics of the response. Studies report that there are both broadly tuned, and finely tuned taste responsive neurons in the PbN (Rosen et al., 2011). PbN neurons generally produce a higher magnitude response for one particular tastant over the others; researchers use this to categorise PbN neurons into “best”-stimulus groups for comparison. Although it has also recently been shown that, despite this observed fine-tuning to a “best” taste stimulus, neuronal responses to their “best” taste stimulus (for PbN and NTS neurons) can change over a number of days; either disappearing, appearing, or simply shifting in magnitude (Sammons et al., 2016). Suggesting that the taste-tuning observed in these structures is somehow malleable and plastic.

Electrophysiological recordings have given some insight into the distribution of taste responsive neurons throughout the PbN. Tokita and Boughter (2016) observed a larger amount of salt-best, sour-best, and bitter-best neurons in the lateral PbN, but a larger amount of sweet-best neurons in the medial PbN. Results such as these have led to theories suggesting a possible hedonic distinction between the lateral and medial sub-nuclei, with aversive stimuli being processed via the lateral PbN, and appetitive stimuli being processed via the medial PbN.

Electrophysiology also provides an interesting method to compare neural responses to taste information in the PbN to the preceding taste structure, the NTS. Neural activation in the PbN following taste stimulation shows more variability than that seen in the NTS in terms of spike magnitude (Di Lorenzo & Victor, 2003, 2007); however the temporal characteristics (distribution, amount, proportion, & precision) of neural responses to taste in the PbN were similar to those seen in the NTS (Di Lorenzo & Victor, 2003, 2007; Rosen et al., 2011). Interestingly, broadly tuned taste-responsive PbN neurons encode more information through temporal coding (i.e. spike timing) than neurons with narrower tuning (Rosen et al., 2011), a pattern also seen in the NTS (Di Lorenzo et al., 2009; Di Lorenzo & Victor, 2003). Although the specificity provided by electrophysiological methods is beneficial on a small scale, this narrow scope of observation limits the use of this method for studying taste activation at a larger scale, such as observing whole neuron populations.

Larger scale investigations of neuronal activation can be carried out using immediate early genes such as c-*fos*. Yamamoto et al. (2009) used c-*fos* immunohistochemistry (IHC) as a marker for recently activated neurons following different protocols of taste stimulation. Yamamoto et al. (2009) studied c-*fos* expression following taste stimulation in several different experimental paradigms to characterise the functions of PbN subnuclei. These paradigms included: novel versus familiar taste stimulation, hedonically positive versus negative taste stimulation, and highly versus poorly nutritious substances. Their findings suggest that functions related to general visceral responses, hedonically negative stimuli, and aversive stimuli are processed via the external lateral PbN; whereas functions related to hedonically positive stimuli, appetitive stimuli, and familiar stimuli are processed via the dorsal lateral PbN; and that sodium taste is processed via the central medial PbN. Although this method does provide a larger scale investigation of taste responsive neurons it is limited to one taste stimulation per animal, eliminating the possibility to draw within-subject comparisons of neural activation by two or more tastants.

More recently, the development of optogenetic tools in neuroscience has allowed researchers to molecularly target specific populations of neurons and either activate or silence them to investigate their function (Deisseroth, 2011). This method has been used to study CGRP neurons in the PbN, which are mostly innervated by glucagon-like 1 peptide neurons originating in the NTS (Richard et al., 2014). Carter et al. (2015) were able to show that activating CGRP neurons in the external lateral PbN was sufficient to induce a conditioned taste aversion (CTA). Then, by optogenetically silencing this population of neurons, they were able to show that they were in fact necessary for the formation of a normal CTA response. This method is very useful for examining behaviour elicited by artificial stimulation of specific populations of neurons, however in the field of taste information processing, there is still much to be uncovered in terms of endogenous neural responses to taste stimulation before researchers can begin artificially recreating them. Additionally, the molecular targets for taste processing still need to be confirmed before it is possible to optogenetically recreate a neural taste response.

1.4 Immediate early genes as tools in neuroscience

Immediate early genes (IEGs) are a family of genes that are activated in response to intra- or extra-cellular stimuli, such as synaptic transmission or action potentials. They are rapidly and transiently expressed, which has led to them being used in the brain as markers for recent neural activation (Fowler et al., 2011; Pérez-Cadahía et al., 2011; Sheng & Greenberg, 1990). The use of IEGs as markers of neural activation is well established (for review, see Hoffman et al., 1993). Although it is understood that the absence of IEG induction should not always be assumed to mean that no neuronal activation has occurred. One way in which this has been demonstrated is through the use of multiple different IEGs following the same intervention, resulting in variations in expression between the IEGs, suggesting that they may have different requirements for induction (Cullinan et al., 1995).

1.4.1 The immediate early gene *Arc*

Arc was identified in 1995 by two labs working independently of each other, Lyford et al. (1995) named it *Arc* for activity-regulated cytoskeleton associated protein, and Link et al. (1995) named it *Arg3.1* for activity-regulated gene 3.1. For simplicity, the term *Arc* will be used hereafter. Unlike other activity-regulated genes, *Arc* shows a unique expression pattern, in that *Arc* messenger ribonucleic acid (mRNA), once synthesised, is rapidly transported to dendrites where it localises near sites of recent synaptic activity that

are sufficient to activate N-methyl-D-aspartate (NMDA) receptors (Steward et al., 2015; Steward et al., 1998; Steward & Worley, 2001). Due to its dynamic expression which is highly correlated to neuronal activation, *Arc in situ* hybridisation (ISH) and IHC methods are being used more frequently to mark recently activated neurons (Guzowski et al., 2000; Guzowski et al., 1999).

Arc has been implicated in synaptic plasticity and memory consolidation due to its involvement in α-amino-3-hydroxy-5-methyl-4-isoxazolepropionic acid (AMPA) receptor endocytosis (Chowdhury et al., 2006; Shepherd et al., 2006). Additionally, it has been hypothesised that *Arc* is expressed in an "experience-dependent" manner. Kelly and Deadwyler (2002) studied *Arc* expression in animals following a simple operant-task comparing groups who had received different amounts of training to complete the task; they found that animals with the least training showed significantly higher *Arc* expression than animals who had received extensive training. This finding suggests that *Arc* may play an important role in processing novel experiences and acquiring new learned behaviours.

In addition to neural plasticity, *Arc* has also been implicated in the neural processing of taste information. *Arc* has been shown to be required for rats to acquire conditioned taste aversion memories (Plath et al., 2006), suggesting it plays a key role in taste-related learning. This is supported by research from Montag-Sallaz et al. (1999) using *Arc* to study the processing of novel tastes in various brain structures including the dentate gyrus, cingulate cortex, and parietal cortex; all of which showed elevated *Arc* expression following taste stimulation with a novel taste compared to a familiar taste. Additionally, in the insular cortex Inberg et al. (2013) showed that familiar tastes result in asymmetrical *Arc* expression, whereas novel tastes produce a more lateralised *Arc* expression. They also showed that inhibiting protein synthesis in the insular cortex in only one hemisphere resulted in significant memory impairment; suggesting that this hemispheric lateralisation of *Arc* expression is necessary for processing novel taste information. This evidence of a clear connection with taste processing makes *Arc* an interesting candidate IEG for studying the neural representation of taste responses.

1.4.2 The development of the *Arc* catFISH method

While developing a specific fluorescent *in situ* hybridisation (FISH) protocol to detect *Arc* mRNA, Guzowski et al. (1999) observed three distinct *Arc* staining profiles in hippocampal neurons. Upon further exploration, they determined that these different patterns of *Arc* distribution were time-dependent. Within the first 2 – 16 minutes following

the activation of an *Arc*-expressing neuron, the *Arc* mRNA is only observed within the cell nucleus. Then, from ~20 to 45 minutes following the activation of the neuron *Arc* mRNA is transported out of the nucleus, resulting in a cytoplasmic staining. By 60 minutes after activation of the neuron, the *Arc* signal is no longer present in the perikaryon. In addition to these nuclear and cytoplasmic staining profiles, they also observed a third staining profile which showed a double staining – this appeared in twice-activated neurons which showed both cytoplasmic and nuclear staining (example images of these three staining profiles can be seen in **Figure 3.5** in the methods section 3.7 on page 42).

Following on from their observations they developed a technique exploiting the precise temporal changes in intracellular distribution of *Arc* mRNA in order to observe neural activation patterns in the same population of neurons following two discrete behavioural experiences. The technique was termed *Arc* catFISH (cellular compartment analysis of temporal activity by fluorescent in-situ hybridisation). Using this method in conjunction with a carefully timed stimulation protocol in which animals receive two distinct stimulation events it is possible to distinguish which neurons responded to each stimulation event by observing the intracellular location of their *Arc* expression. This technique allows an intra-subject comparison, comparing neural activation from two separate events within the same animal. This technique has been used successfully in paradigms studying auditory-cued learning (Carpenter-Hyland et al., 2010), neural encoding of novel environments (Guzowski et al., 1999), and neural convergence of information about conditioned stimulus and unconditioned stimulus during Pavlovian fear conditioning (Barot et al., 2009).

1.4.3 Using the *Arc* catFISH method to study taste responsive neurons

The *Arc* catFISH method has also been developed to study neural responses to taste stimulation (Töle, 2014) to bridge the shortcomings of previously used methods by allowing observation of large populations of taste-responsive neurons across two separate taste-stimulations. In a recent study exploring neural responses to taste information, Töle (2014) found that the immediate early gene *Arc* is a marker for some type of bitter-specific activation in the NTS. Results also showed that the NTS contained distinct, yet overlapping populations of neurons activated by different bitter tastants (Töle, 2014).

Taken together, the roles of both the PbN and *Arc* in the formation of conditioned taste aversion memories (Carter et al., 2015; Plath et al., 2006), the bitter-specificity of taste-responsive *Arc* expression in the NTS (Töle, 2014), and the fact that the parabrachial

nucleus is the main target for gustatory NTS neurons, the parabrachial nucleus is a clear candidate for further study using this method.

1.5 Aim

The aim of this thesis is to investigate neural activation following taste stimulation in the parabrachial nucleus in naïve and conditioned mice using the IEG *Arc* as a neural activity marker. Specifically, observing whether the PbN, like the NTS, also shows a bitter-specificity in naïve mice; whether prior learning experience with tastants changes the rate of *Arc* expression in the PbN; and lastly, determining which neuropeptides are involved in this bitter-specific *Arc* expression. To this end, *Arc* expression patterns are observed in the PbN following different taste stimulation protocols in naïve and conditioned mice using the *Arc* catFISH protocol. The taste protocol for naïve animals includes a single stimulation with compounds from each taste quality, as well as three bitter compounds for comparison. A second taste stimulation experiment includes double stimulation protocols in which mice receive two temporally separate taste stimulations either with a different tastant each time or with two stimulations of the same tastant; stimuli include different combinations of the three bitter stimuli as well as a control stimulus. The rate of *Arc* expression triggered by taste stimulation with each stimulus is measured, and the rate at which neurons are reactivated by a second taste stimulation (either with the same, or with a different taste stimulus) is determined. Additionally, the distribution of *Arc* expression in the PbN is measured to see if higher expression levels are present in the lateral or medial PbN subnuclei.

In order to observe how prior exposure affects taste-responsive *Arc* expression, animals are conditioned to find either a bitter or an umami tastant aversive using a one-time pairing of the tastant with a lithium chloride injection. These mice then receive a single taste stimulation with either the stimulus they were conditioned to find aversive, or a control stimulus, and *Arc* expression in the PbN is analysed.

An extended FISH protocol is then established to include a second RNA probe in order to stain for neuropeptide ribonucleic acid (RNA) expression present in the *Arc*-expressing neurons. This is performed with genes that are known to be present in PbN neurons: calcitonin (Calca), glucagon like 1 peptide receptor (Glp1r), gastrin-releasing peptide (Grp), hypocretin receptor 1 (Hcrtr1), and neurotensin (Nts). Once the new, extended protocol is established the rate of *Arc* neurons co-expressing each of these genes is determined.

1.5.1 Hypotheses

It is expected that bitter taste stimulation will produce an increase in *Arc* expression in the PbN similar to what has previously been shown in the NTS. It is also hypothesised that mice stimulated twice with the same tastant will show a higher rate of neurons showing a twice-stimulated *Arc* expression (*Arc* in both the nucleus and in the cytoplasm), compared to mice stimulated twice with a different tastant for each stimulation event. It is also hypothesised that *Arc* expression in the PbN following bitter taste stimulation will be distributed more heavily in the lateral PbN.

Umami taste stimulation is expected to result in a low rate of *Arc* expression in naïve animals compared to controls, whereas due to *Arc*'s known function in CTA learning, mice conditioned to find umami aversive are expected to show an increase in the rate of *Arc* expression following umami taste stimulation compared to naïve animals. This aversive-umami *Arc* expression is also expected to be more heavily distributed in the lateral PbN.

The neuropeptide candidate genes were all selected due to their known functions or locations in the PbN to increase the likelihood of finding a neuropeptide that is co-expressed in *Arc*-expressing PbN neurons. Therefore, it is expected that they will all show some *Arc* co-expressing cells. Calcitonin in particular is expected to show a high rate of co-expression with bitter-responsive *Arc*-expressing neurons due to its role in aversion processing.

Materials

This section contains the tools and supplies used to carry out the experiments discussed in this thesis. Basic materials and molecular biology laboratory equipment are not explicitly listed.

2.1 Devices

Table 2.1: Devices

Device	Manufacturer
Automated microscope Mirax MIDI	Carl Zeiss Microscopy, Jena
Centrifuge 5417R	Eppendorf AG, Hamburg
Colibri - Spectrophotometer	Biozym Scientific, GmbH, Hessisch Olendorf
Confocal laser scanning microscope LCS SPX	Leica Microsystems, Wetzlar
Cryomicrotome HM 560 CryoStar	Thermo Fisher Scientific, Dreieich
Davis MS 160-Mouse, Lickometre	DiLog Instruments, Tallahassee, FL, USA
Fluorescence microscope Axioplan 1	Carl Zeiss Microscopy, Jena
Gel Documentation System - Gene Genius	Synoptics, Cambridge, UK
pH meter HI 9024	HANNA Instruments, Kehl am Rhein
pH meter Lab 850	SI Analytics, Mainz
Liquid Handling System, Freedom EVO 150	Tecan, Crailsheim
Power supply for electrophoresis EPS 601	BioRad, Munich
Automatic tissue stainer Shandon Varistain 24-4	Thermo Fisher Scientific, Dreieich
Spectrophotometer NanoDrop ND-1000	NanoDrop Technologies, Wilmington, DE, USA
ThermoMixer compact	Eppendorf AG, Hamburg
Thermal Cycler PTC-200	MJ Research, Waltham, MA, USA
Thermocycler TProfessional	Biometra, Munich
Thermocycler TProfessional Basic	Biometra, Munich
TissueLyser II	Qiagen, Hilden
Vortex-Genie 2	Scientific Industries, Bohemia, NY, USA
Water bath 1003	Society for Laboratory Technology, Castle Wedel
Water bath OLS200	Grant Instruments, Shepreth, UK

A commercially available multi-channel lickometre (Davis MS 160 – Mouse: DiLog Instruments, Tallahassee, FL) measured the licking behaviour of the mice. The apparatus consists of a testing chamber (dimensions; 14.5 cm wide, 30 cm deep, 15 cm tall), a 16-channel taste stimulus delivery system, and a dedicated computer programmed to control stimulus delivery and to record licking behaviour. The apparatus detects licking behaviour and measures cumulative licks, latency until first lick, inter-lick interval, and the rate of licking (for more details, see Glendinning, Gresack, et al., 2002).

2.2 Software

Table 2.2: Software

Program	Manufacturer
Davis Collect Data	DiLog Instruments, Tallahassee, FL, USA
Excel 2010, 2013	Microsoft Corporation, Redmond, WA, USA
GeneSnap 6:01	Synoptics, Cambridge, UK
ImageJ	Wayne Rasband, NIH, Bethesda, MD, USA
LAS X 2.0.0.14332	Leica Microsystems, Wetzlar
MIRAX Scan 1.12	Carl Zeiss Microscopy, Jena
MIRAX Viewer 1.12	Carl Zeiss Microscopy, Jena
Photoshop CS3, CS6	Adobe Systems, San Jose, CA, USA
SigmaPlot 12.3	Systat Software, Erkrath
Tecan EVOware 2.3, 2.5	Tecan, Crailsheim
Venn Diagram Plotter 1.5	Kyle Littlefield, Matthew Monroe, PNNL, Richland, WA, USA

2.3 Chemicals and consumables

Table 2.3: Chemicals and consumables

Substance (Abbreviation)	Purity	Manufacturer	Catalogue #
2-Methylbutane	for synthesis, ≥99 %	Carl Roth, Karlsruhe	3927.1
3-(N-Morpholino)propanesulfonic acid (MOPS)	≥99 %	Carl Roth, Karlsruhe	6979.4
4',6-Diamidinie-2'-phenylindole dyhydrochloride (DAPI)		Thermo Fisher Scientific, Dreieich	D1306
4-Nitro blue tetrazolium chloride (NBT), 100 mg·ml $^{-1}$ in 70 % in Dimethylformamide	>95 %	Roche Applied Science, Mannheim	11383213
5-Bromo-4-chloro-3-indolyl phosphate (BCIP) 50 mg·ml^{-1} in dimethylformamide	>95%	Roche Applied Science, Mannheim	11383221
Acetic Acid ($C_2H_4O_2$)	extra pure	Carl Roth, Karlsruhe	6755.1
Acetic anhydride	puriss. P.a., *ACS reagent* ≥99.0 %	Sigma-Aldrich, Steinheim	45830
Agar		Invitrogen, Life Technologies, Darmstadt	30391023
Agarose, UltraPure		Invitrogen, Life Technologies, Darmstadt	16500500
Agarose, Wild Range		SERVA, Heidelberg	11406
Ammonium chloride (NH_4Cl)	*BioUltra, for molecular biology*, ≥99.5 %	Sigma-Aldrich, Steinheim	09718
Ampicillin		Sigma-Aldrich, Steinheim	
Aquick Gel Extraction Kit		Qiagen, Hilden	28704
Blocking reagents		Roche Applied Science, Mannheim	11096176
Bromophenol Blue, Sodium Salt		USB Corp., Cleveland, OH, USA	12370
Chloroform	p.a., EMSURE	Merck KGaA, Darmstadt	1.02445
Daily System Clean		LVL technologies, Crailsheim	2001
Deoxynucleotide Triphosphates (dNTPs)	≥99 %	Fermentas, St.-Leon-Rot	R0181

Substance (Abbreviation)	Purity	Manufacturer	Catalogue #
DIG RNA Labelling Mix		Roche Applied Science, Mannheim	1277073
Dimethyl Sulfoxide (DMSO)	BioUltra, ≥99.5 %	Sigma-Aldrich, Steinheim	41639
Disodium Phosphate (Na_2HPO_4)	*ReagentPlus*, ≥99 %	Sigma-Aldrich, Steinheim	S0876
DNA- standard size "Gene-Ruler DNA Ladder Mix"		Fermentas, St.-Leon-Rot	SM0331
Electro Insulation Tape		Carl Roth, Karlsruhe	1256.1
Ethanol (EtOH)	p.a., EMSURE	Merck KGaA, Darmstadt	1.00983
Ethidium Bromide, aqueous, 10 $mg \cdot ml^{-1}$ (EtBr)	BioReagent	Sigma-Aldrich, Steinheim	E1510
Ethylenediaminetetraacetic acid, Disodium Salt, Dihydrate ($Na_2H_2EDTA \cdot 2H_2O$)	*ACS reagent*, 99.0 – 101.0 %	Sigma-Aldrich, Steinheim	E4884
Fluorescein-Avidin-D, 5 $mg \cdot ml^{-1}$		Vector Laboratories, Burlingame, CA, USA	A-2001
Fluorescein RNA Labelling Mix		Sigma-Aldrich, Steinheim	11685619910
Fluorescent Mounting Medium		Dako, Hamburg	S302380-2
Formalin, aqueous, ≥36 %	BioReagent	Sigma-Aldrich, Steinheim	47608
Formamide		Roche Applied Science, Mannheim	1814320
High Pure PCR Product Purification Kit		Roche Applied Science, Mannheim	11732668
Hydrochloric acid, fuming, 37 %	p.a.	Carl Roth, Karlsruhe	X942.1
Hydrogen peroxide (H_2O_2), 30 % (w/w)	ACS reagent	Sigma-Aldrich, Steinheim	216763
In Situ Hybridisation Buffer		Ambion, Life Technologies, Darmstadt	B8807G
Iodoacetamide	SigmaUltra, ≥99 %	Sigma-Aldrich, Steinheim	I1149
Lamb Serum		Gibco, Life Technologies, Darmstadt	16070-096
Levamisole	≥99 % (GC)	Sigma-Aldrich, Steinheim	L9756
Magnesium chloride hexahydrate ($MgCl_2 \cdot 6H_2O$)	p.a., EMSURE	Merck KGaA, Darmstadt	1.05833
Magnesium sulphate ($MgSO_4$)		Thermo Fisher Scientific, Dreieich	52044
Maleic Acid	*ReagentPlus*	Sigma-Aldrich, Steinheim	M0375
Methanol (MeOH)	p.a., EMSURE	Merk KGaA, Darmstadt	1.06009
Microscope slides SuperFrost Plus		Carl Roth, Karlsruhe	H867.1
MiniPax, silica gel absorbent packets, 10 g		Sigma-Aldrich, Steinheim	Z163597
Monopotassium phosphate (KH_2PO_4)	*ReagentPlus*	Sigma-Aldrich, Steinheim	P5379
Neutravidin-Alkaline-Phosphatase		Thermo Fisher Scientific, Dreieich	31002
One Shot® TOP10 Chemically Competent *E. coli* kit		Invitrogen, Life Technologies, Darmstadt	C404010
Paraformaldehyde (PFA)	Reagent Grade	Sigma-Aldrich, Steinheim	P6148
PCRx Enhancer System		Invitrogen, Life Technologies, Darmstadt	11495-017
Plasmid mini- and midipreparation kit		Qiagen, Hilden	27405 12843
Polysorbate 20 (Tween 20)		Fisher Scientific, Schwerte	BP337
Potassium Chloride (KCl)	*ReagentPlus*, ≥99 %	Sigma-Aldrich, Steinheim	P4504
Random Primers		Invitrogen, Life Technologies, Darmstadt	48190-011
RNA ladder "Ribo-Ruler High		Fermentas, St.-Leon-Rot	SM1821

Substance (Abbreviation)	Purity	Manufacturer	Catalogue #
Range RNA Ladder"			
Set Up Clean		LVL technologies, Crailsheim	2000
Sodium Acetate (NaAc)	p.a., EMSURE	Merck KGaA, Darmstadt	1.06268
Sodium Bicarbonate ($NaHCO_3$)	p.a. EMSURE	Merck KGaA, Darmstadt	1.06329
Sodium chloride (NaCl)	*BioUltra, for molecular biology*, ≥99.5 %	Sigma-Aldrich, Steinheim	71376
Sodium Citrate, Dihydrate (Na-Citrate · $2H_2O$)	≥98 %	Sigma-Aldrich, Steinheim	C7254
Sodium Hydroxide	Pure, >97.0 %	Merck KGaA, Darmstadt	1.06462
TO-PRO-3 Iodide, 1 mM in DMSO		Invitrogen, Life Technologies, Darmstadt	T3605
Triethanolamine	*BioChemika*, ≥99.0 %	Sigma-Aldrich, Steinheim	90279
Tris(hydroxymethyl)-aminomethane (Tris)	≥99.0 %	Sigma-Aldrich, Steinheim	T1503
TRIzol Reagent		Ambion, Life Technologies, Darmstadt	15596-018
Tryptone		Sigma-Aldrich, Steinheim	T9410
TSA Biotin System		PerkinElmer, Rodgau-Jügesheim	NEL700001KT
Yeast Extract		Carl Roth, Karlsruhe	2363.2

2.4 Enzymes

Table 2.4: Enzymes

Enzyme	Manufacturer	Catalogue #
Advantage 2 Polymerase Mix	Clontech, CA, USA	S1798
Deoxyribonuclease I, *Amplification Grade*	Invitrogen, Life Technologies, Darmstadt	18068-015
Pfu-Polymerase	Promega, Mannheim	M7741
*Pfu*Ultra High-Fidelity DNA Polymerase	Agilent Technologies, CA, USA	300380
Proteinase K, recombinant, *from Pichia pastoris, PCR Grade*	Roche Applied Science, Mannhein	3115828
Reverse Transcriptase SuperScript II	Invitrogen, Life Technologies, Darmstadt	18064-014
Ribonuclease-Inhibitor RiboLock	Fermentas, St.-Leon-Rot	EO0381
T3 RNA Polymerase	Roche Applied Science, Mannhein	11031163001
T7 RNA Polymerase	Roche Applied Science, Mannhein	10881767001
TURBO DNase	Ambion, Life Technologies, Darmstadt	AM2238

Restriction Enzymes	Manufacturer	Catalogue #
ApaI	New England BioLabs	R0114S
BgllI	Fermentas, St.-Leon-Rot	ER0081
Eco 88	Fermentas, St.-Leon-Rot	ER0381
NotI	Fermentas, St.-Leon-Rot	ER0571
SalI	Fermentas, St.-Leon-Rot	ER0641
XmnI	New England BioLabs	R01945

2.5 Antibodies

Table 2.5: Dyes/secondary antobodies

Epitope (Abbreviation)	Origin	Manufacturer	Catalogue #	Dilution
Anti-Digoxigenin-POD	Sheep, polyclonal	Roche Applied Science, Mannheim	11207733910	1:500
Anti-Fluorescein-POD	Sheep, polyclonal	Roche Applied Science, Mannheim	11426346910	1:1500

2.6 Oligonucleotides

The oligonucleotides used for polymerase chain reaction (PCR) were purchased lyophilised from Eurofins MWG Operon, Ebersberg. They were then each dissolved in deionised, UV-irradiated water to a final concentration of 100 µm and stored at -20˚C.

Table 2.6: Oligonucleotides that were used for the generation of RNA probes.

Designation	Sequence
T3-***Arc* ABA** fwd.	AATTAACCCTCACTAAAGGG **TGGAAGAGTACCTGCGGC**
T7-***Arc* ABA** rev.	TAATACGACTCACTATAGGG **ACCCAAAGAGCCCTGGAC**
T3-**NtsABA**-fwd.	AATTAACCCTCACTAAAGGG **AGAAGAAGATGTGAGAGCCCTG**
T7-**NtsABA**-rev.	TAATACGACTCACTATAGGG **CTGCTTTGGGTTAATAACGCTC**
Sal-**CalcaABA**-fwd.	GGGGGG GTCGAC **AGCACTGCCTGGCTCCAT**
Not-**CalcaABA**-rev.	GGGGGG GCGGCCGC **CCAGATGACTGCCCTTGC**
Sal-**Glp1rABA**-fwd.	GGGGGG GTCGAC **CTCAAGTGGATGTATAGCACGG**
Not-**Glp1rABA**-rev.	GGGGGG GCGGCCGC **ACTCCATCTGGACCTCATTGTT**
Sal-**Hcrtr1ABA**-fwd.	GGGGGG GTCGAC **ACCCACTGTTGTTCAAGAGCAC**
Not-**Hcrtr1ABA**-rev.	GGGGGG GCGGCCGC **TTGCCACTGAGGAAGTTGTAGA**
Sal-**GrpABA**-fwd.	GGGGGG GTCGAC **CACGGTCCTGGCTAAGATGTAT**
Not-**GrpABA**-rev.	GGGGGG GCGGCCGC **CCAGTAGAGTTGACGTTTGCAG**

2.7 Taste stimuli

Table 2.7: Taste stimuli for *Arc* analysis

Taste Quality	Substance (Abbreviation)
Control stimulus	25 mM KCl, 2.5 mM $NaHCO_3$ (ctrl.)
Umami	100 mM Monosodium glutamate (NaGlu)
Sweet	0.5 M Sucrose (Sucr)
Salty	0.8 M Sodium Chloride (NaCl)
Sour	0.03 M Citric Acid (Citr.)
Bitter	0.5 mM Cycloheximide (Cyx) 10 mM Quinine Hydrochloride (Qui) 1 mM Cucurbitacin I (Cuc)

Table 2.8: Taste stimuli for short-term preference test and CTA

Taste Quality	Substance (Abbreviation)
Control stimulus	H_2O
Umami	20 mM Monosodium Glutamate (Umami)
Sweet	300 mM Sucrose (Sucr)
Sour	50 mM Citric Acid (Citr.)
Bitter	1 µM Cycloheximide (Cyx) 0.1 µM Quinine Hydrochloride (Qui) 30 µM Cucurbitacin I (Cuc) 1 µm Papaverin 1 µm Sucrose Octaacetate (SOA)

2.8 Solutions and buffers

Unless otherwise stated, all solutions were prepared with deionised water (conductivity maximum 0.06 $\mu S \cdot cm^{-1}$). Diethylpyrocarbonate (DEPC) was not added to the solutions to deactivate ribonucleases (RNases). Instead, containers were sterilised either at 200 ˚C for two hours or, for temperature-sensitive materials, working surfaces were sterilised using RNase-AWAY solution. Bottles used to store or prepare solutions intended for RNase-sensitive methods were treated periodically with DEPC. The solutions were stored at room temperature, unless otherwise indicated.

2.8.1 Solutions for the agarose gel electrophoresis

TAE (Tris-Acetate-EDTA-Buffer), 50×
2 M Tris-Base
1 M Acetic Acid
$^1/_{10}$ volume 0.5 M EDTA, pH 8

Running buffer for denaturing RNA gels
$^1/_{10}$ volume of 10× MOPS-Buffer
0.67 % Formaldehyde

MOPS-Buffer for denaturing RNA-Gels, 10×
0.2 M MOPS
50 mM Sodium Acetate
10 mM EDTA
pH 7.0
Autoclave
Store at 4 ˚C

Loading buffer for agarose gel electrophoresis, 6×
60 % Glycerol
60 mM EDTA
10 mM Tris-HCl, pH 7.6
0.03 % Bromophenol Blue
0.03 % Xylene Cyanole
Store at -20 ˚C

2.8.2 Solutions for pre-treatment

4 % PFA in PBS
PFA dissolved at approx. 65 ˚C
in 0.2 mM NaOH
Add $^1/_{10}$ volume 10× PBS
Adjust pH 7.4
Make fresh

Triethanolamine Buffer
0.1 M Triethanolamine
pH 8 adjusted with HCl
Make fresh

2.8.3 Solutions for *in situ* hybridisation

The stock solutions listed below were used to prepare the aqueous solutions used in the pipetting robot. Tween-20 was added to all aqueous (except the hybridisation buffer) solutions to reduce the surface tension. With a few exceptions (0.6 % hydrogen peroxide in methanol, hybridisation buffer, Tyramide-biotin in Amplification Diluent, and the system liquid), the solutions were degassed by applying a vacuum prior to being placed in the pipetting robot. This was to avoid the formation of bubbles under the cover glass which could affect the distribution of the aqueous solutions over the slides.

PBS (phosphate-buffered saline), 10×
0.1 M Na_2HPO_4
17.64 mM KH_2PO_4
26.83 mM KCl
1.369 M NaCl
pH 7.4
Autoclave

SSC (saline sodium citrate), 20×
0.3 M Sodium Citrate
3 M NaCl
pH 7
Autoclave

TN (Tris-NaCl-Buffer), 10×
1 M Tris-Base
1.5 M NaCl
pH 7.4
Autoclave

NTE (NaCl-Tris-EDTA-Buffer), 5×

2.5 M NaCl
50 mM Tris-Base
25 mM $Na_2H_2EDTA \cdot 2H_2O$
pH 8
Autoclave

MWB (maleate wash buffer)
0.15 M NaCl
0.1 M Maleic Acid
0.2 M NaOH
pH 7.4
Store at 4 ˚C

Proteinase-K Buffer, 2×
0.1 M Tris-Base
10 mM $Na_2H_2EDTA \cdot 2H_2O$
pH 8 (HCl)
Autoclave

20 % PFA in PBS
PFA dissolved at 65 ˚C
in 0.2 mM NaOH
Add $^1/_{10}$ volume 10× PBS
Adjust pH 7.4
Store at -20 ˚C

4 % PFA in PBS
$^1/_3$ volume 20 % PFA in PBS
Add $^1/_{10}$ volume 10× PBS
Top up with water

TNB (Tris-NaCl-Buffer with Blocking Reagent)
Dissolve 0.5 % Blocking Reagent (PerkinElmer)
at 55 ˚C in TN
Store at -20 ˚C

BR (Blocking Reagent)
Dissolve 1 % Blocking Reagent (Roche)
at 55 ˚C in MWB
Make fresh

2.8.4 Solutions for molecular cloning

Lysogeny Broth (LB) Medium
10 g/l Tryptone
5 g/l Yeast extract
10 g/l NaCl
Autoclave
pH 7.5

Terrific Broth (TB) Medium
800 ml H_2O
12 g Tryptone
24 g Yeast extract
4 ml Glycerol
Adjust volume to 900 ml with H_2O
Autoclave, allow to cool to less than 60 °C
Add 100 ml potassium phosphate solution

LB Agar Plates
LB medium
15 g/l Agar
Autoclave
Cool to 55 °C
Add 100 µg/ml Ampicillin and plate
Cool until solidified
Store inverted in sealed bags at 4 °C

Potassium Phosphate Solution
0.17 M KH_2PO_4
0.72 M K_2HPO_4
Autoclave

2.9 Experimental animals

2.9.1 Naïve taste stimulation animals

The experimental animals used in the naïve taste stimulation experiments were 90 male C57BL/6 mice. The animals were purchased from: Société Janvier, Le Genest Saint Isle, France; Charles River Laboratories, Wilmington, MA, USA; Harlan Laboratories, Eystrup, or were from our own breeding colony. At the time of the experiments the animals were 8-19 weeks old, and had been housed for at least one week in our animal husbandry facility for acclimatisation.

2.9.2 Conditioned taste aversion animals

The experimental animals used in the behavioural experiment were 32 male C57BL/6 mice. The animals were purchased from Société Janvier, Le Genest Saint Isle, France. At the time of the experiments the animals were 8-10 weeks old, and had acclimatised for least one week in the experiment room.

The mice lived in standardised conditions in a temperature-controlled room on a 12hr/12hr light/dark cycle. During the water restriction phases of the experiment the mice were weighed daily to ensure they maintained 80 % of their baseline bodyweight.

Methods

This section is intended to provide an overview of the methods used to carry out these experiments. First, the steps involved in the generation of the ribonucleic acid (RNA) probes to detect expression of *Arc* and neuropeptide/neuropeptide receptor RNA are described. Then the animal stimulation protocol is explained, followed by a description of the preparation of the brain tissue, and the preparation of the cryosections. Finally, the training and testing protocols used in the short-term taste preference testing are described.

3.1 Generation of the *Arc* RNA probe

The *Arc* RNA probe used in the *in situ* hybridisation experiments corresponds to 862 nucleotides of the first exon of the *Arc* gene (nucleotides 869 to 1730, see Ensembl database:

[http://www.ensembl.org/Mus_musculus/Transcript/Exons?db=core;g=ENSMUSG00000022602;r=15:74669083-74672570;t=ENSMUST00000110009]. *Arc* probes were generated from a piece of deoxyribonucleic acid (DNA) that was amplified by polymerase chain reaction (PCR). The primer sequences used for probe generation are listed in Table 2.6 on page 21. The sequence linked above was flanked by promoters for T7 (antisense) and T3 RNA polymerase (sense).

Agarose gel electrophoresis was used to check the results of each step of the probe generation. 1 % agarose gels with 1× triethanolamine (TAE) buffer were used for DNA and the separation was performed at 12 $V \cdot cm^{-1}$ for 25 – 30 minutes. Denaturing gels with 1.5 % agarose, 0.67 % formaldehyde and 1× 3-(N-Morpholino)propanesulfonic acid (MOPS) buffer were used for RNA, separated at 8.4 $V \cdot cm^{-1}$ for about 25 minutes. The composition of the buffers is given in section 2.8.1 on page 22.

3.1.1 RNA extraction

Total RNA was extracted from the mouse brain using the guanidinium thiocyanate-phenol-chloroform method (Chomczynski & Sacchi, 1987) and a ready-made mixture (TRIzol; Invitrogen).

The brain tissue was homogenised with 1 ml per 100 mg of tissue using TRIzol TissueLyzer II and then centrifuged for 10 minutes at 12,000 *g* and 4 ˚C. The supernatant was removed and incubated at room temperature for 5 minutes. 0.2 ml of chloroform per millilitre of TRIzol was added and the mixture was shaken vigorously for 15 seconds, and

incubated for 2 – 3 minutes at room temperature. The mixture was centrifuged for 15 minutes at 12,000 *g* and 4 ˚C. The upper aqueous phase was collected and added to 0.5 ml isopropanol per millilitre of TRIzol to precipitate the RNA. This was incubated for 10 minutes at room temperature and then centrifuged for 10 minutes at 12,000 *g* and 4 ˚C. The supernatant was discarded and the RNA pellet was washed and denatured with 1 ml of 75 % ethanol per millilitre of TRIzol. After another 5 minutes of centrifugation at 7,500 *g* and 4 ˚C the supernatant was discarded and the RNA pellet was dried at room temperature. The dried precipitate was then dissolved in deionised water at 55-60 ˚C.

The quality of the RNA extraction was checked by electrophoresis using a denaturing 1.5 % agarose gel. The concentration of the extracted RNA was determined by ultra violet (UV) spectrometry.

3.1.2 Complimentary DNA synthesis

The complimentary (cDNA) synthesis was performed using a genetically modified reverse transcriptase Superscript II (Invitrogen) and total RNA from the mouse brain as a template.

First any residual DNA not removed during RNA extraction was removed by deoxyribonuclease (DNase) digestion. For this purpose, 150 $ng \cdot \mu l^{-1}$ of the extracted RNA, 10× DNase buffer $^1/_{10}$ volume, 1 mM dithiothreitol (DTT), 1:33 μl^{-1} Ribolock RNase inhibitor and 0.067 $U \cdot \mu l^{-1}$ DNase I (Invitrogen) were mixed for a batch of 15-30 µl.

The mixture was then incubated at room temperature for 1 hour, next the DNase was inactivated by adding 2 mM ethylenediaminetetraacetic acid (EDTA) and heating to 68 ˚C for 15 minutes. For the subsequent reverse transcription $^1/_3$ of the reaction mixture was added to 12.5 $ng \cdot \mu l^{-1}$ Random Primer and incubated for 5 minutes at 72 ˚C, and then rapidly cooled on ice. The remainder of the reaction mixture was added to an equal volume of deionised, UV-irradiated water, and stored at -80 ˚C to serve as a control to test the success of the DNase I digestion ("-RT").

Then, for the Reverse Transcription the ⅔ of the original volume of the DNase I digestion was combined with $^2/_5$ of the original volume of 5× Reverse Transcriptase Buffer, deoxynucleotide triphosphates (dNTPs, each 0.5 µM), 3 mM magnesium chloride ($MgCl_2$), 0.5 $U \cdot \mu l^{-1}$ Ribolock RNase Inhibitor, and 10 $U \cdot \mu l^{-1}$ Superscript II. The final volume was $^4/_3$ the original volume.

The Reverse Transcription was performed at 42 ˚C for 1 hour. Ten minutes before the end 10 $U \cdot \mu l^{-1}$ Superscript II was added again. Finally, the reaction was stopped by heating

to 72 ˚C for 15 minutes. For subsequent PCRs 1µl samples of the Reverse Transcriptase ("+RT") and the –RT control were used.

3.1.3 Polymerase chain reaction

A Polymerase Chain Reaction (PCR) was carried out to generate starting material for the *in vitro* transcription using cDNA from a mouse brain as a template. First, the optimum temperature was determined during the annealing step in 25 µl batches. For this, a PCR program with a gradient of various temperatures during the annealing step across the individual reaction tubes was used.

For the *Arc*-specific primers a gradient of six temperatures ranging from 56 ˚C to 66 ˚C were chosen, this is because the calculated melting temperature of the primer-template hybrid was approximately 64 ˚C. This PCR determined a 58 ˚C optimum annealing temperature, resulting in an intense band of the expected size, without side bands on the agarose gel.

A PCR was then carried out on a larger scale (using reaction tubes of 50 µl) to obtain enough starting material. The PCR approach is summarised as follows:

25 µl batch	50 µl batch	
11.5 µl	24 µl	Deionized and UV irradiated water
2 µl	4 µl	10× Polymerase buffer
2 µl	4 µl	dNTP mix (2.5 mM each)
0.5 µl	1 µl	Forward primer (10 µM)
0.5 µl	1 µl	Reverse primer (10 µM)
2.5 µl	5 µl	10× PCR Enhancer Solution
1 µl	1 µl	cDNA template
20 µl	40 µl	

The polymerase was prepared separately with polymerase buffer and water and then cooled on ice. Polymerase buffer was added manually during the first step of the PCR program.

25 µl batch	50 µl batch	
4 µl	8 µl	Deionized and UV irradiated water
0.5 µl	1 µl	10× Polymerase buffer
0.5 µl	1 µl	*Pfu*-Polymerase (2-3 $U \cdot \mu l^{-1}$)
5 µl	10 µl	

The sequence of the PCR program for the amplification of the template for the *Arc*-RNA probe was as follows:

1. 95 ˚C, 5 minutes – extended denaturing step for the addition of the polymerase
2. 95 ˚C, 30 seconds – denaturing the double stranded DNA template
3. 58 ˚C, 30 seconds – primer hybridisation (annealing)
4. 73 ˚C, 2 minutes – elongation: synthesis of the new DNA strands

[Steps 2-4 were run 40 times]

5. 73 ˚C, 10 minutes – final synthesis phase
6. 4 ˚C, cooling until removal

After completion of the PCR, the reaction mixtures were purified using a commercially available PCR product purification kit (such as High Pure PCR Product Purification Kit, Roche) according to the manufacturer's instructions and dissolved in deionised water. The concentration of the DNA was then estimated by applying 1 µl and 2 µl samples to a 1 % agarose gel alongside varying volumes of DNA Ladder (1 µl, 2 µl, 5 µl, and 10 µl).

3.1.4 *In vitro* transcription

The RNA probes used for *in situ* hybridisation were obtained by means of the RNA polymerase of bacteriophage T3 (sense probe) or T7 (antisense probe). The starting material used was a purified DNA fragment, amplified by PCR, containing the desired sequence of the probe, which was flanked by a T3 and T7 promoter.

The reaction mixture for the *in vitro* transcription contained 4-6 $ng \cdot \mu l^{-1}$ DNA template as a starting material, $^{1}/_{10}$ volume 10× transcription buffer, $^{1}/_{10}$ volume 10× digoxigenin-nucleoside triphosphate (NTP) mix, 0.9 $U \cdot \mu l^{-1}$ Ribolock RNase inhibitor and 0.9 $U \cdot \mu l^{-1}$ RNA polymerase. Due to the large quantity of RNA probe required, reaction mixtures of 500 µl were used, resulting in a yield of about 200 – 250 µg RNA probe.

The *in vitro* transcription was performed at 37 ˚C for 3.5 hours. Then $^{1}/_{25}$ volume Turbo DNase (2 $U \cdot \mu l^{-1}$) was added and incubated for 30 minutes at 37 ˚C to degrade the DNA starting material. To precipitate the RNA probe ¼ volume of ammonium acetate (final concentration: 2 M) was added and then ethanol to a final concentration of 70 %. The precipitation was carried out either for 12 hours at -20 ˚C, or for 1 hour at -80 ˚C. The RNA probe was precipitated by centrifugation for 30 minutes at 20,000 *g* and 4 ˚C. The precipitate was washed using twice the original volume of 80 % ethanol and centrifugation for 20 minutes at 20,000 *g* and 4 ˚C. After removing the supernatant, the precipitate dried

in the open air and was then dissolved in the original volume of water. Then the precipitation was repeated and the dried precipitate was dissolved once again in the original volume of water. The quality and concentration of the probes was determined by investigating one aliquot was using agarose gel electrophoresis and UV spectrometry, which determined the quotient of optical density (OD) at four different wave lengths. The optical density of a nucleic acid solution depends on the pH of the solution and thus of the solvent (Wilfinger et al., 1997). The values given here refer to pure water as a solvent. An OD ratio at the wavelengths 260 and 280 (OD_{260}/OD_{280}) of less than 1.85 points in RNA dissolved in water indicates contamination by proteins. An OD_{260}/OD_{230} value less than 2 indicates contamination by dithiothreitol, phenol, salts, or carbohydrates. An OD260/OD270 value provides further evidence of contamination with phenol, which has an absorption maximum near 270 nm. For our purposes this value should be around 1.2. Probe concentrations were adjusted to 400–500 $ng \cdot \mu l^{-1}$ for use in the *in situ* hybridisation protocol. The RNA probes were then stored at -80 ˚C until further use.

3.2 Preparation of the neuropeptide probes

In order to maximise the likelihood of observing neuropeptide RNA co-expressed in *Arc*-expressing neurons, a range of candidate genes were selected. First, a long-list of genes was created based on data observed in the PbN using the Allen Brain Atlas gene search tool (http://mouse.brain-map.org/), the five genes selected for this experiment were chosen based on their known taste- or food-related functions or for their expression pattern in the PbN appearing in similar areas to *Arc*-expression. Five probes were selected and primers were designed based on the probes used in the Allen Brain Atlas. These included calcitonin-related polypeptide alpha, the gene product encoding for calcitonin, (Calca) (probe number: RP_071204_02_D02), glucagon-like peptide 1 receptor (Glp-1r) (probe number: RP_051130_01_A07), hypocretin receptor 1 (Hcrtr1) (probe number: RP_070129_02_E06), gastrin-releasing peptide (Grp) (probe number: RP_071204_04_F07), and neurotensin (Nts) (probe number: RP_051213_01_A07). Each primer was designed to have specific sequences attached that are recognised by restriction enzymes for subsequent cloning into a plasmid (reference to table with primer sequences).

Following the same RNA extraction and cDNA synthesis steps used for the *Arc* probes (see sections 3.1.1 and 3.1.2, respectively) a different approach was used to produce the subsequent probes. The DNA was cloned into plasmid vectors and inserted into

Escherichia coli (E. coli) host cells, as this allows long-term storage and easy amplification of probes for future experiments.

This process involves amplification of the probe sequence of the selected neuropeptides by reverse-transcriptase polymerase chain reaction (RT-PCR) to create the DNA insert. This was then followed by preparation of a cloning vector and DNA insert by using restriction enzymes to generate complementary ends. The prepared DNA insert was then ligated into the prepared vector. At this point chemically competent E. coli bacteria were transformed using the plasmids containing the sequence for the RNA probes. After checking for the right sequences, the transformed E. coli were either stored at -80 °C after adding glycerol or taken to amplify the plasmid DNA, which was then harvested and used in the next *in vitro* transcription step.

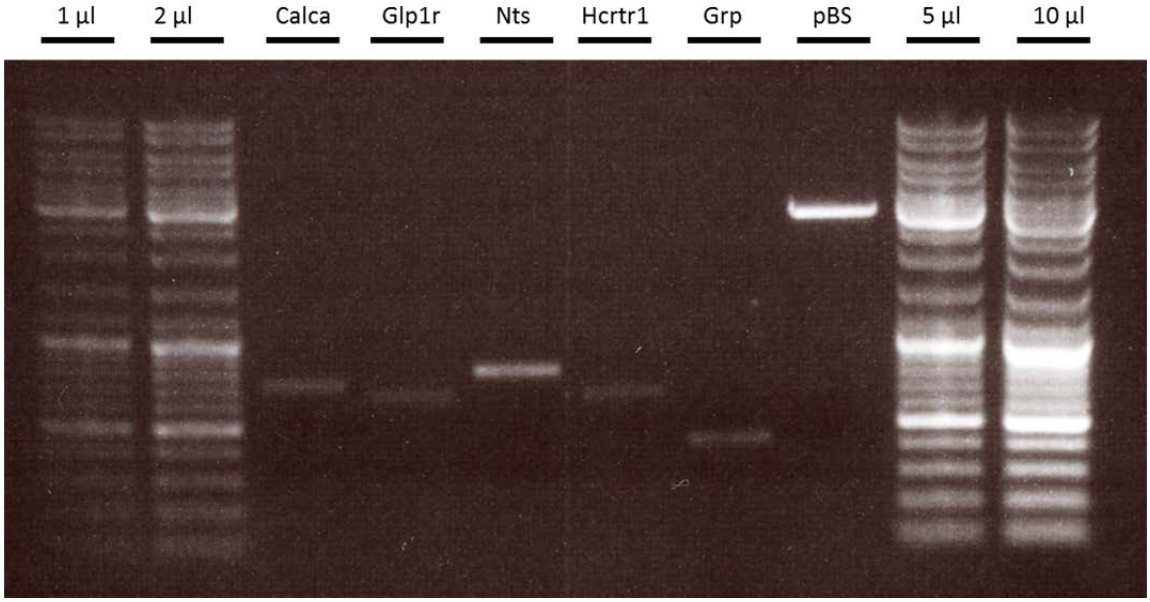

Figure 3.1 Gel photograph of the purified PCR products and linearised plasmid vector they were cloned into.
Calca: calcitonin, Glp1r: glucagon-like peptide 1 receptor, Nts: neurotensin, Hcrtr1: hypocretin receptor 1, Grp: Gastrin-relesing peptide, pBS: linearised pBluescript KS+ vector.

3.2.1 Isolation of the DNA fragments

The DNA was amplified by RT-PCR using the specially designed primers for each neuropeptide (see Table 2.6, page 21). The reaction volumes were 50 µl. The PCR approach for each of the candidate genes is summarised below, the polymerase was always prepared separately with polymerase buffer and water and cooled on ice until added manually for the first step of the PCR. The PCR products were then agarose gel extracted and purified.

3.2.1.1 Glucagon-like peptide 1 receptor and gastrin-releasing peptide

25 µl	Deionized and UV irradiated water
5 µl	10× Polymerase buffer
2 µl	dNTP mix (2.5 mM each)
1 µl	Forward primer (10 µM)
1 µl	Reverse primer (10 µM)
5 µl	10× PCR Enhancer Solution
1 µl	cDNA template
40 µl	

8.5 µl	Deionized and UV irradiated water
1 µl	10× Polymerase buffer
0.5 µl	Pfu-Polymerase (2-3 U·µl-1)
10 µl	

The sequence of the PCR program for the amplification of the template for the Glp1r and Grp probes was as follows:

1. 95 ˚C, 1:30 minutes – extended denaturing step for the addition of the polymerase
2. 95 ˚C, 30 seconds – denaturing the double stranded DNA template
3. 58 ˚C, 30 seconds – primer hybridisation (annealing)
4. 72 ˚C, 2 minutes – elongation: synthesis of the new DNA strands

[Steps 2-4 were run 35 times]

5. 72 ˚C, 5 minutes – final synthesis phase
6. 4 ˚C, cooling until removal

3.2.1.2 Hypocretin receptor 1

23 µl	Deionized and UV irradiated water
4 µl	10× Polymerase buffer
4 µl	dNTP mix (2.5 mM each)
1 µl	Forward primer (10 µM)
1 µl	Reverse primer (10 µM)
1 µl	MgSO4 5 µM
5 µl	10× PCR Enhancer Solution
1 µl	cDNA template
40 µl	

8 µl	Deionized and UV irradiated water
1 µl	10× Polymerase buffer
1 µl	*Pfu*-Ultra Polymerase (2-3 U·µl^{-1})
10 µl	

The sequence of the PCR program for the amplification of the template for the hypocretin receptor 1 probe was as follows:

1. 95 ˚C, 2 minutes – extended denaturing step for the addition of the polymerase
2. 95 ˚C, 30 seconds – denaturing the double stranded DNA template
3. 60 ˚C, 30 seconds – primer hybridisation (annealing)
4. 72 ˚C, 1 minute – elongation: synthesis of the new DNA strands

[Steps 2-4 were run 35 times]

5. 72 ˚C, 10 minutes – final synthesis phase
6. 4 ˚C, cooling until removal

3.2.1.3 Neurotensin

29 µl	Deionized and UV irradiated water
4 µl	10× Polymerase buffer
4 µl	dNTP mix (2.5 mM each)
1 µl	Forward primer (10 µM)
1 µl	Reverse primer (10 µM)
1 µl	cDNA template
40 µl	

8 µl	Deionized and UV irradiated water
1 µl	10× Polymerase buffer
1 µl	Advantage Taq 2-Polymerase (2-3 $U \cdot \mu l^{-1}$)
10 µl	

The sequence of the PCR program for the amplification of the template for the neurotensin probe was as follows:

1. 95 ˚C, 1 minute – extended denaturing step for the addition of the polymerase
2. 95 ˚C, 30 seconds – denaturing the double stranded DNA template
3. 68 ˚C, 30 seconds – primer hybridisation (annealing)
4. 68 ˚C, 1 minute – elongation: synthesis of the new DNA strands

[Steps 2-4 were run 35 times]

5. 68 ˚C, 5 minutes – final synthesis phase
6. 4 ˚C, cooling until removal

Following the PCR, the neurotensin PCR product continued directly to the *in vitro* transcription step (section 3.2.7, page 35) as the primers included promotors for T3/T7 polymerase and cloning was not necessary.

3.2.2 Problems with probe generation

Despite trying multiple primer pair combinations and various commercially available polymerases, isolation and amplification of the Calca primers by PCR was unsuccessful. Instead, the DNA sequence containing the information for the Calca probe was synthesised by Eurofins Genomics. The DNA sequence was delivered in the vector pEX-A2, and was then sub-cloned into our pBluescript KS+ vector. These problems may have been due to a repetitive sequence in the gene.

Unlike the other neuropeptide probes, the neurotensin probe was generated using the same method as for the *Arc* probe generation due to problems during ligation and transformation steps. The neurotensin primers were redesigned flanked with T3 and T7 promoters and prepared using the same method as described for the *Arc* probe.

3.2.3 Restriction digest

For cloning the PCR fragments into the pBluescript KS+ vector, the PCR fragments and the target vector were digested using restriction enzymes NotI and SalI (Fermentas, St.-Leon-Rot). The target vector was also dephosphorylated to prevent re-ligation. This was carried out using a commercially available kit as per the manufacturer's instructions (Roche - Rapid DNA Dephos & Ligation Kit, Sigma-Aldrich; Ref. 04898117001). Restriction digests were performed using the following 20 µl reaction recipe:

DNA	5 µl
10x Restriction Enzyme Buffer	2 µl
H_2O	12.5 µl
Restriction Enzymes	0.5 µl (0.25 µl NotI + 0.25 µl SalI)
	20 µl

Mix, spin down, and incubate for 2 hours at 37 °C

The results of the digest were checked via agarose gel electrophoresis.

3.2.4 Vector dephosphorylation

Linearised vector DNA	17 µl
rAPid Alkaline Phosphatase 10x Buffer	2 µl
rAPid Alkaline Phosphatase Enzyme	1 µl

Incubate at 37 °C for 30 minutes
Incubate at 75 °C for 2 minutes
Immediately cool on ice.

3.2.5 Ligation

The PCR fragment was ligated into the linearized dephosphorylated vector using the Rapid DNA Dephos & Ligation Kit (Roche/Sigma-Aldrich, Ref. 04 898 117 001) as indicated by the manufacturer, ensuring the molar ratio of vector:insert was ~1:3 with a maximum of 200 ng of DNA. The vector, insert, DNA dilution buffer, and water was combined into a 10 µl volume reaction and mixed before the addition of 10 µl DNA Ligation Buffer and 1 µl T4 DNA Ligase; this reaction was incubated at room temperature for 10 minutes. The resulting plasmids contained the DNA information for the chosen RNA probes.

3.2.6 Transformation

The plasmid DNA was then introduced into a bacteria host cell using the One Shot® TOP10 Chemically Competent *E. coli* kit (Invitrogen, Ref. C404010), as per manufacturer instructions. This process is called transformation.

2 µl of the ligation mixture was added to an aliquotof 50 µl chemically competent *E. coli*, and incubated for 30 minutes on ice. This is followed by a heat shock step, in which the reaction tube was kept at 42 °C for 30 seconds, followed by 2 minutes on ice. Then 250 µl of room temperature super optimal broth with catabolite repression (S.O.C., provided by the manufacturer of the One Shot® TOP10 kit) was added to the tube followed by one hour at 37 °C, shaking.

30 µl and 100 µl samples were then plated on Ampicillin Agar plates and incubated overnight at 37 °C. Approximately 10 colonies were selected the following day and used to inoculate 3 ml of lysogeny broth (LB) medium containing Ampicillin. After approximately 16 hours of incubation at 37 °C, plasmid DNA was purified using a commercially available plasmid preparation kit (Qiagen, Hilden). Control digests were performed to check the plasmids and 2-3 candidate samples were chosen for sequencing (Eurofins Genomics). Once the correct sequences were confirmed a larger scale plasmid preparation was carried out using a commercially available midiprep-kit (Qiagen, Hilden) as per the manufacturer's instructions to gain a sufficient amount of plasmid DNA.

3.2.7 In vitro transcription

For in vitro transcription the plasmid DNA was linearised using the restriction enzymes NotI (antisense) or SalI (sense) (Fermentas, St.-Leon-Rot) and purified by gel electrophoresis. The restriction digest protocol can be found in section 3.2.3 on page 33.

The *in vitro* transcription protocol was identical as for the *Arc* probes (as described in section 3.1.4 on page 28) with one exception: Fluorescein RNA labelling mix (Roche via Sigma-Aldrich) was used to generate probes that were labelled with fluorescein instead of digoxigenin.

3.3 Stimulation and tissue sampling

The animal stimulation experiments were performed within the animal facilities of the German Institute of Human Nutrition (Max Rubner Laboratory). The experiments were performed in accordance with the German animal protection law and were approved by the Brandenburg State Office for Environment, Health, and Consumer Protection in animal experiment applications with the reference numbers: 23-2347-8-10-2008, 23-2347-21-2014, and 23-2347-2-2016. The tests took place in the morning between 9:00 am and 1:00 pm. Food and water bottles were removed from the cage approximately an hour before the start of experiments to avoid confounding taste stimulation.

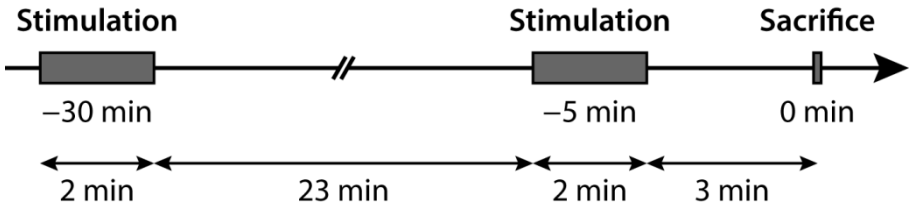

Figure 3.2 The taste-stimulation protocol
Image from Dr. Jonas Töle (DIfE, Nuthetal).

For the stimulation the animals were individually removed from the cage and restrained by holding the scruff of the neck and the tail. Each animal received 1-2 ml of taste stimuli over a two minute period. The tastant was administered equally throughout the oral cavity by means of a gastric gavage needle attached to a syringe. Distribution of the tastant throughout the oral cavity was also aided by tongue and jaw movements occurring in response to the stimulation. Generally the animals remained calm during the stimulation, with a small increase in activity in the last 30-60 seconds of stimulation.

After the first stimulation, the mice were placed into an empty cage to prevent other animals coming into contact with the taste solution left around the animal's mouth and on their fur. This isolation also facilitated the observation of the animals after stimulation. Depending on the protocol, the animal would then either wait 3 minutes until being sacrificed or they would wait 23 minutes for a second, identical stimulation with either the same or a different taste stimulus, after which they would wait 3 minutes until sacrifice. The sacrifice of the animals was carried out by decapitation. Subsequently, the brain was rapidly removed by dissection of the skull, placed in a square, plastic shell, and coated with embedding medium, then frozen in 2-methylbutane chilled over dry ice. The sacrifice and removal of the brain usually took less than two minutes. The tissue was then stored at -80 ˚C until further use.

3.4 Preparation of tissue sections

The mouse brains were sliced into 14 µm thick horizontal sections using a cryomicrotome at -12 ˚C. Each glass microscope slide held four brain-tissue sections. The tissue sections were organised in a series of six slides so that each slide had four brain slices that were 6 slices apart. For example, the slide 001 would have the first, seventh, thirteenth, and nineteenth slices (see **Figure 3.3**).

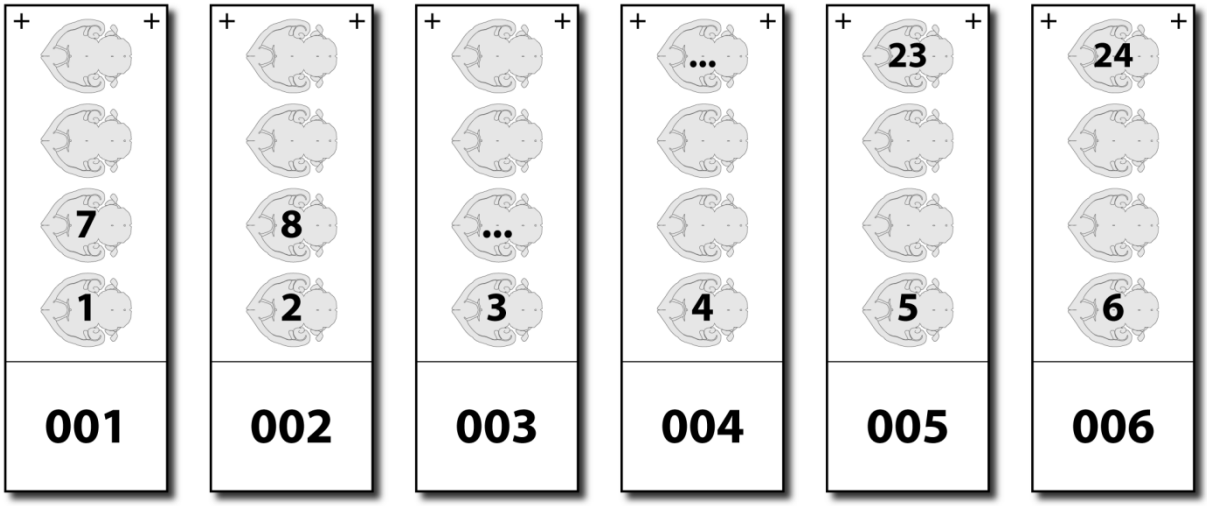

Figure 3.3 The sequence of brain-slice placement during collection.
This images shows a series of six slides (001 - 006) which hold the first 24 brain slices. Image from Dr. Jonas Töle (DIfE, Nuthetal).

During slicing, a mouse brain atlas (Franklin & Paxinos, 2007) was used for orientation. Brains were cut from dorsal to ventral and sections were collected from the point at which a breakthrough between the cerebellum and the pons (the superior cerebellar peduncule) was visible (Fig. 152 in Franklin & Paxinos, 2007). This occurs just before the

appearance of the parabrachial nucleus. From here, the sections were continuously collected until the end of the ventral hypothalamus was reached. At this point, there were only a few brain areas, predominantly the cerebral cortex, left uncollected. Typically, one mouse brain resulted in twelve series, providing 72 slides holding 288 brain slice sections.

After mounting, the slides were allowed to dry, and were then frozen in the cryomicrotome. Upon completion of the slicing process, a silica gel dryer packet was placed into the slide boxes which were then hermetically sealed with electrical insulation tape and stored at -80 ˚C until further use.

3.5 *In situ* hybridisation

3.5.1 Pre-treatment of tissue sections

The pre-treatment of brain sections, consisting of fixation and acetylation, was carried out in an automatic stainer. The slides were thawed in their airtight containers at 37 ˚C to prevent condensation of water on the slides. Subsequently, the slides were arranged in a metal frame and placed into the stainer, which automatically immerses the slides into the appropriate solutions (the program for the automatic stainer can be found in the Appendix, section, page 99). First, the fixation of the tissue was performed by incubating the slides for 10 minutes in 4 % PFA in PBS (the composition of the solutions can be found in section 2.8.2 on page 22). Subsequently, the slides were washed twice, for two minutes each time in 0.9 % NaCl solution. After the washing step the program was interrupted and the Acetylation step was performed manually in a staining trough. For this purpose, 1.875 ml of acetic anhydride was added to 750 ml of triethanolamine buffer. A magnetic stirrer was used to mix the buffer and the acetic anhydride; it continued to stir throughout the acetylation step. Immediately after the Acetic anhydride was pipetted into the triethanolamine buffer, the metal frame holding the slides was then immersed and removed from the buffer ten times in quick succession before being left to sit in the solution. After five minutes, the procedure was repeated again by adding an additional 1.875 ml of acetic anhydride to the buffer, and immersing and removing the slides from the buffer ten times before leaving them to sit in the solution. After an additional 5 minutes immersed in the solution the slides were brought back to the automatic stainer to continue the program. After a two minute wash in PBS and then 0.9% NaCl solution, the dehydration of the sections was carried out in an ascending series of alcohol solutions (30 %, 50 %, 70 %, 80

%, 95 %, 100 %, 100 %, for 2 minutes each). After the slides had dried, they were stored in an airtight container at -80 ˚C again, until further use.

3.5.2 Carrying out the *in situ* hybridisation

The actual *in situ* hybridisation was carried out using a pipetting robot, which performs pipetting operations automatically. The Tecan Freedom EVO platform is based on a liquid-filled pipetting system, which allows precise pipetting. After each pipetting operation the tube system was flushed with the system liquid (deionised water) to prevent cross-contamination. Reagents were added to the reservoirs on the working surface table of the machine as needed at specific time-points throughout the program. In addition to plastic containers of different volumes, there were also four heated glass containers for the solutions used in the stringency washing steps. The arrangement of the reagent vessels can be found in the Appendix (page 100).

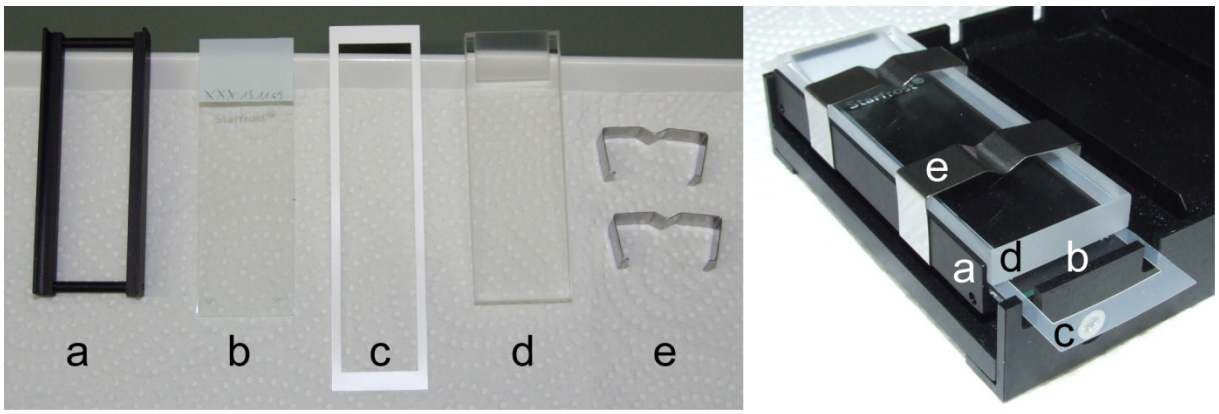

Figure 3.4 The components of the flow-through chambers and their arrangement during the *in situ* hybridisation.
a: metal frame, **b:** microscope slide, **c:** spacer, **d:** glass block with a wedge-shaped reservoir at the upper end, **e:** retaining clips. Image from Dr. Jonas Töle (DIfE, Nuthetal).

Slides were fastened into the flow-through chambers; the components of a flow-through chamber are shown in **Figure 3.4**. To this end slides were thawed in their airtight containers at 37 ˚C. Slides (b) with the tissue sections facing up were placed on a metal frame (a), covered by a glass block (d), and fastened together with retaining brackets (e). The slide and the glass block were separated by a very thin spacer (c) at the very edge of the glass block down the long edge creating a space between the slide and the glass block that could hold a volume of approximately 90 µl. This cavity was open along the short edges of the glass block, allowing inflow and outflow of the solutions. Along the short upper-edge of the glass block, there was a wedge-shaped cavity. The glass blocks and

slides were placed together so that this diagonal cut-out formed a wedge-shaped reservoir between the slide and the glass block. This reservoir could hold approximately 570 µl, and this is where the solutions were pipetted into. The solutions pipetted into the reservoir would then flow down the cavity between the glass block and the slide, wetting the brain tissue on the slides, and then flowing out of the cavity, being collected in the bottom of the flow chambers.

In the first step, 0.6 % hydrogen peroxide in methanol was applied to the slides to inhibit endogenous peroxidase. Beginning the process with methanol also facilitated the first liquid treatment of the tissue sections, since it has a much lower surface tension than water. Subsequently, 0.2 M hydrochloric acid was applied to permeabilise the cells. After equilibration with proteinase K buffer, 0.0159 $U \cdot ml^{-1}$ proteinase K was added to proteolytically degrade the tissue. Then slides were incubated in 4 % PFA in PBS to stop the proteinase K digestion and fix the tissue again. Next, equilibration was performed with hybridisation buffer, during this step the temperature of the slides was increased to 64 ˚C within approximately 15 minutes. Once the hybridisation temperature was reached, RNA probe dissolved in hybridisation buffer at a final concentration of 600 $ng \cdot ml^{-1}$ was added to the slides. This step has repeated three hours into the six-hour incubation period. During the prehybridisation steps, the tissue samples were rinsed with PBS between each step. All of the aqueous solutions, with the exception of the hybridisation buffer, contained 0.05 % Tween 20 in order to reduce the surface tension of the solutions. The hybridisation buffer as well as the RNA probe dissolved in hybridisation buffer were both incubated for 10 minutes at 65 ˚C and then cooled rapidly on ice before deployment in the pipetting robot.

Following the hybridisation, the stringency washing steps were carried out to remove any excess or non-specifically bound RNA probe. The temperature of the slide was lowered to 62 ˚C and the wash solutions were preheated to 62 ˚C. The first washing step was performed using 5× saline-sodium citrate (SSC), followed by 2× SCC in 50 % formamide, 1× SCC in 50 % formamide, and finally with 0.1× SSC. During the last washing step the temperature of the slide was lowered to 24 ˚C.

Then, 20 mM iodoacetamide in NaCl-Tris-EDTA (NTE) buffer was added to alkylate sulfhydryl groups. Then, epitope masking was carried out by treating the tissue sections sequentially with 4 % lamb serum in Tris-sodium chloride buffer (TN), TN with blocking reagent (TNB), and 0.5 % blocking reagent in maleate wash buffer (MWB).

This was followed by the addition of anti-digoxigenin antibody conjugated with horseradish peroxidase in TNB. In the subsequent amplification step, the peroxidase

caused the Tyramide Biotin dissolved in Amplification Diluent to react and bind to the tissue. Finally, the fluorescent dyes were added to the slides: Avidin-Cy3 conjugate to detect the biotin residues of the tyramide biotin and 4',6-Diamidinie-2'-phenylindole dihydrochloride (DAPI) as nuclear counterstaining. The slides were then rinsed with deionised water.

Between the steps following the stringency wash steps, the tissue was washed in each case with TN. When solutions were made with a buffer other than TN, for example MWB or NTE, after the TN washing step the tissue was washed with its corresponding buffer before and after the addition of the solution, followed by an additional TN washing step.

Upon completion of the TECAN program the flow chambers were disassembled and the stained sections were covered using a mounting medium optimised for fluorescent dyes. They were then stored at 4 ˚C, in a dark dry room, until further use.

3.6 Changes involved in double FISH protocol

In the subsequent double fluorescent *in situ* hybridisation (FISH) the TECAN machine followed a similar program except that there was no addition of iodoacetamide and there were also three additional steps which occurred after the application of the Tyramide Biotin dissolved in Amplification Diluent (TSA) and before the addition of the fluorescent dyes (for an overview of both the single and double FISH protocols, see Appendix, Table A.2, page 101 and Table A.3, page 103).

The initial TSA step was followed by application of 0.05 M hydrogen chloride (HCl) to the slides to inactivate the peroxidase coupled to the first antibody. This was then followed by the addition of anti-fluorescein antibody conjugated with peroxidase in TNB, then fluorescein tyramide diluted in Amplification buffer. No further conjugate was necessary. Following these steps the program progressed as described in the previous section, moving onto the addition of the fluorescent dyes.

3.7 Evaluation

Experiments were evaluated by digitising the stained brain sections, allowing the identification of the relevant brain regions and the quantification of *Arc* expression using an image-processing program.

3.7.1 Digitisation of tissue sections

Once the mounting medium on the slides had dried enough to ensure sufficient adhesion of the cover slips to the slides, an automated fluorescence microscope (Mirax Midi, Zeiss) digitised the slides using a short-arc mercury lamp as a light-source. Fluorescent dyes were detected using the Zeiss filter sets 43 (excitation filter: central wavelength 545 nm usable bandwidth of 25 nm, beam splitter 570 nm, emission filter: central wavelength 605 nm usable bandwidth of 70 nm), 49 (excitation filter: 365 nm, beam splitter: 395 nm, emission filter: 445 nm usable bandwidth 50 nm), and 44 (excitation filter: central wavelength 475 nm usable bandwidth of 40 nm, beam splitter 500 nm, emission filter: central wavelength 530 nm usable bandwidth of 50 nm).

At each frame, seven images were taken around the autofocus level, evenly spaced 1 µm apart. The imaging software then carried out a process similar to deconvolution, combining the image information of the seven levels into one plane. The algorithms that underlie this process are integrated in the microscope software and are not described by the manufacturer exactly. The individual images were finally combined into a large two-dimensional image and saved to disk. Relevant areas were exported as a TIF file for analysis.

3.7.2 Counting of *Arc*-expressing neurons

The TIF files were then uploaded into Adobe Photoshop for quantification and a mouse brain atlas was used as a guide to locate the PbN (Franklin & Paxinos, 2007). The outline of the PbN was determined using surrounding anatomical landmarks and the Cy3 channel as a guide. Surrounding anatomical landmarks used for identification of the PbN included: the 4th ventricle, lobules 2 and 3 of the cerebellar vermis, the superior cerebellar peduncle (SCP), the dorsal nucleus of the lateral lemniscus, and the vestibular nucleus.

Secondly, any defects in the tissue section, such as tears, creases, or holes caused by air bubbles were outlined. Then the image was analysed at its original magnification and *Arc*-expressing neurons were marked by hand with coloured circles. The circles were colour-coded in order to represent the intracellular distribution of RNA (for examples see **Figure 3.5 G-I**)

After labelling the *Arc*-expressing neurons, the PbN was further subdivided by tracing the centre of the SCP, which transects the PbN with the lateral PbN located lateral to the SCP, and the medial PbN located medial to the SCP (**Figure 3.5 C**).

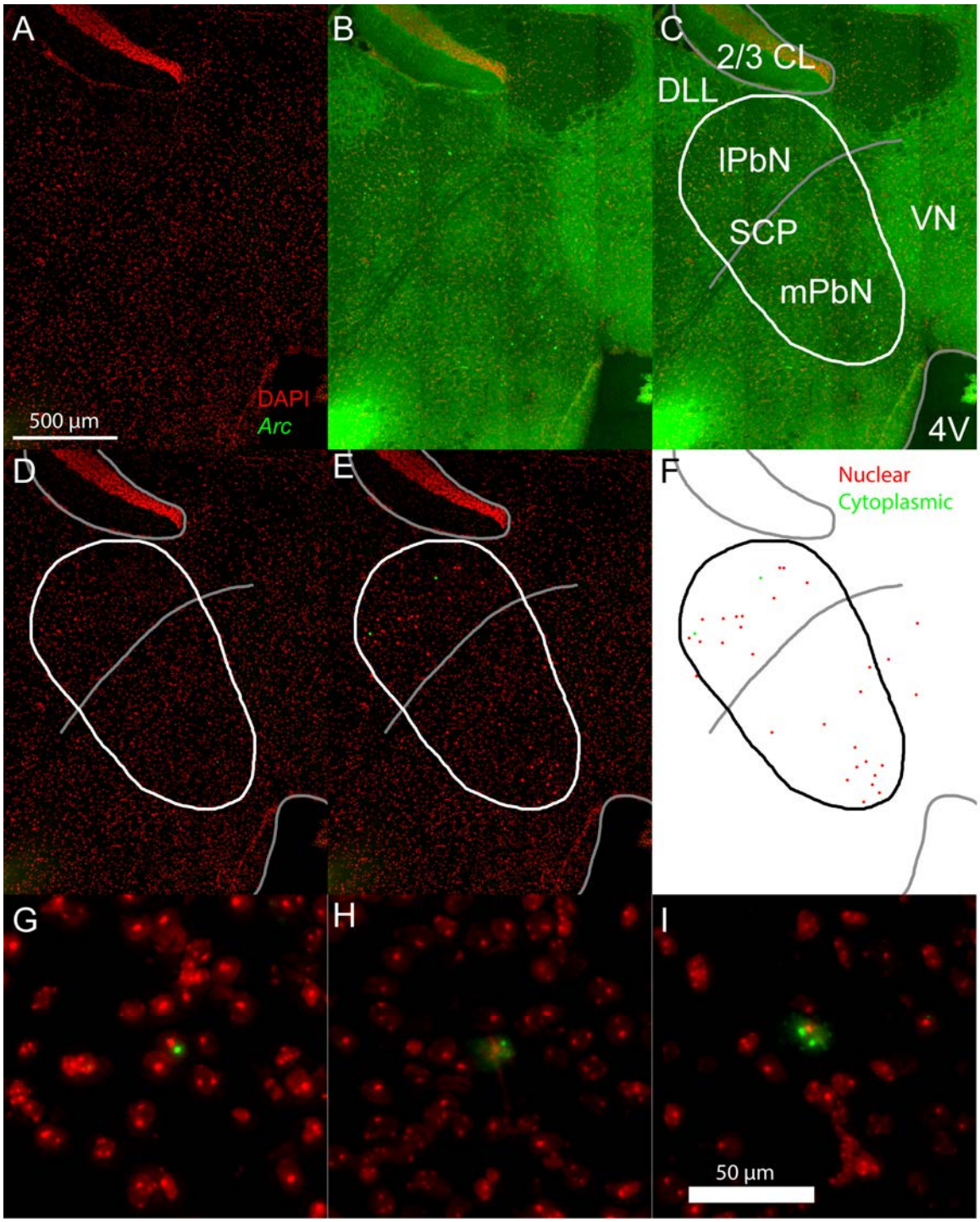

Figure 3.5 Location of the PbN and quantification of *Arc* expression.
A: raw image of the PbN showing cell nuclei (red) and *Arc* RNA (green); **B**: raw image with the Cy3 (*Arc*) channel enhanced to better observe surrounding structures; **C**: The outline of the PbN and SCP with surrounding structures labelled, 2/3 CL: lobules 2 and 3 of the cerebellar vermis, DLL: dorsal nucleus of the lateral lemniscus, lPbN: lateral parabrachial nucleus, SCP: superior cerebellar peduncle (or brachium conjunctivum), mPbN: medial parabrachial nucleus, VN: vestibular nucleus, 4V: fourth ventricle, **D**: the outline of the PbN (white) shown with the Cy3 channel unenhanced, **E**: the PbN with *Arc*-expressing neurons marked according to the intracellular distribution of *Arc* (red: nuclear; green: cytoplasmic), **F**: The outline of the PbN (black) and marks corresponding to *Arc*-expressing neurons, **G**: a cell showing nuclear *Arc* expression, **H**: a cell with cytoplasmic *Arc* expression, **I**: a cell with both nuclear and cytoplasmic *Arc* expression.

Finally, the *Arc*-expressing neurons were counted, for each of the lateral, medial, and whole PbN. In order to compare the results between animals and subdivisions, the density of *Arc* expression was calculated by determining the number of *Arc*-expressing neurons and the area of the relevant subdivision. This produced a number representing the rate of expression (*Arc*-expressing neurons per mm^2 of whole/lateral/medial PbN), allowing the comparison of subdivisions regardless of any difference in size.

The manual analysis was performed in Adobe Photoshop on separate layers, so that the original image remained unaltered. In individual cases, the intracellular distribution of *Arc* RNA was not clearly determined on the digitised section. When this occurred, the corresponding tissue section was examined more closely using fluorescence microscopy.

3.7.3 Statistical analysis

Statistical analysis was performed using the programs Microsoft Excel and SigmaPlot. T-tests and a factorial analysis of variance (ANOVA) were used to test for statistically significant differences between groups. The significance level α was set at 0.05.

3.8 Behavioural training

The animal stimulation experiments were performed within the animal facilities of the German Institute of Human Nutrition (Max Rubner Laboratory). The experiments were performed in accordance with the German animal protection law and were approved by the Brandenburg State Office for Environment, Health, and Consumer Protection in animal experiments application with the reference number 23-2347-2-2016.

For each mouse the behavioural paradigm ran for 15 days from the first training session to the final taste stimulation. An overview of the protocol can be seen in **Figure 3.6** on page 46. Animals were allowed free access to food throughout the behavioural experiments.

3.8.1 Bottle/shutter training

During the first day the animals received a training session (Bottle Training) in which they were introduced to the Davis Rig lickometre testing chamber with a water-spout presented and were allowed 30 minutes of unlimited access to water. The purpose of this training session was for the animals to acclimate to the testing environment and to learn to promptly locate the drinking system.

Over the following two days animals received Shutter Training, which consisted of 30 minutes of either 10-second (Day 1) or 5-second (Day 2) trials of water access. The start of a trial is triggered by the mouse's first lick after the shutter opens. Trials were followed by 7.5-second intervals during which a new water-bottle would be positioned behind the shutter. Trials would end after 60 seconds if a mouse did not initiate licking behaviour, this would also be followed by a 7.5-second break to change to another water-bottle. The purpose of these training sessions is to familiarise the animals with the shutter process and any noises it creates during the actual testing paradigm.

Training sessions were performed in the morning between 8:00 am and 1:00 pm. During the three days of training the animals are kept on an 18-hour water deprivation schedule in order to ensure the animals were motivated to drink.

3.8.2 Baseline short-term preference test

The animals then performed two sessions of short-term preference testing in the lickometre over the following two days. Over a 20-minute testing session animals were presented with numerous different tastants in order to measure their licking-behaviour in response to each taste.

The solutions were presented individually according to a schedule programmed into the computer. Upon the first lick, the mouse triggered a 5-second measurement, after which the shutter closed and remained closed for 7.5-seconds while the next solution is brought into position for the next trial. As in the shutter training sessions, if a mouse should not initiate licking behaviour during a trial the trial ended after 60 seconds, followed by a 7.5-second break during which the bottles move, and then the same tastant was presented for a second trial. If the mouse should not lick the spout for another 60 seconds during the second trial, the trial ended and the next trial started with the next solution. The purpose of this test was to determine the animals' baseline responses to the different tastants presented.

Due to the short time frame in which the animals can respond to the different taste stimuli, it diminishes the possibility for post-ingestive effects to influence the animals' licking behaviour, as can occur in longer-term taste-preference tests. This is especially important when studying bitter tastants, many of which are toxic, and thus have negative post-ingestive effects such as nausea/increased heart rate etc.

Animals were presented with a variety of different solutions including water (6 bottles), sodium glutamate (2 bottles), sucrose (1 bottle), citric acid (1 bottle),

cycloheximide (Cyx) (2 bottles), quinine (2 bottles), papaverin (1 bottle), and sucrose octaacetate (SOA) (1 bottle) (for more information on solutions see Table 2.8 on page 21). The solutions were presented in a random order which was controlled by the Davis Rig software.

Short-term preference tests were performed in the morning between 8:00 am and 1:00 pm. During the three days of training the animals are kept on a 22.5-hour water deprivation schedule in order to ensure the animals were motivated to drink. After their training, animals were given free access to water until their water restriction for the following training session began.

3.8.3 Conditioned taste aversion

The day after the second short-term preference test session the animals had a rest day on which they had free access to water. This was followed by two days on which water access was restricted to twice each day: first from 9:00 am for 30 minutes, and then again in the afternoon from 2:30 pm for another 30 minutes. This resulted in the animals having a 5-hour water restriction during the day, and 18-hour water restriction overnight, ensuring that the animals were motivated to drink during the conditioning session, even if they were presented with a mildly aversive solution.

3.8.4 Post-conditioned taste aversion short-term preference test

The conditioned taste aversion (CTA) session took place in the animal's home cage, at 9:00 am animals were given 15 minutes access to a tastant (either umami or a mild concentration of cycloheximide, for more details see Table 2.8 on page 21. Another 15 minutes after the tastant had been taken away (approximately 9:30 am) the mice received a 20 ml/kg intraperitoneal injection of either 150 mmol/l Lithium Chloride (LiCl) - which leads to malaise and is well established to produce conditioned taste aversion (John et al., 2005) - or 150 mmol/l Sodium Chloride (NaCl, which triggers no discomfort other than the actual injection process and is thus considered an adequate control substance for this paradigm). After the CTA session the animals were given free access to water and were monitored for 3-6 hours to ensure no unexpected adverse side-effects occurred. The following day the animals received no intervention to allow the animals to recover.

The animals then performed two additional sessions of short-term preference testing in the Davis Rig over the following two days. The testing sessions were performed exactly

as the first two sessions in order to determine if the CTA session resulted in any changes in licking behaviour.

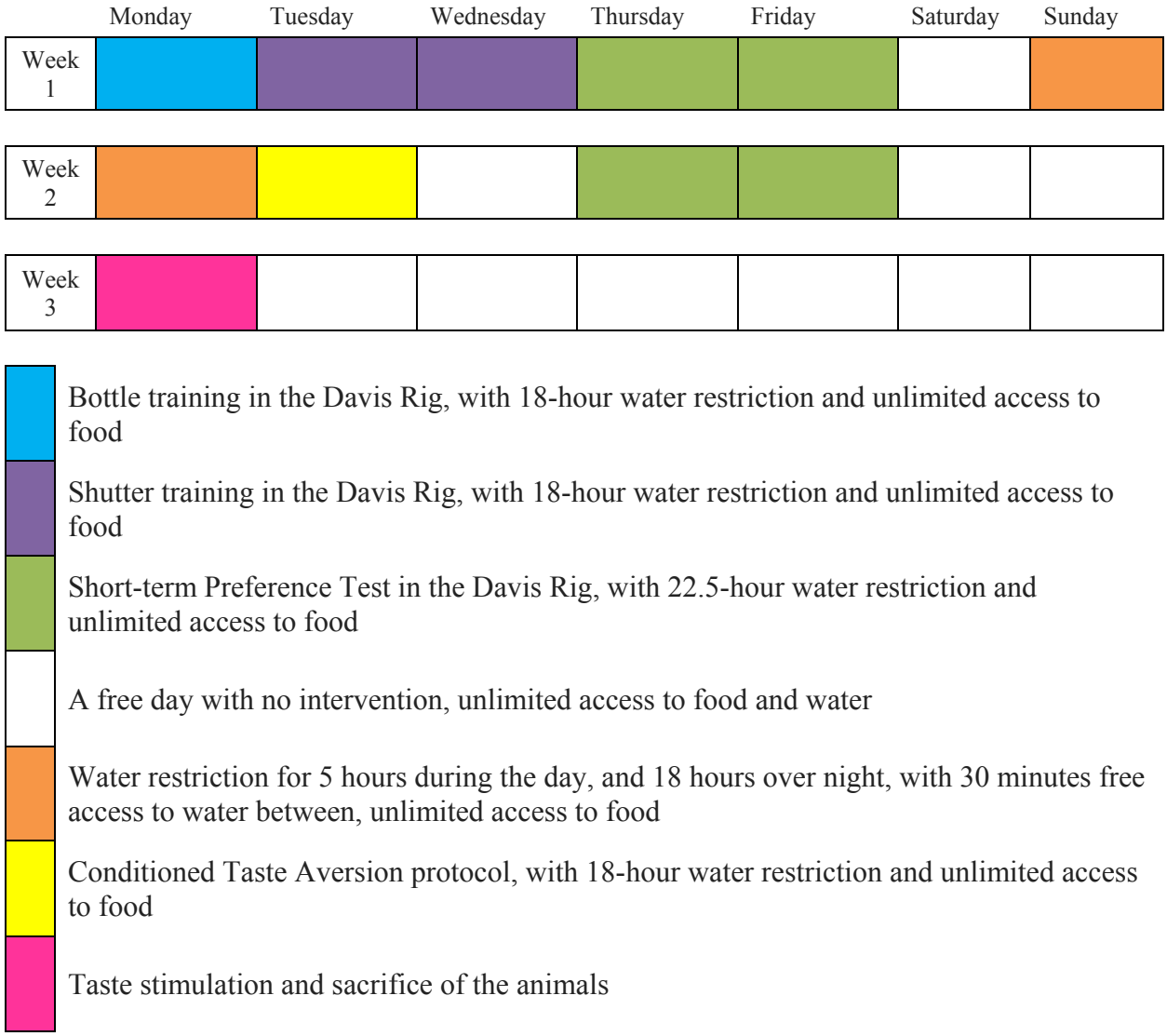

Figure 3.6. Behavioural protocol schedule

3.8.5 Oral stimulation and tissue sampling for *Arc* analysis

For the oral stimulation procedure the CTA animal groups (Umami-LiCl, Umami-NaCl, Cyx-LiCl, and Cyx-NaCl) were each randomly divided in two, and half of the subjects received a control saliva-like stimulus, and the other half received a stronger concentration of the stimulus they received during the CTA session. The concentrations, oral stimulation, and tissue sampling were identical to the stimulation protocol used in section 3.3 (page 35). Five minutes after stimulus onset the animals were sacrificed.

The tissue collected was then prepared, treated, and analysed as described in the initial *Arc* analysis experiment (for more information see sections 3.4 Preparation of tissue sections on page 36; 3.5 *In situ* hybridisation on page 37; and 3.7 Evaluation on page 40).

3.8.6 Evaluation of short-term taste preference behaviour

The short term taste preference tests were carried out to confirm the successful conditioning of conditioned taste aversions. The licking behaviour measured by the Davis Rig software was collected and within-group comparisons were drawn comparing licking behaviours such as latency until first lick and total number of licks both within and across trials. These were compared before and after CTA training for the relevant stimuli.

Statistical analysis was performed using the programs Microsoft Excel and SigmaPlot. T-tests were used to test for statistically significant differences between lickometre sessions. The significance level α was set at 0.05.

Results

This section presents the results of this work, starting with the investigation of *Arc* expression in the parabrachial nucleus (PbN) after single or double taste stimulation in naïve animals. Then behavioural and neural responses to conditioned taste aversion (CTA) will be reported. Lastly, this section will cover the results gathered while establishing the double fluorescent *in situ* hybridisation (FISH) protocol.

4.1 *Arc* expression in the PbN after single stimulation

Initially, animals were stimulated once, with one tastant, either five or thirty minutes prior to sacrifice. The stimuli used included solutions representing the five basic taste qualities, umami (1 mM monosodium glutamate), sweet (0.5 M saccharose), salty (0.8 M sodium chloride), sour (30 mM citric acid), and three bitter stimuli: 0.5 mM cycloheximide (Cyx), 10 mM quinine hydrochloride (hereinafter quinine, Qui), and 1 mM cucurbitacin I (hereinafter cucurbitacin, Cuc). All stimuli were dissolved in an aqueous solution which consisted of deionised water, 25 mM potassium chloride (KCl), and 2.5 mM sodium bicarbonate ($NaHCO_3$). This solution is tasteless to humans (De Araujo et al., 2003), and was also used in this experiment as an additional control stimulus (control).

Representative results of the *in situ* hybridisation for the detection of *Arc* ribonucleic acid (RNA) are shown in **Figure 4.1** on the next two pages. Among the stimuli used, only the three bitter stimuli (cycloheximide, quinine, and cucurbitacin) resulted in an increase in *Arc* expression in the PbN (p-values: Cyx < 0.01; Qui < 0.01; Cuc = 0.01). Taste stimulation with sweet, salty, sour, or umami tastants did not produce a significant increase in the rate of *Arc*-expressing neurons above that seen in animals stimulated with a control stimulus (p-values: sweet = 0.63 ; salty = 0.42 ; sour = 0.42 ; umami = 1.0). The rate of *Arc*-expressing neurons appeared to be particularly dense in the lateral PbN (see enlarged sections in **Figure 4.1A**). Additionally, the total rate of *Arc*-expressing neurons was consistent across the animals stimulated either 5 minutes, or 30 minutes prior to sacrifice. The cellular distribution of *Arc* also appeared to be consistent with the stimulation time-point, with animals stimulated 30 minutes before sacrifice showing predominantly cytoplasmic *Arc* expression, and animals stimulated 5 minutes prior to sacrifice showed predominantly nuclear staining. **Figure 4.2** shows the rate of *Arc*-expressing neurons seen in the PbN following taste stimulation with each of the tastants, including the distinction between nuclear, cytoplasmic, and *Arc* expression in both compartments.

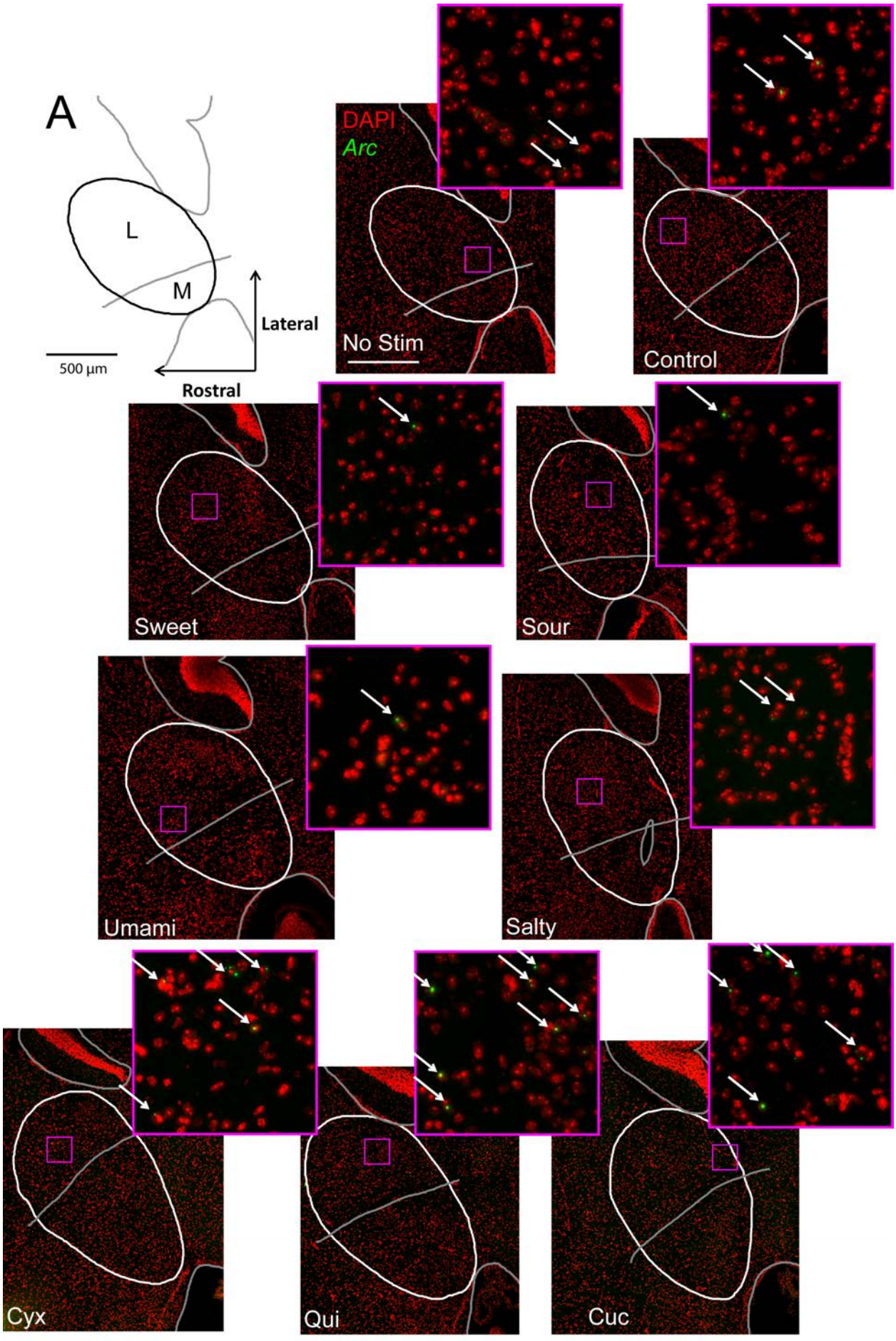
A
L
M
Lateral
Rostral
500 µm
DAPI
Arc
No Stim
Control
Sweet
Sour
Umami
Salty
Cyx
Qui
Cuc

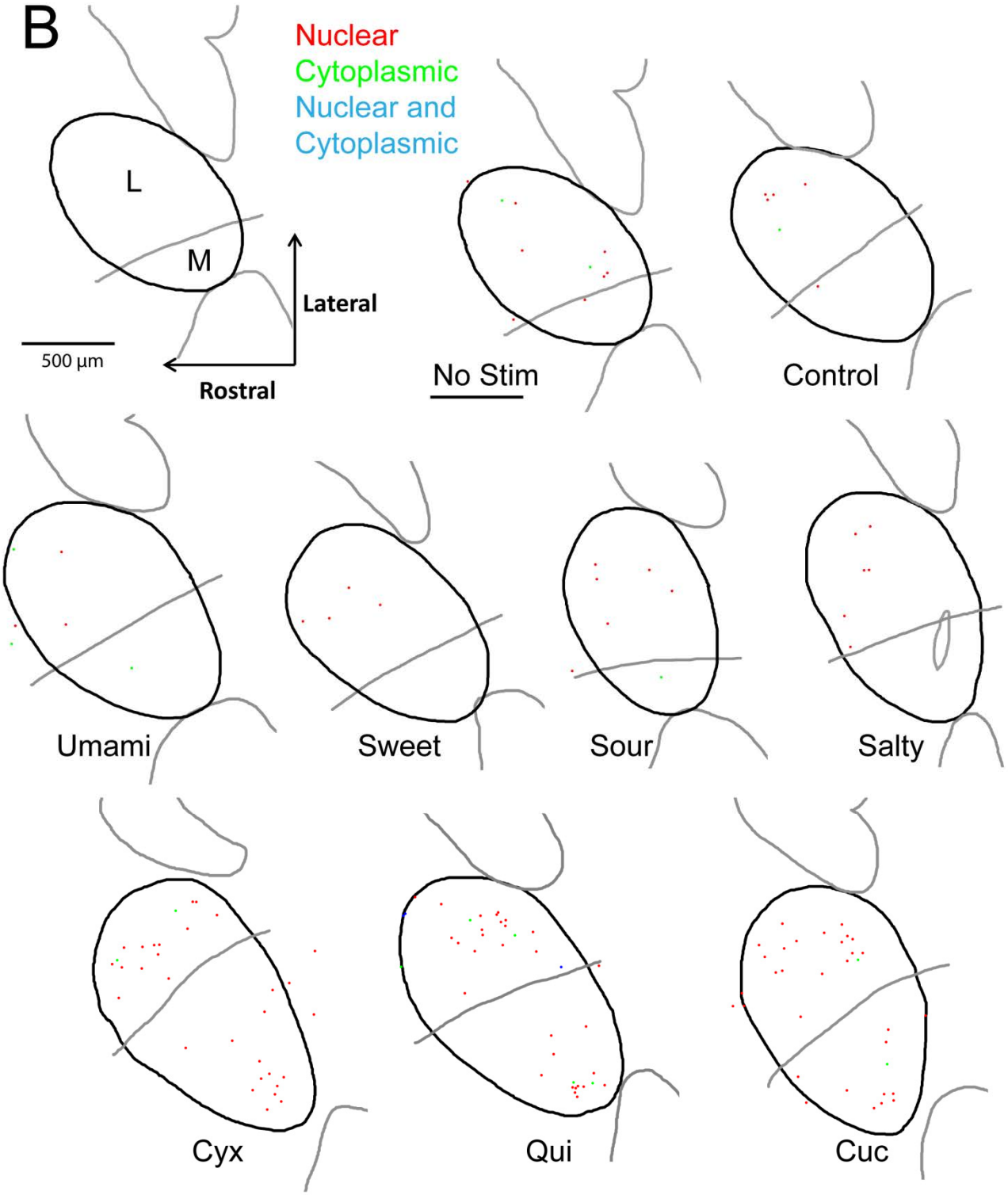

Figure 4.1 *Arc* expression in the PbN after single stimulation in naïve animals.
Examples from animals stimulated 5 minutes prior to sacrifice. **A:** representative results of fluorescent *in situ* hybridisation. The white line marks the outline of the PbN, with a grey line transecting the PbN showing where the superior cerebellar peduncle (brachium conjunctivum) lies. The cell nuclei are labelled with the fluorescent dye DAPI (red), and the *Arc* RNA is shown in green. The cut-outs are 8x magnifications in the lateral PbN. **B:** Representative results of the counting of the sections shown in A. The coloured dots mark neurons expressing *Arc* RNA; red: nuclear, green: cytoplasmic, and blue: nuclear and cytoplasmic localisation of *Arc* RNA.

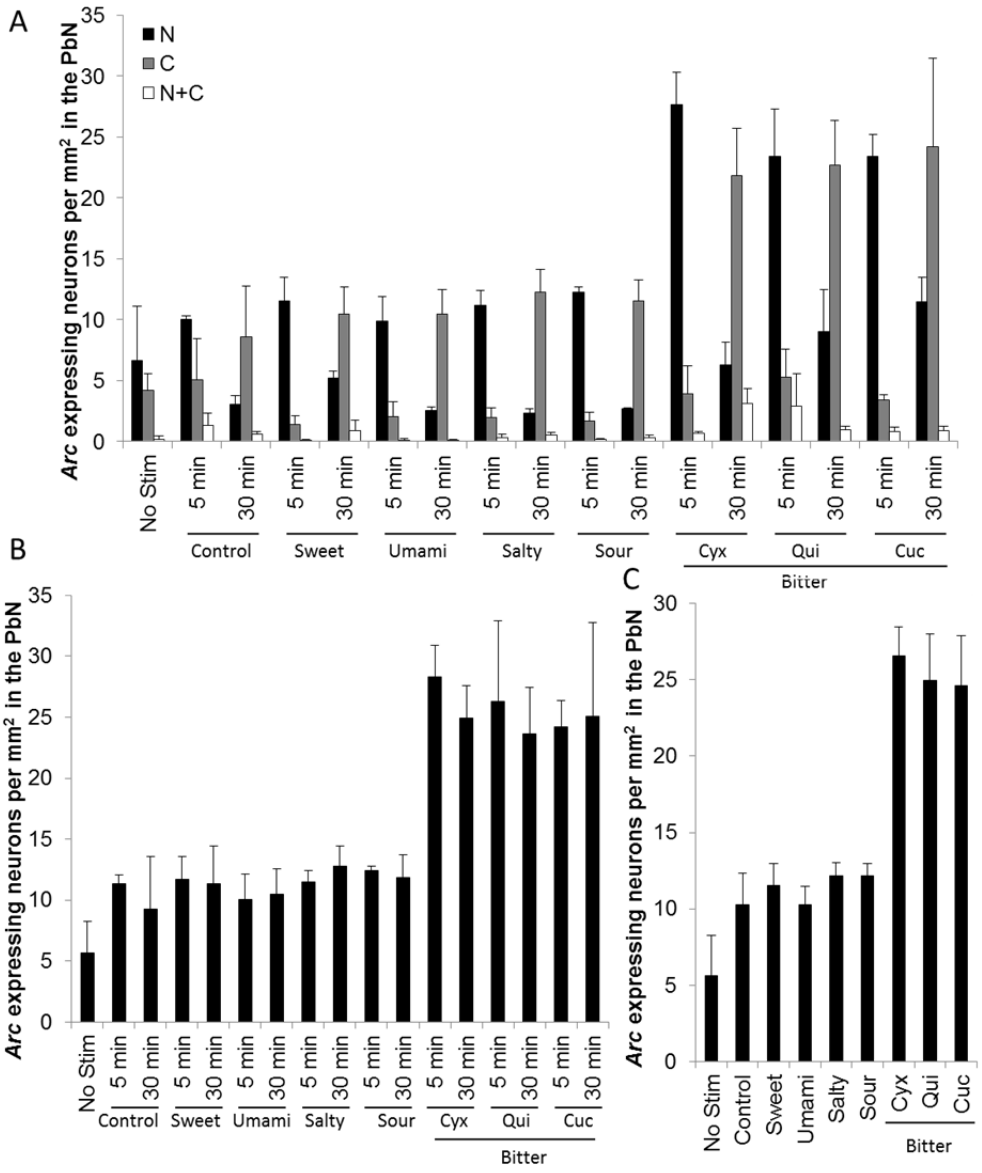

D	No Stim	Control	Umami	Sweet	Salty	Sour	Cyx	Qui
Control	-							
Umami	-	-						
Sweet	-	-	-					
Salty	-	-	-	-				
Sour	-	-	-	-	-			
Cyx	#	#	#	#	#	#		
Qui	#	#	#	#	#	#	-	
Cuc	#	#	#	#	#	#	-	-

Figure 4.2 *Arc* expression in the whole PbN following a single stimulation in naïve animals. **A:** Intracellular distribution of *Arc* RNA; black: nuclear staining (N), grey: cytoplasmic staining (C), and white: both nuclear and cytoplasmic staining (N+C). n = 2-3. **B:** *Arc* expression corresponding to the relevant time-point: neurons which showed *Arc*-RNA in the nucleus in animals stimulated 5 minutes prior to sacrifice, and neurons which showed *Arc*-RNA in the cytoplasm in animals stimulated 30 minutes prior to sacrifice, n = 2-3. **C:** Summarised values of relevant expression of both stimulation time points, n = 3-6. The figures show mean values of the *Arc*-expressing neurons per mm^2 PbN and standard error. **D:** Statistical analysis of the data shown in C**.** The relevant *Arc* expression induced by various stimuli was checked by analysis of variance and subsequent pairwise comparison using the Holm-Šídák method: # significant difference, - no significant difference.

Additionally, statistical analysis was carried out to draw comparisons between the three bitter stimuli. It was shown that there was no statistical difference in the rate of *Arc*-expressing neurons in animals stimulated with one bitter tastant compared with either of the other bitter tastants (Cyx v Qui: $p = 0.55$; Cyx v Cuc: $p = 0.57$; Qui v Cuc: $p = 0.99$). Raw data for all stimuli can be found in the Appendix (Table A.4, page 104). These results show a response in the PbN that is specific to bitter stimuli resulting in increased *Arc* expression.

4.2 *Arc* expression in the PbN after two stimulations

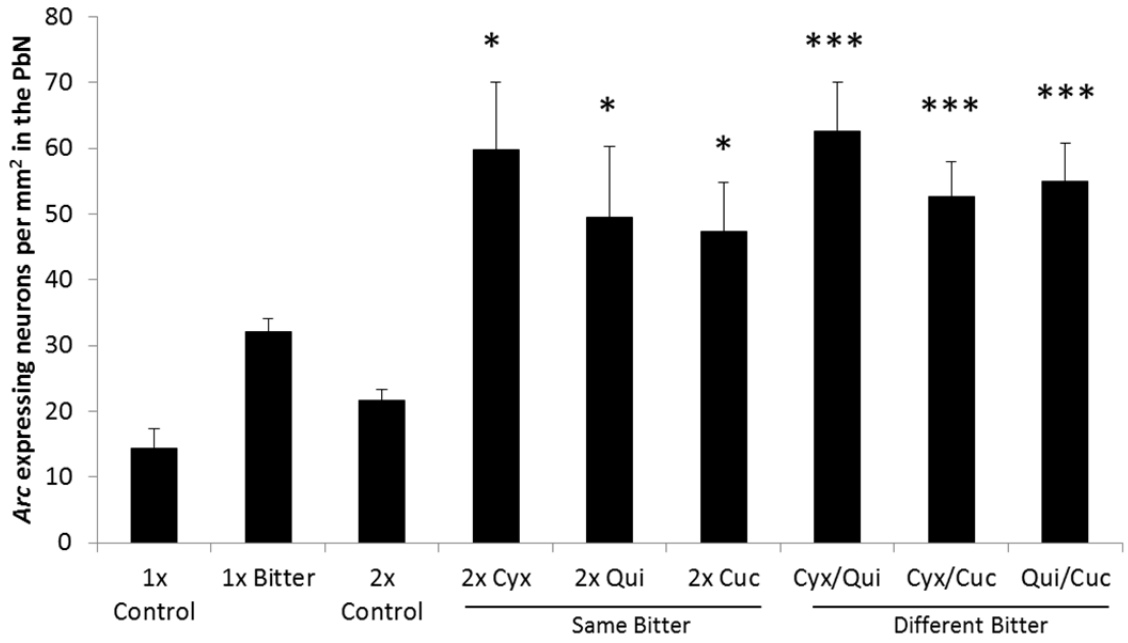

Figure 4.3 Total *Arc* expression following a single or double taste stimulation protocol with control or bitter stimuli in naïve animals.
The density of *Arc*-expressing neurons throughout the PbN are shown here for all double stimulation protocols. Single stimulation groups for each taste category are shown for comparison. All groups stimulated twice with the same bitter stimuli (bars 4-6) as well as the groups stimulated with two different bitter stimuli (bars 7-9) showed a statistically significant increase in *Arc* expression compared to animals stimulated twice with the control stimulus. However there were no significant differences in *Arc* expression between the bitter stimuli. Differences between the control stimulus and bitter stimuli were tested by t-test (* $p \leq 0.05$, *** $p \leq 0.001$), differences between the bitter stimuli were tested by analysis of variance. Shown are the mean values of *Arc*-expressing neurons per mm^2 PbN and standard error, n = 6-10.

In order to further explore the bitter-specific increase in *Arc* expression found in the previous experiment, mice were submitted to a double-stimulation protocol which involved two taste stimulations: 30 minutes and 5 minutes prior to sacrifice with bitter stimuli. Mice were either stimulated twice with the same bitter stimulus (2× Cyx, etc.) or with two different stimuli, one at each time point. All possible combinations of the three bitter

substances were included: Cyx/Qui, Cyx/Cuc, and Qui/Cuc, and both possible sequences for each combination (Qui, Cyx; Cyx, Qui). A control group received two stimulations with a control stimulus.

Animals stimulated twice with the same bitter stimulus showed a statistically significant increase in *Arc* expression throughout the PbN in comparison to animals stimulated twice with a control stimulus (2x Cyx p = 0.01; 2x Qui p = 0.03; 2x Cuc p = 0.01) (**Figure 4.3**). An analysis of variance showed no significant difference in the rate of *Arc* expression between the three bitter substances (2x Cyx v. 2x Qui p = 0.5 ; 2x Cyx v. 2x Cuc p = 0.35; 2x Qui v. 2x Cuc p = 0.87). Additionally, there was no statistically significant difference in *Arc* expression when comparing any of the animals stimulated twice with the same bitter tastant or with two different bitter tastants (see **Figure 4.3**).

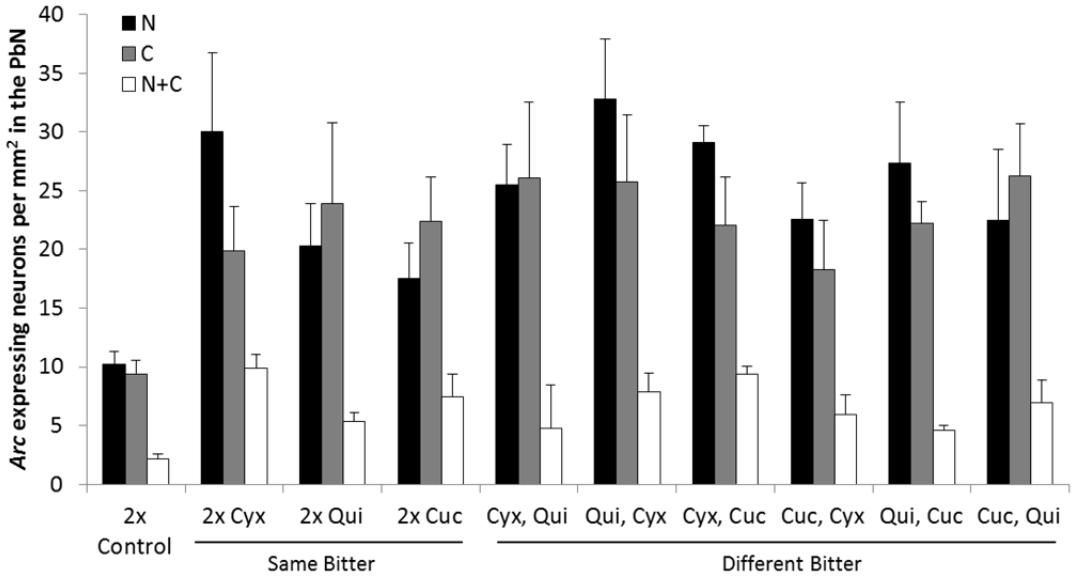

Figure 4.4 Intracellular distribution of *Arc* expression after two stimulations with bitter substances in naïve animals.
The *Arc*-expressing neurons are presented according to the intracellular distribution of *Arc* RNA; black: nuclear (N), grey: cytoplasmic (C), white: nuclear and cytoplasmic (N+C) staining. For all stimuli, only a small portion of neurons was activated by both stimulations, this is manifested by the appearance of *Arc* RNA in the nucleus and cytoplasm. Shown are the mean values of *Arc*-expressing neurons per mm^2 PbN and the standard error, n = 3-10.

Initial analysis showed a significant increase in *Arc* expression in animals stimulated twice compared to animals stimulated only once with the same stimulus (2x control p = 0.00; 2x Cyx p = 0.02; 2x Qui p = 0.05; 2x Cuc p = 0.02). In order to study the twice-stimulated animals further, the data was then analysed according to the intracellular distribution of *Arc* RNA (see **Figure 4.4**). These results showed that, in animals stimulated with two bitter tastants, each individual taste stimulation triggered increased *Arc*

expression to a rate of approximately 30 cells per mm^2, with approximately 5 – 10 cells per mm^2 being activated by both taste stimulation events.

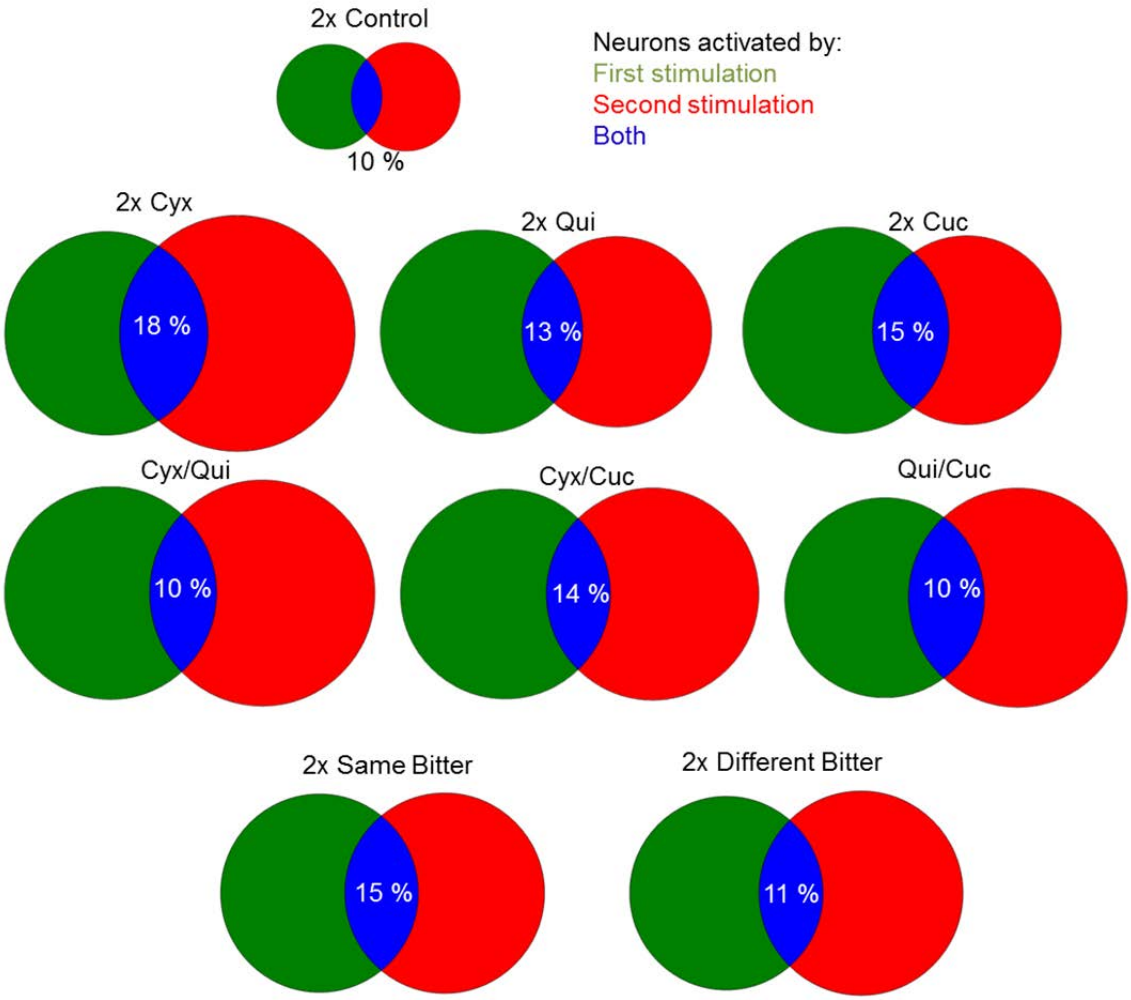

Figure 4.5 PbN cell populations responding to each taste stimulation following double taste stimulation protocols with control and bitter stimuli.
Green: fraction of cells that responded to the first taste stimulation alone (i.e. cytoplasmic *Arc* expression); red: fraction of cells that responded to the second stimulation alone (i.e. nuclear *Arc* expression); and blue: fraction of cells that responded to both taste stimulations (i.e. nuclear and cytoplasmic *Arc* expression). The area of the circles represents the density of *Arc* expressing cells responding to the particular stimulation.

Closer examination of the twice-activated neurons (neurons which expressed *Arc* both in the nucleus and in the cytoplasm) revealed a low rate of *Arc*-expressing neurons exhibiting *Arc* RNA in both the cytoplasm and the nucleus across all experimental groups (**Figure 4.5**) (Control: 10 % ± 1 % standard error (SE); Cyx: 18 % ± 3 % SE; Qui: 13 % ± 2 % SE; Cuc: 15 % ± 2 % SE; Cyx/Qui: 10 % ± 2 % SE; Cyx/Cuc: 14 % ± 2 % SE; Qui/Cuc: 10 % ± 1 % SE). This suggests a low incidence of neurons being reactivated by the second stimulation, whether or not it was the same bitter stimulus.

Although there was a trend for animals stimulated twice with the same stimulus to show a higher rate of twice-activated neurons, this was not a significant difference when comparing the groups as individual tastants. However, when analysing the bitter-stimulated animals in two groups – "Same bitter" (2x Cyx, 2x Qui, and 2x Cuc) or "Different bitter" (Cyx/Qui, Cyx/Cuc, and Qui/Cuc), as seen in **Figure 4.5** – the Same Bitter animals show a significantly higher rate of twice-activated neurons (15 % ± 1 % SE) compared to the Different Bitter animals (11 % ± 1 % SE) ($p = 0.03$). This could mean that a very small percentage of these twice-stimulated bitter-responsive *Arc*-expressing neurons (approximately 4 %) may be responding specifically to one bitter tastant, and are not activated by other bitter tastants.

4.3 Distribution of *Arc*-expressing neurons in the PbN

Looking at the raw data (**Figure 4.1 B**) an unequal distribution of *Arc*-expressing cells in the PbN is apparent, with clusters of *Arc* expressing cells present in the lateral portion of the PbN. In order to quantify the patterns of *Arc* distribution throughout the PbN, sections were subdivided along the brachium conjunctivum, creating a distinction between the medial and lateral sub regions. A visual representation of this subdivision can be seen illustrated in **Figure 3.5** on page 42.

Statistical analysis determined that the lateral PbN has a significantly higher density of *Arc*-expressing neurons following taste stimulation compared to the medial PbN across the majority of tastants (**see Figure 4.6**). This increase in *Arc* expression in the lateral PbN was not specific to bitter tastants, as it is also true for animals stimulated with sweet ($p = 0.02$), umami ($p = 0.02$), salty ($p = 0.01$), and sour ($p = 0.07$) tastants. Animals that received a control stimulus also show a trend ($p = 0.1$) toward higher *Arc* expression in the lateral compared to the medial PbN. Animals that received no stimulation ($p = 0.91$) show no significant difference between the rate of *Arc* expression in the lateral versus the medial parabrachial nuclei.

Although the results show a higher density of *Arc*-expression in the lateral PbN statistical analysis reveals that the bitter-specific increase in *Arc* expression seen in the whole PbN analysis is present in both subnuclei. Cyx-stimulated animals show significantly higher *Arc*-expression in the lateral ($p < 0.01$) and medial ($p < 0.01$) PbN compared to control-stimulated animals. This is also true for Qui-stimulated animals (lateral: $p = 0.01$; medial: $p < 0.01$) and Cuc-stimulated animals (lateral: $p = 0.02$; medial:

p = 0.01). This suggests that the bitter-responsive *Arc*-expressing neurons are distributed more heavily in the lateral PbN.

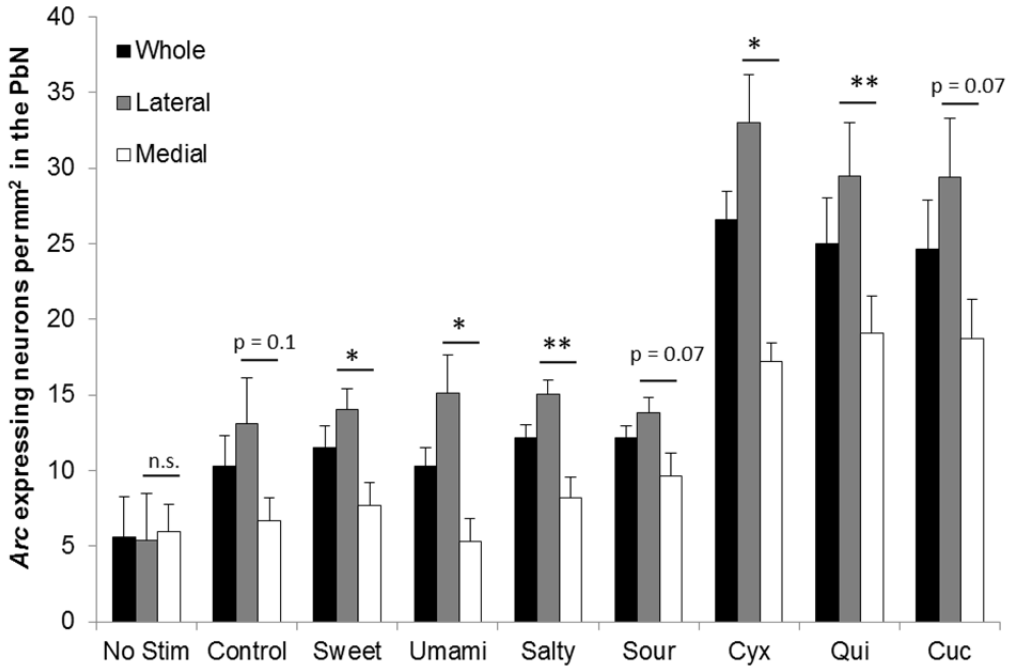

Figure 4.6 Distribution of *Arc*-expressing neurons in the subdivisions of the PbN after a single stimulation in naïve animals.
Black: whole PbN; grey: lateral PbN; and white: medial PbN. Differences within the stimuli between the lateral and medial sub-regions were determined by t-test (* $p \leq 0.05$, ** $p \leq 0.01$, *** $p \leq 0.001$), n = 3 – 6. Figure shows the mean values of *Arc*-expressing neurons per mm^2 PbN and standard error.

4.4 Behavioural responses to taste stimulation after CTA

The lateral PbN has been strongly implicated in the formation of conditioned taste aversion memories (Carter et al., 2015; Sakai & Yamamoto, 1997; Sakai & Yamamoto, 1998; Yamamoto et al., 1995; Yamamoto, Shimura, Sako, et al., 1994). In order to investigate whether an increase in *Arc* expression in the PbN could be triggered by a non-bitter tastant that animals have been conditioned to find aversive, it was first necessary to condition a taste aversion. This was done using a one-time pairing of an umami tastant with a lithium chloride (LiCl) injection; controls received an equivalent sodium chloride (NaCl) injection. For comparison, an additional group was included that received a CTA protocol using the bitter compound (Cyx).

In order to confirm whether the conditioned taste protocol successfully produced an aversion to umami, the lick behaviour of the animals was measured in the Davis MS 160 Mouse lickometre (DiLog Instruments, Tallahassee, FL, USA). Animals were exposed to numerous tastants including water, umami, and cycloheximide, and their licking behaviour

was measured before, and again after the completion of the conditioned taste aversion protocol. The total number of licks as well as the latency until first lick was analysed for both the umami tastant and cycloheximide across the four groups (for mean and SE see Table 4.1 on page 58). These groups are referred to according to the substance they were conditioned with and whether they received a LiCl or a NaCl injection as part of the CTA protocol, i.e. Umami-LiCl animals received umami paired with a LiCl injection during the CTA protocol.

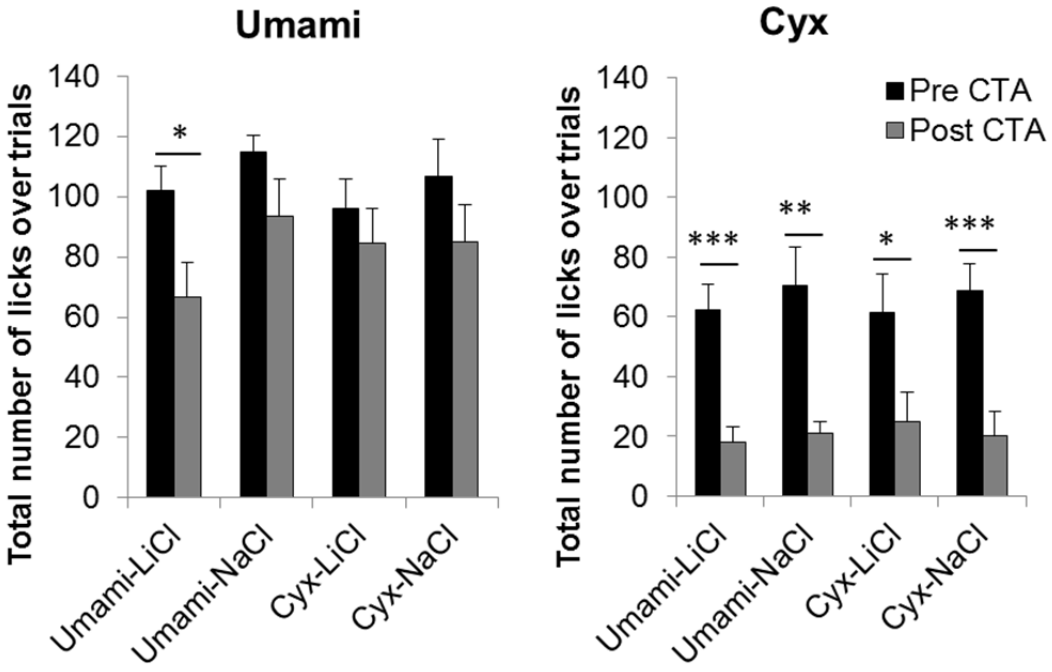

Figure 4.7 Licking behaviour before and after CTA I.
The total number of licks across all umami and Cyx solution trials in the lickometre over a 20 minute recording session, measured before and after animals were conditioned to find either umami (Umami-LiCl) or Cyx (Cyx-LiCl) aversive, and non-conditioned controls (Umami-NaCl, Cyx-NaCl). Statistical difference with animals between pre- and post-CTA recording sessions was determined by t-test (* $p \leq 0.05$, ** $p \leq 0.01$, *** $p \leq 0.001$), n = 8.

The total number of licks of the umami tastant was significantly decreased in the Umami-LiCl animals after the CTA paradigm ($p = 0.04$), this was not seen in any of the other groups (**Figure 4.7**). The total number of licks of cycloheximide was reduced following CTA across all of the experimental groups (Umami-LiCl, $p < 0.01$; Umami-NaCl, $p = 0.01$; Cyx-LiCl, $p = 0.05$; Cyx-NaCl, $p < 0.01$). These results suggest that the CTA paradigm successfully induced a conditioned taste aversion to umami, but did not enhance the averseness of the already aversive Cyx solution.

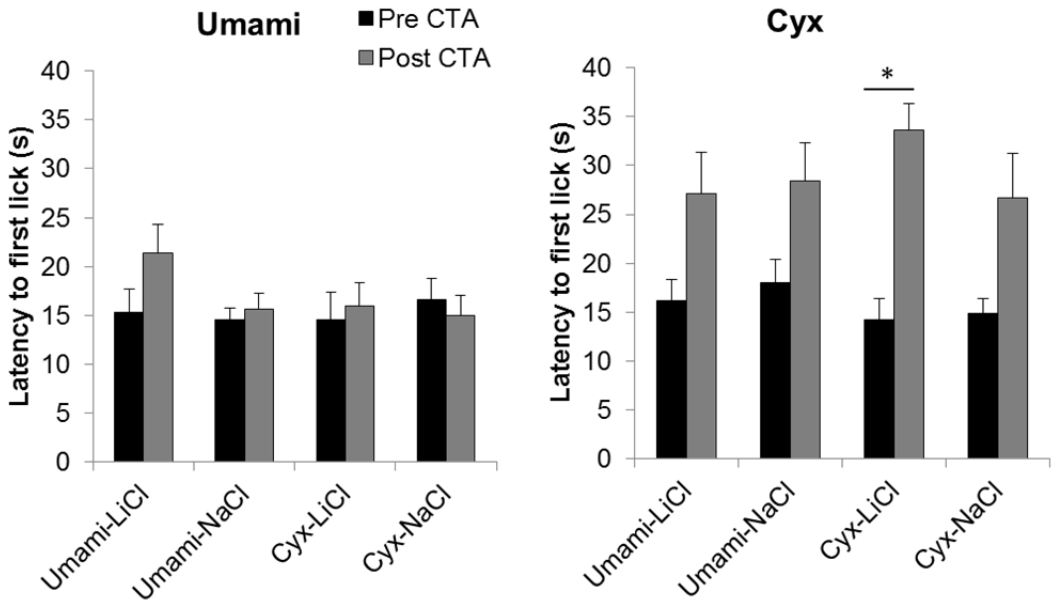

Figure 4.8 Licking behaviour before and after CTA II.
The average latency until first lick (s) across all umami and Cyx solution trials in the lickometre over a 20 minute recording session, measured before and after animals were conditioned to find either umami (Umami-LiCl) or Cyx (Cyx-LiCl) aversive, and non-conditioned controls (Umami-NaCl, Cyx-NaCl). Statistical difference with animals between pre- and post-CTA recording sessions was determined by t-test (* $p \leq 0.05$), n = 8.

All of the experimental groups showed an increase in latency until the first lick of cycloheximide (**Figure 4.8**), however, only the Cyx-LiCl group showed a statistically significant increase (Cyx-LiCl, $p < 0.01$; Cyx-NaCl, $p = 0.06$; Umami-LiCl, $p = 0.06$; Umami-NaCl, $p = 0.06$). The latency until first lick of the umami tastant was not statistically different following CTA, there was, however a slight, non-significant increase in the Umami-LiCl group ($p = 0.10$). This increased latency could mean that the animals are able to determine Cyx stimulus trials without licking the spout, resulting in an increased latency until first lick.

Table 4.1 Licking behaviour before and after CTA

			Total # licks		Latency until first lick	
			Pre-CTA	Post-CTA	Pre-CTA	Post-CTA
	CTA Group	n	Mean ± SE	Mean ± SE	Mean ± SE	Mean ± SE
Umami	Umami-LiCl	8	102.13 ± 8.01	66.81 ± 11.54	15.29 ± 2.42	21.40 ± 2.91
	Umami-NaCl	8	115.00 ± 5.55	93.44 ± 12.34	14.53 ± 1.25	15.69 ± 1.63
	Cyx-LiCl	8	96.25 ± 9.45	84.75 ± 11.25	14.57 ± 2.83	15.96 ± 2.33
	Cyx-NaCl	8	106.69 ± 12.33	85.13 ± 12.17	16.66 ± 2.12	15.04 ± 1.98
Cyx	Umami-LiCl	8	62.44 ± 8.56	18.13 ± 5.03	16.20 ± 2.12	27.09 ± 4.21
	Umami-NaCl	8	70.63 ± 12.52	21.19 ± 3.65	18.06 ± 2.30	28.45 ± 3.86
	Cyx-LiCl	8	61.56 ± 12.75	25.06 ± 9.53	14.25 ± 2.14	33.60 ± 2.78
	Cyx-NaCl	8	68.75 ± 8.96	20.38 ± 8.02	14.85 ± 1.51	26.65 ± 4.61

4.5 *Arc* expression in the PbN after CTA

To analyse the *Arc* expression in the CTA animals we compared animals conditioned to find either Umami or Cyx aversive (Umami-LiCl and Cyx-LiCl, respectively) with their relative CTA control groups (Umami-NaCl and Cyx-NaCl) as well as naïve animals from the single stimulation experiment described in section 4.1. Representative images of the *Arc* distribution of each of the groups are shown in **Figure 4.9**, group mean results are shown in **Figure 4.10**, and group means are displayed in Table 4.2.

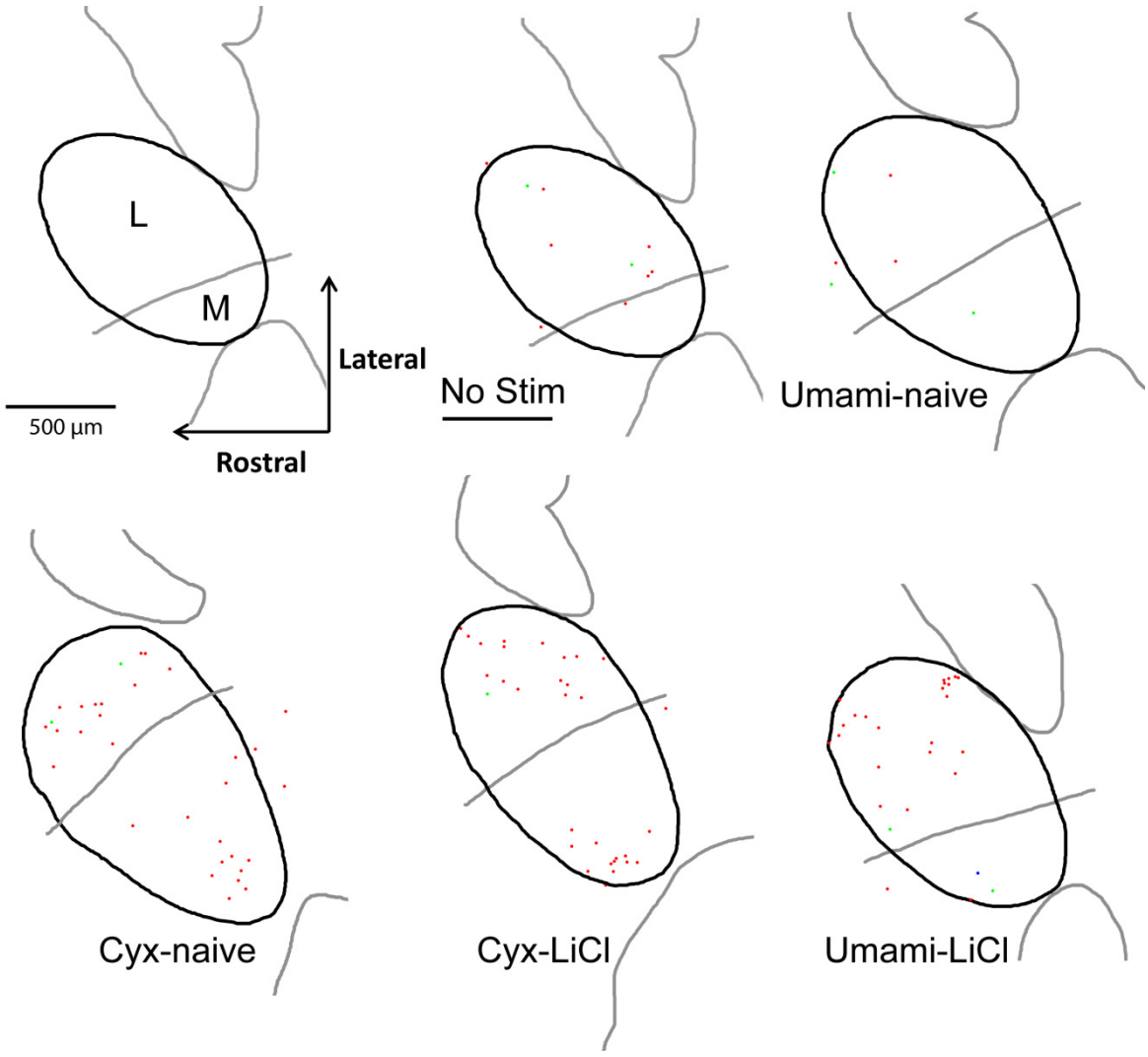

Figure 4.9 *Arc* expression in the PbN after single stimulation in naïve and conditioned animals.
Representative results of the counting of naïve animals stimulated with Umami and Cyx, and animals stimulated with Umami and Cyx after having been conditioned to find them aversive. The coloured dots mark neurons expressing *Arc* RNA; red: nuclear, green: cytoplasmic, and blue: nuclear and cytoplasmic localisation of *Arc* RNA. The black line marks the outline of the PbN, with a grey line transecting the PbN showing where the superior cerebellar peduncle (brachium conjunctivum) lies.

Umami-LiCl animals showed a significant increase by approximately 2.5 fold in *Arc* expression after Umami taste stimulation compared to naïve animals ($p = 0.01$), Umami-NaCl animals ($p = 0.01$), and naïve animals stimulated with a control stimulus ($p < 0.01$). Additionally, the rate of *Arc* expression in Umami-LiCl animals stimulated with Umami was not statistically different from naïve animals stimulated with Cyx ($p = 0.87$).

Conversely, Cyx-LiCl animals showed no significant increase in *Arc* expression following Cyx stimulation, compared to naïve animals stimulated with Cyx ($p = 0.23$) or Cyx-NaCl animals stimulated with Cyx ($p = 0.39$). They did, however show an increase in *Arc* expression when compared to animals stimulated with a control stimulus ($p < 0.01$) as seen before in naïve animals (section 4.1 page 48).

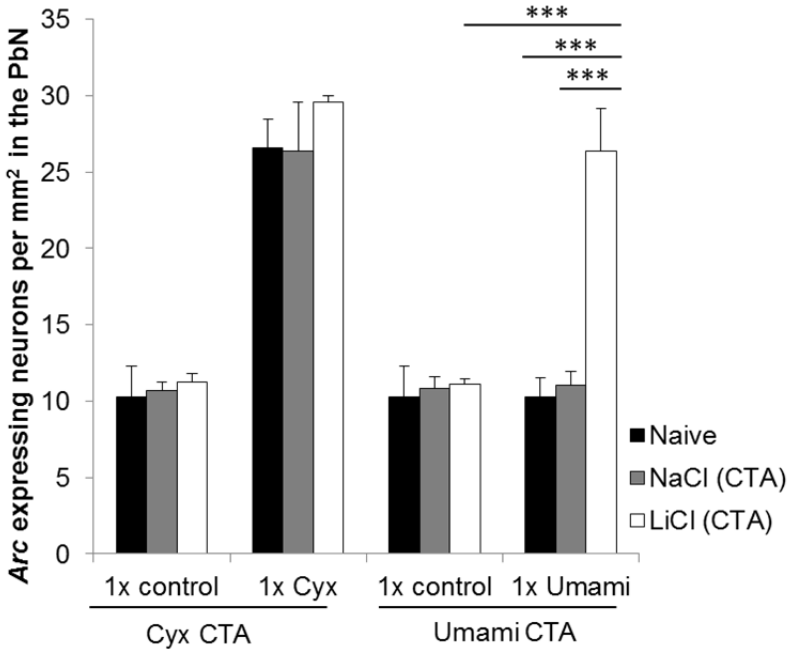

Figure 4.10 *Arc* expression in the PbN following a single stimulation in naïve and conditioned animals.
Conditioned animals were either conditioned with umami or Cyx solutions. Black: naïve animals with no prior exposure to the tastants before the taste stimulation; grey: control CTA animals that received a NaCl injection paired with a tastant during the CTA protocol; and white: animals that received a LiCl injection paired with a taste stimulus during the CTA protocol. The *Arc* expression induced by various stimuli was checked by analysis of variance (*** $p \leq 0.01$), $n = 3 – 6$.

In order to further explore the post-conditioning increase in *Arc* expression seen in Umami-LiCl animals stimulated with an Umami tastant, the pattern of distribution was calculated across the lateral and medial sub-nuclei (**Figure 4.11**). As was previously seen in bitter stimulated animals, Umami-stimulated Umami-LiCl animals showed a significantly higher rate of *Arc* expression in the lateral PbN compared to the medial PbN

(p = 0.03). This was also true for the Cyx-stimulated Cyx-LiCl animals (p = 0.05). These results suggest that this *Arc* expression is processed predominantly via the lateral PbN.

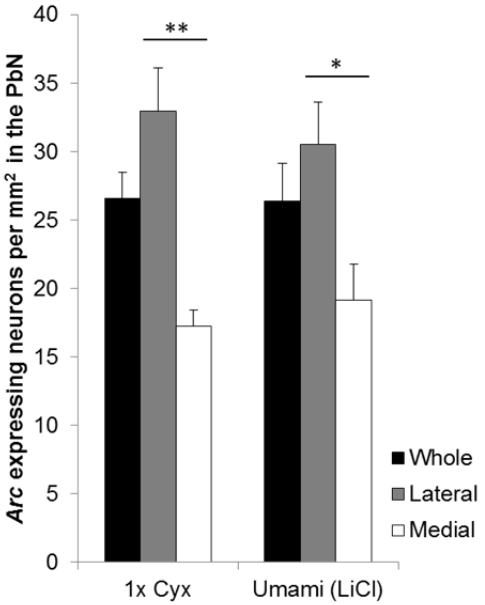

Figure 4.11 Distribution of *Arc*-expressing neurons in the subdivisions of the PbN after a single stimulation in naïve and conditioned animals.
Black: whole PbN; grey: lateral PbN (non-gustatory PbN); and white: medial PbN. Differences within the stimuli between the lateral and medial sub-regions was determined by t-test (* $p \leq 0.05$, ** $p \leq 0.01$), n = 4 – 5. Figure shows the mean values of *Arc*-expressing neurons per mm^2 PbN and standard error.

Table 4.2 *Arc*-expressing cells per mm^2 in naïve and conditioned animals

			Whole		Lateral		Medial	
Tastant	CTA Group	n	Mean	± SE	Mean	± SE	Mean	± SE
Control	Naive	6	10.28	± 2.03	13.11	± 3.04	6.65	± 1.55
	Umami-NaCl	3	10.79	± 0.80	12.98	± 1.05	7.05	± 0.71
	Umami-LiCl	3	11.12	± 0.30	12.76	± 0.27	8.19	± 0.86
	Cyx-NaCl	3	10.68	± 0.55	12.85	± 0.78	6.24	± 0.99
	Cyx-LiCl	3	11.27	± 0.52	13.45	± 0.78	7.72	± 0.55
Umami	Naive	4	10.27	± 1.22	15.11	± 2.53	5.32	± 1.53
	Umami-NaCl	3	11.06	± 0.91	13.44	± 1.04	7.17	± 0.73
	Umami-LiCl	4	26.37	± 2.78	30.55	± 3.09	19.18	± 2.63
Cyx	Naive	5	26.59	± 1.87	32.98	± 3.16	17.23	± 1.21
	Cyx-NaCl	4	26.34	± 3.23	28.73	± 3.64	20.86	± 3.94
	Cyx-LiCl	3	29.57	± 0.39	32.96	± 0.65	22.71	± 2.52

4.6 Neuropeptides present in *Arc*-expressing PbN neurons

In order to examine the molecular identity of *Arc*-expressing neurons of the PbN the *Arc* catFISH protocol was adapted to include a second RNA probe to analyse the expression of a variety of neuropeptide candidate genes. Two of the main criteria for

candidate gene selection were: known taste- or food-related functions and known expression in the PbN, particularly in the lateral portion. The genes selected were: calcitonin (Calca), glucagon like 1 peptide receptor (Glp1r), gastrin-releasing peptide (Grp), hypocretin receptor 1 (Hcrtr1), and neurotensin (Nts).

4.6.1 Optimisation of the new extended protocol

While establishing the extended *Arc* catFISH protocol three steps required optimisation: finding appropriate probe concentrations and antibody dilutions, and finding a suitable method to quench the peroxidase activity between the two tyramide signal amplification (TSA) steps.

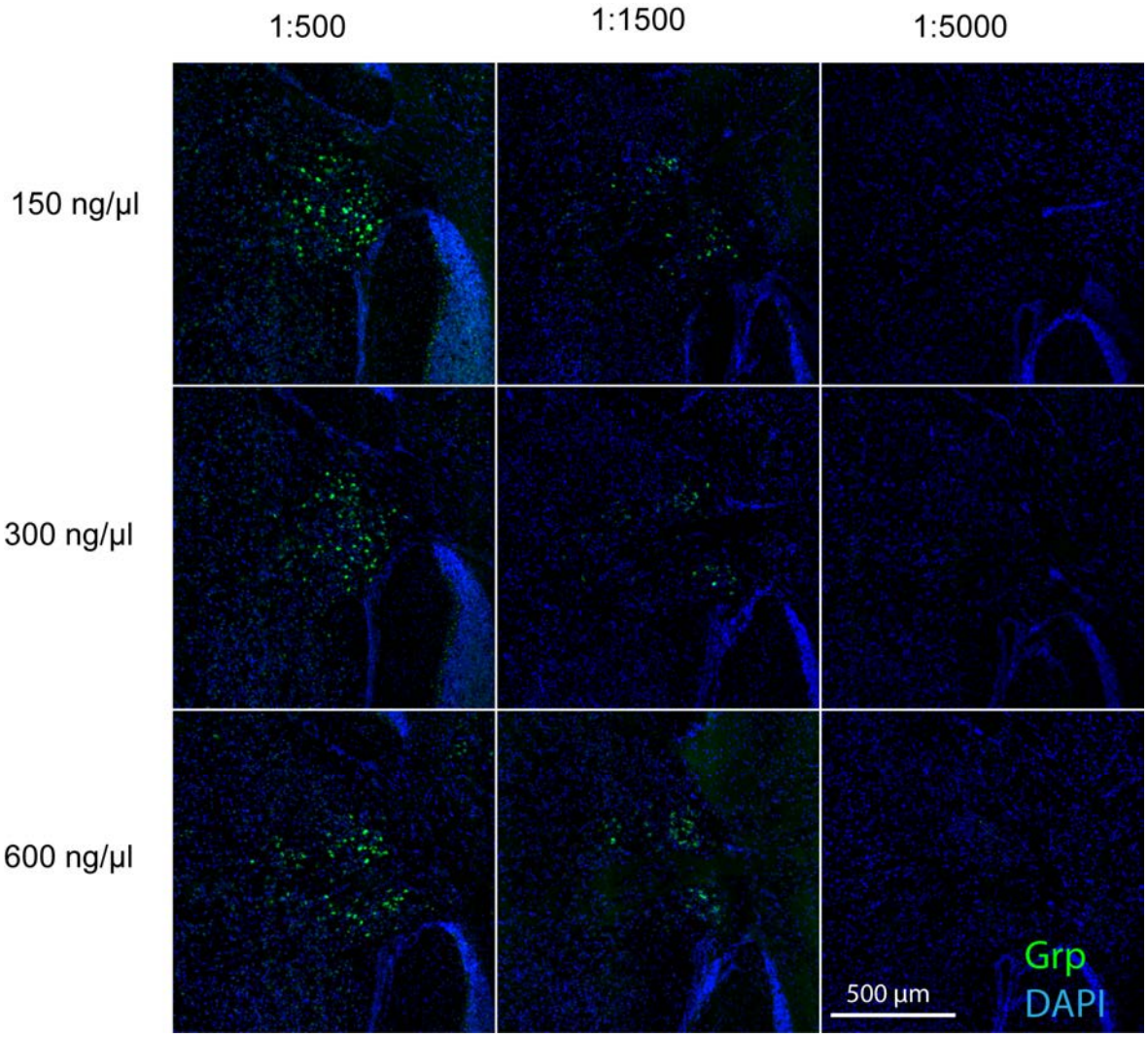

Figure 4.12 Optimisation of double FISH protocol I.
Testing different probe concentrations (150, 300, and 600 ng/µl) and anti-Fluorescein antibody dilutions (1:500, 1:1500, and 1:5000), green: gastrin-releasing peptide (Grp) RNA detected by secondary probe, blue: cell nuclei stained with DAPI.

Initially, the concentration of the second RNA probe and the Anti-Fluorescein antibody, which was used to detect the second probe were the same as those used for the *Arc* probe and the Anti-Digoxigenin antibody. However, the high level of background staining made it necessary to test a series of different probe concentrations and antibody dilutions. The concentrations 150 ng/µl, 300 ng/µl, and 600 ng/µl were tested alongside the antibody dilutions 1:500, 1:1500, and 1:5000 (examples using Grp shown in **Figure 4.12**) for all probes. After comparing the background signal in these stainings it was determined that 150 ng/µl probe concentration and 1:1500 anti-Fam POD yielded the best signal to background ratio.

Two tyramide signal amplification (TSA) kits and antibodies are used in the extended double-FISH protocol. The first TSA kit (which will be referred to as TSA 1 kit) and Anti-Digoxigenin antibody amplify the *Arc* signals, and the second TSA kit (TSA 2 kit) and Anti-Fluorescein antibody amplify signals from the secondary probe. Both TSA steps rely on the same method using horseradish peroxidase coupled to the antibodies to enzymatically activate numerous tyramide conjugates that are directly or indirectly visualized and thus lead to a stronger fluorescent signal. Using two TSA steps requires quenching of the peroxidase in between to avoid bleeding through of the signal of the first TSA step.

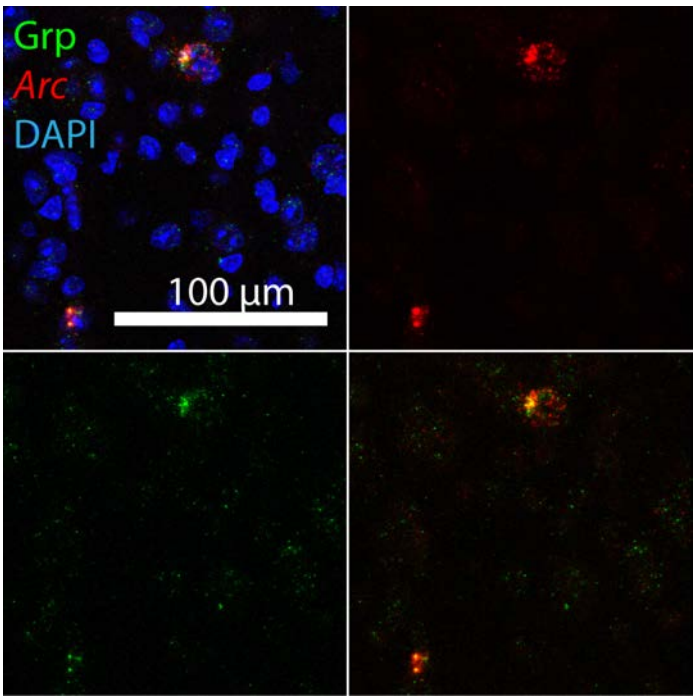

Figure 4.13 Optimisation of double FISH protocol II.
Using 100 mM sodium azide for the peroxidase quenching step after the first TSA kit it appeared that the first TSA kit was not successfully inactivated. Blue: cell nuclei stained with DAPI, red: *Arc* RNA visualized by first TSA kit, green: gastrin-releasing peptide (Grp) RNA visualized by second TSA kit.

Initially, 100 mM sodium azide was used for this step; however it appeared that some of the signals amplified by the TSA 2 kit were occurring in the same location as *Arc* signals (see **Figure 4.13**). To be sure that this was not due to unsuccessful inactivation of the TSA 1 kit, a different method was explored using 0.05 M hydrochloric acid which successfully inactivated the TSA 1 kit, and was used for subsequent experiments (**Figure 4.14**).

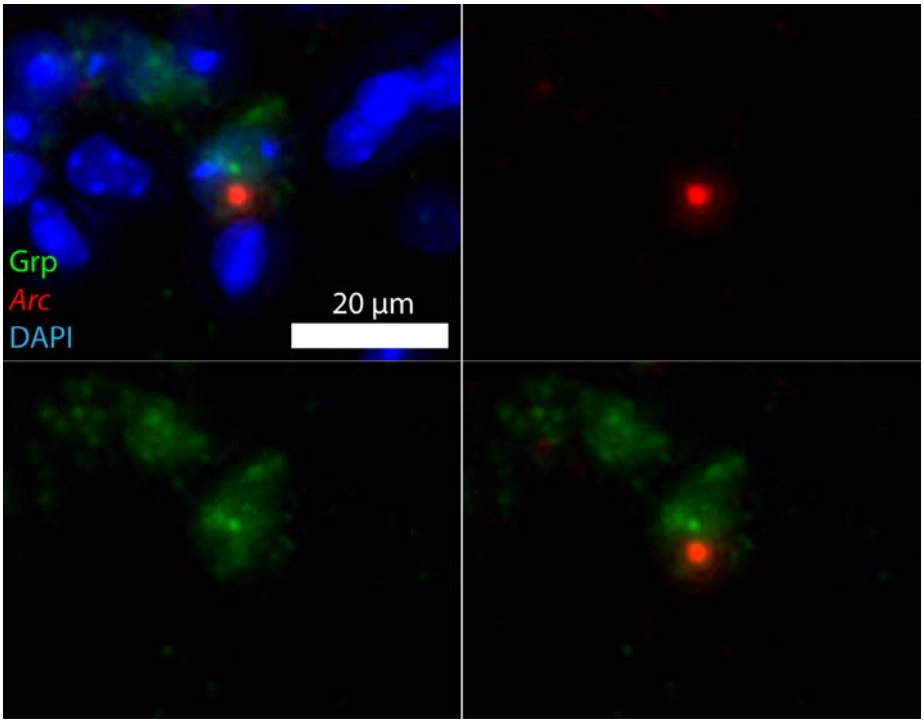

Figure 4.14 Optimisation of double FISH protocol III.
Using 0.05 M hydrochloric acid for the peroxidase quenching step after the first TSA kit it appeared to successfully inactivate the first TSA kit. Blue: cell nuclei stained with DAPI, red: *Arc* RNA visualized by first TSA kit, green: gastrin-releasing peptide (Grp) RNA visualized by second TSA kit.

4.6.2 Distribution of gene expression and co-expression in the PbN

In order to determine the rate of co-expression between *Arc*-expressing cells and cells expressing RNA of the candidate genes the analysis compared animals stimulated twice with two bitter stimuli and animals stimulated twice with a control stimulus. Results were analysed to observe the distribution of each of these genes within the PbN and to observe the rate at which each of the genes was co-expressed with *Arc*. Calca, Glp1r, Hcrtr1, Grp, and Nts were all shown to be present in the PbN, in both the lateral and medial subnuclei (representative FISH images are displayed in **Figure 4.16**).

The distribution throughout the subnuclei of the PbN was calculated for each gene (see Table 4.3 on page 67). Calca, Glp1r, and Nts neurons were expressed in a similar rate through both the medial and the lateral PbN (**Figure 4.15**). Interestingly, Hcrtr1 and Grp

neurons were expressed at a higher rate in the medial PbN, although this was only significant for Hcrtr1 neurons ($p < 0.01$) and not Grp neurons ($p = 0.26$).

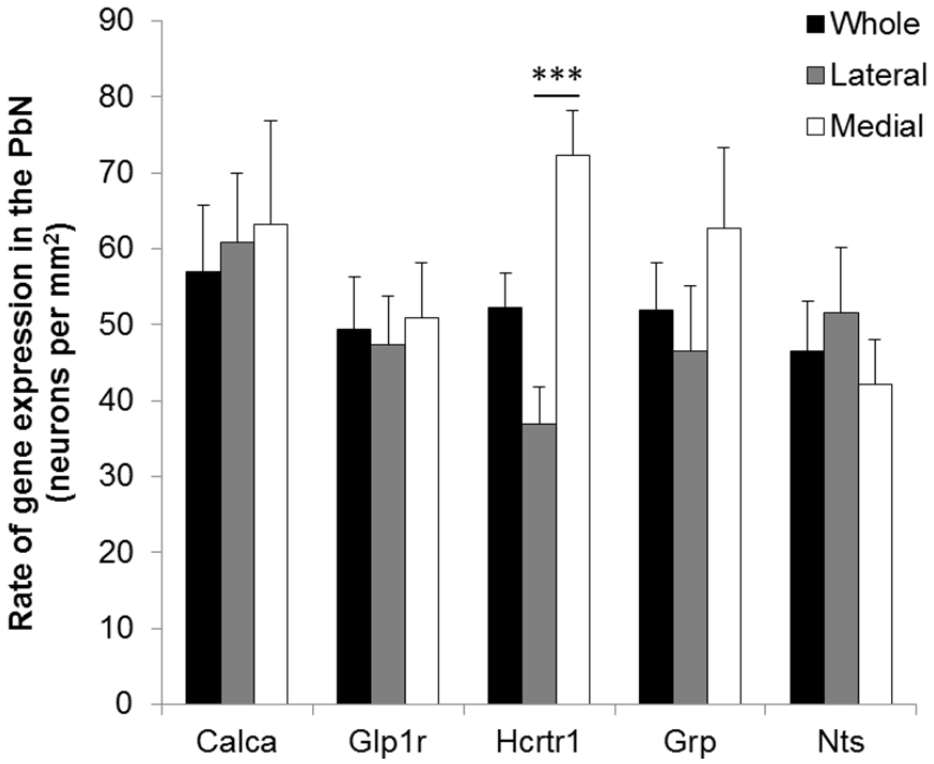

Figure 4.15 Distribution of Calca-, Glp1r-, Hcrtr1-, Grp-, and Nts-expressing neurons in the subdivisions of the PbN.
Black: whole PbN; grey: lateral PbN (non-gustatory PbN); and white: medial PbN (gustatory PbN). Differences within the animals between the lateral and medial sub-regions were determined by t-test (*** $p \leq 0.001$), n = 6 – 7. Figure shows the mean values of neurons expressing each of the genes per mm^2 PbN and standard error.

The rate of cells co-expressing both *Arc* and each neuropeptide was calculated for the whole, lateral and medial PbN. This analysis was carried out in animals that had received two taste stimulations either twice with a control stimulus, or twice with a bitter stimulus. The results from this analysis are shown in **Figure 4.17**. All of the genes analysed using the 2x FISH protocol showed a very low rate of co-expression with *Arc* in animals stimulated twice with a control stimulus (Calca = 0.82 ± 0.25 cells per mm^2; Glp1r = 1.3 ± 0.36 cells per mm^2; Hcrtr1 = 0.44 ± 0.22 cells per mm^2; Grp = 0.07 ± 0.07 cells per mm^2; Nts = 0.68 ± 0.68 cells per mm^2).

In animals stimulated twice with a bitter substance Calca and Glp1r neurons co-expressed *Arc* signals at a similar rate (Calca = 8.85 ±1.79 cells per mm^2; Glp1r = 9.03 ± 2.89 cells per mm^2) with no significant difference seen between the lateral and medial PbN (Calca: $p = 0.3$; Glp1r: $p = 0.3$). The rate of cells co-expressing *Arc* and Calca was

significantly higher in 2x bitter stimulated compared with 2x control stimulated animals ($p = 0.02$). This was also true for the rate of cells co-expressing *Arc* and Glp1r ($p = 0.05$). This analysis showed that 16% of *Arc* expressing neurons co-expressed Calca (± 1 % SE) and 17 % of *Arc* expressing neurons co-expressed Glp1r (± 5 % SE) in 2x bitter stimulated animals (compared to 9 % and 11 %, respectively, in 2x control stimulated animals).

Hcrtr1 was co-expressed with *Arc* at a rate of 8.00 ± 2.22 neurons per mm^2 in 2x bitter stimulated animals. This was significantly higher compared to 2x control stimulated animals ($p = 0.04$). Additionally, 2x bitter stimulated animals showed a higher rate of neurons co-expressing *Arc* and Hcrtr1 in the medial PbN compared to the lateral PbN ($p = 0.05$). According to this data 17 % of *Arc* expressing neurons co-expressed Hcrtr1 in 2x bitter stimulated animals (compared to 4 % in 2x control stimulated animals).

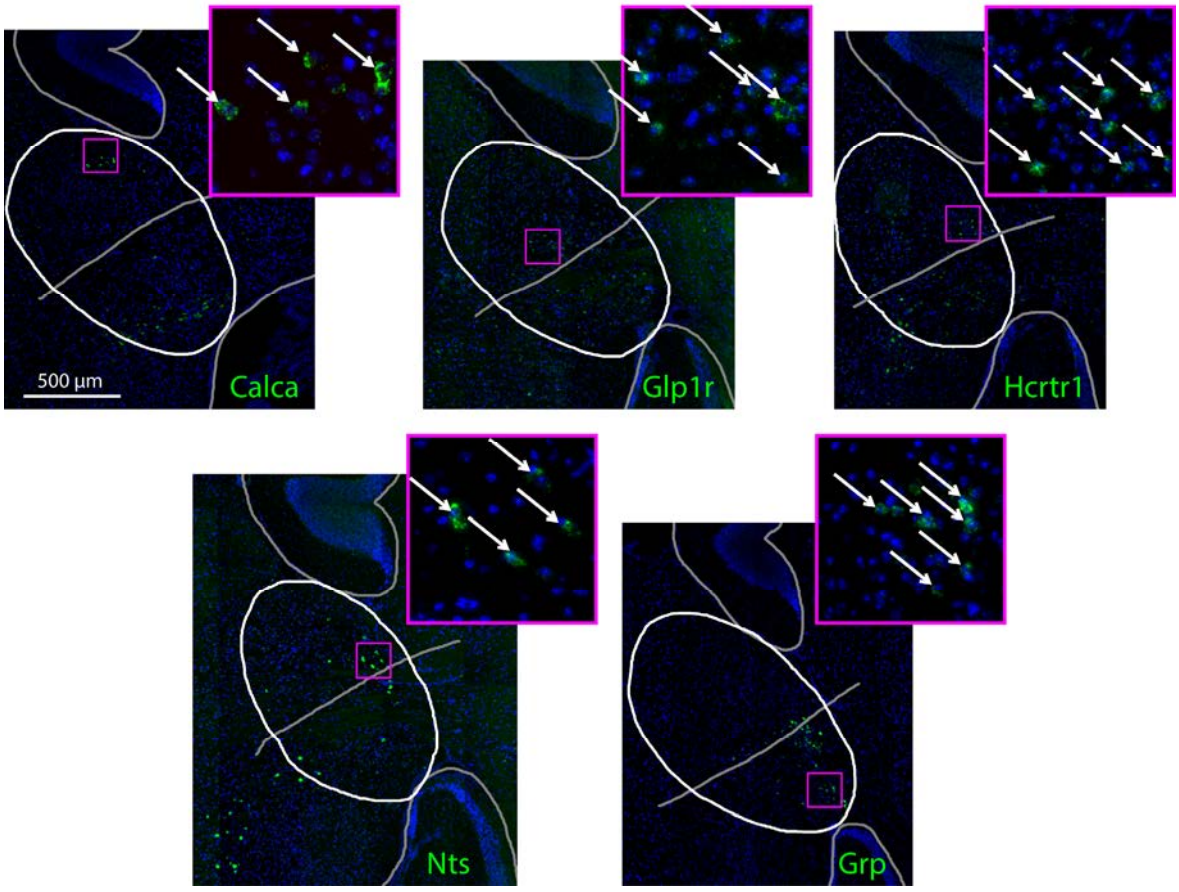

Figure 4.16 RNA expression patterns for candidate neuropeptides
Representative results of fluorescent *in situ* hybridisation of the neuropeptide candidate gene probes. The white line marks the outline of the PbN, with a grey line transecting the PbN showing where the superior cerebellar peduncle (brachium conjunctivum) lies. The cell nuclei are stained blue by DAPI, and the candidate genes RNA are shown in green. The cut-outs are 6x magnifications in the lateral PbN.

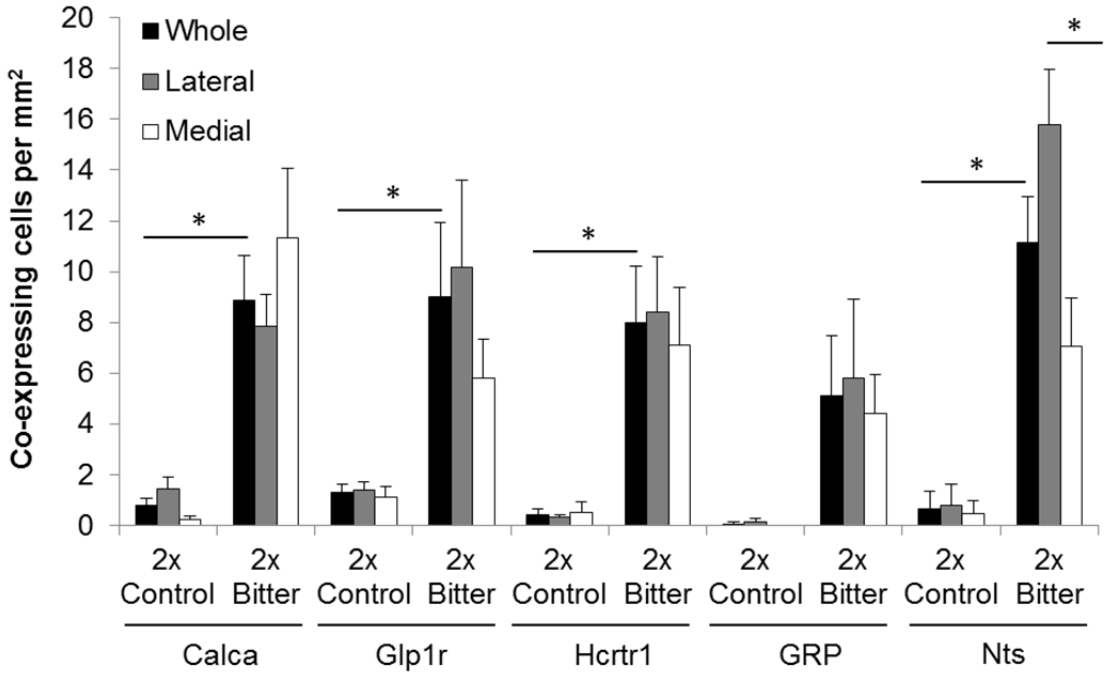

Figure 4.17 Distribution of Calca-, Glp1r-, Hcrtr1-, Grp-, and Nts-expressing neurons which co-express *Arc* in the subdivisions of the PbN.
Black: whole PbN; grey: lateral PbN (non-gustatory PbN); and white: medial PbN (gustatory PbN). Differences within the animals between the lateral and medial sub-regions were determined by t-test (* $p \leq 0.05$), n = 3 – 4. Figure shows the mean values of neurons expressing each of the genes per mm^2 PbN and standard error.

Grp showed the lowest rate of co-localization with *Arc* expressing neurons (5.10 ± 2.36 SE cells per mm^2) in 2x bitter stimulated animals. This was not significantly higher compared to 2x control stimulated animals ($p = 0.12$). Additionally, 2x bitter stimulated animals showed a similar rate of neurons co-expressing *Arc* and Grp in the lateral PbN compared to the medial PbN ($p = 0.71$). According to this data 9 % of *Arc* expressing neurons co-expressed Grp in 2x bitter stimulated animals (compared to 1 % in 2x control stimulated animals).

Table 4.3 Distribution of candidate genes in the PbN

Probe	n	Whole		Lateral		Medial	
		Mean	SE	Mean	SE	Mean	SE
Calca	7	56.94	± 8.72	60.76	± 9.12	63.18	± 13.69
Glp1r	7	49.36	± 6.88	47.38	± 6.29	50.94	± 7.20
Hcrtr1	7	52.27	± 4.59	36.93	± 4.80	72.30	± 5.81
Grp	7	51.93	± 6.18	46.46	± 8.59	62.60	± 10.68
Nts	6	46.44	± 6.59	51.64	± 8.57	42.08	± 6.00

Nts showed the highest rate of co-localization with *Arc* expressing neurons (11.15 ± 1.80 SE cells per mm^2) in 2x bitter stimulated animals. This was significantly higher

compared to 2x control stimulated animals (p = 0.01). Additionally, 2x bitter stimulated animals showed a higher rate of neurons co-expressing *Arc* and Nts in the lateral PbN compared to the medial PbN (p = 0.02). According to this data 20 % of *Arc* expressing neurons co-expressed Nts in 2x bitter stimulated animals (compared to 5 % in 2x control stimulated animals). Comparatively, when calculating the proportion of candidate gene-expressing cells which co-express *Arc*, it was observed that 0-3 % of PbN neurons expressing one of the candidate genes co-expressed *Arc* in control-stimulated animals, compared to 13-20 % in bitter-stimulated animals (data shown in Appendix Table A.7 page 105).

Table 4.4 Proportion of *Arc*-expressing PbN cells co-expressing candidate genes

Probe			Whole		Lateral		Medial	
	Stimulus	n	Mean	SE	Mean	SE	Mean	SE
Calca	2x Control	3	9%	± 4%	12%	± 5%	4%	± 3%
	2x Bitter	4	16%	± 1%	15%	± 2%	18%	± 5%
Glp1r	2x Control	3	11%	± 5%	10%	± 4%	14%	± 4%
	2x Bitter	4	17%	± 5%	18%	± 5%	16%	± 5%
Hcrtr1	2x Control	3	4%	± 2%	3%	± 1%	7%	± 5%
	2x Bitter	4	17%	± 3%	16%	± 4%	20%	± 3%
Grp	2x Control	3	1%	± 1%	1%	± 1%	0%	± 0%
	2x Bitter	4	9%	± 3%	9%	± 4%	12%	± 4%
Nts	2x Control	2	5%	± 4%	5%	± 4%	6%	± 5%
	2x Bitter	4	20%	± 6%	22%	± 6%	17%	± 6%

Combining these findings with previous investigations into the function and projections from these specific neurons types in the brain, it will be possible to make some predictions as to the possible function of the bitter-responsive *Arc*-expressing neurons seen in the taste pathway.

Discussion

This chapter contains a summary of the main findings of this research, interpretations of these results and their implications for the understanding of the neural processing of taste information. The rate of taste-responsive neurons will be compared to previous research in the parabrachial nucleus (PbN) in naïve and conditioned mice, as will the distribution of taste-responsive neurons throughout the PbN sub-nuclei. Then possibilities for the neural targets and the functional importance of bitter-responsive *Arc* expression in the PbN will be discussed.

5.1 Summary of main findings

The aim of this thesis was to explore the neural transmission of taste information using the *Arc* catFISH (cellular compartment analysis of temporal activity by fluorescent in-situ hybridisation) method to investigate the pattern of neuronal activation in the PbN following taste stimulation. This was carried out in naïve and conditioned animals to explore possible taste-behaviour correlates with changes in *Arc* expression in the PbN. Additional secondary FISH probes were used to investigate the molecular identity of taste-activated neurons.

As hypothesised, only bitter-stimulated naïve animals showed increased *Arc* expression in the PbN compared to controls, whereas after a conditioned taste aversion (CTA) protocol, in which mice were conditioned with lithium chloride (LiCl) to find umami tastants aversive (umami-LiCl animals), mice showed increased *Arc* expression after umami taste stimulation. Cyx-LiCl animals showed neither enhanced aversive behavioural responses to cycloheximide (Cyx) in the lickometre nor enhanced PbN *Arc* expression following Cyx stimulation compared to naïve Cyx-stimulated animals.

A second taste stimulation resulted in an almost two-fold increase in *Arc* expression in the PbN in both bitter- and control-stimulated animals, and unexpectedly, only a small portion (15 %) of neurons were activated by both taste stimulations when the same bitter tastant was used for both taste stimulations, and a smaller portion (11 %) when a different bitter tastant was used for each taste stimulation.

The extended *Arc* catFISH protocol was established and used to explore the molecular identity of bitter-activated *Arc*-expressing neurons in the PbN. It was determined that, in animals stimulated twice with bitter tastants, approximately 16 % of the *Arc*-expressing neurons co-expressed calcitonin (Calca) ribonucleic acid (RNA); 17 % co-expressed

glucagon-like peptide 1 receptor (Glp1r) RNA; 17 % co-expressed hypocretin receptor 1 (Hcrtr1) RNA; 9 % co-expressed gastrin-releasing peptide (Grp) RNA; and 20 % co-expressed neurotensin (Nts) RNA.

5.2 Taste-induced increase in *Arc* expression in the PbN

Oral stimulation with bitter substances results in a significant increase in *Arc* expression in the PbN compared to animals stimulated with a control, saliva-like, substance. However, this increase is not observed in naïve animals stimulated with sweet, umami, salty, or sour taste stimuli. These findings are similar to previous results seen in the gustatory nucleus of the solitary tract (NTS) (Töle, 2014), which lead Töle to hypothesise that this *Arc* expression may be bitter specific. The bitter-specificity observed in the present experiment using *Arc* has not been seen using other immediate early genes (IEGs) to study taste-responsive neurons in the PbN; Yamamoto, Shimura, Sakai, et al. (1994) observed similar sized clusters of c-*fos* expressing PbN neurons after stimulation with salty, sour, sweet, and bitter taste solutions (umami was not included in the study). Considering *Arc*-expression as a neural-activity marker, the findings of the present study suggest that non-bitter taste solutions do not activate PbN neurons. However, considering the important role of *Arc* in synaptic plasticity (Guzowski et al., 2000), it is more likely that this *Arc* expression represents plastic changes, such as the strengthening of synapses, underlying some form of memory formation. In the present study, this would suggest that bitter taste stimulation triggers a state of enhanced synaptic plasticity in the PbN.

The rate of *Arc* expression observed in the gustatory NTS (Töle, DIfE, 2014) was also similar to that seen in the PbN (~25 *Arc* expressing cells per mm^2 in bitter-stimulated mice). Using the rate of *Arc* expression per mm^2 observed in the whole/lateral/medial PbN and the gustatory NTS it is possible to extrapolate, based on the size of these structures, the total number of *Arc* expressing cells in the gustatory NTS and the PbN subnuclei for comparison. In 1x Cyx stimulated mice the extrapolated number of *Arc* expressing neurons in the whole gustatory NTS is ~477, the whole PbN is ~2003, the lateral PbN is ~1577, and the medial PbN is ~478. Interestingly, the extrapolated numbers suggest a much higher number of *Arc*-expressing neurons in the PbN, which would mean a higher incidence of synaptic plasticity occurring in the PbN following bitter taste stimulation; whereas in the "gustatory" processing areas, the number of *Arc*-expressing neurons in the gustatory NTS and the gustatory PbN (medial) are the same. This higher occurrence of synaptic changes in the PbN may be due to the large number of intra-structural connections within the PbN,

which are believed to underlie the role of the PbN in strengthening the association of taste perception (processed via the medial PbN) with post-ingestive effects (processed via the lateral PbN) (Saper & Loewy, 1980) resulting in taste aversions or preferences. This would suggest that the increase in *Arc* expression following bitter taste stimulation is the result of synaptic strengthening between PbN neurons and their targets (both intra- and inter-structural) to allow the mice to mediate future feeding behaviours. Additionally, the higher incidence of synaptic changes in the PbN compared to the NTS would suggest that the PbN plays a greater role in taste-related learning.

The high rate of bitter-responsive neurons observed in this study in comparison to neurons that respond to other tastants are also notably different to previous electrophysiological studies of taste-responsive neurons in the PbN. Generally in single-unit recording studies, researchers have recorded taste responses from approximately 40 – 100 neurons throughout the PbN. In these studies neurons are categorised according to which tastant elicits the greatest response (i.e., "bitter-best" would mean the neurons show the greatest response following bitter taste stimulation). Unlike the present study, electrophysiological recording studies consistently report bitter-best neurons to be the lowest portion of recorded cells, with only approximately 2 – 10 % of the recorded cells being categorised as bitter-best in the NTS and the PbN (Lemon & Margolskee, 2009; McCaughey, 2007; Spector & Travers, 2005; Tokita & Boughter, 2016; Wilson & Lemon, 2014). Although this cannot be a direct comparison, as these studies do not report the total number of PbN neurons that responded to bitter, but the number of neurons that showed greater responses to bitter stimulation compared to stimulation with other non-bitter tastants. This discrepancy may also be due to the categorisation of neurons into taste-groups, as sweet-best neurons can be activated by bitter tastants – they merely elicit greater responses to sweet tastants. This would result in an under-reporting of the total number of bitter-responsive neurons, and may explain this difference in result. This explanation is supported by a recent study showing that the tuning of taste-responsive NTS and PbN neurons changes over time, with specific taste responses appearing, disappearing, or shifting in magnitude across multiple days of recording (Sammons et al., 2016).

5.2.1 Rate of reactivated neurons in double-stimulation paradigm

In a paradigm testing neuronal activation following two separate (25 mins apart) oral taste stimulations with the same stimulus, the number of *Arc* expressing cells in the PbN was approximately twice the amount shown after a single stimulation. This was true for

both bitter and control taste stimuli, which suggests that the second taste stimulation event results in the activation of a new population of neurons that did not respond to the initial stimulation.

Examining the intracellular distribution of *Arc* in these neurons confirms this, and additionally shows that only a small percentage of PbN neurons activated by the first taste stimulation (control: 10%; cycloheximide: 18%; quinine: 13%; cucurbitacin: 15%) are reactivated by the secondary stimulation of the same stimulus. Within the twice stimulated animals, comparisons were drawn between animals that received the same taste stimulus for both taste stimulations and animals that received a different taste stimulus for each taste stimulation. The percentage of twice-activated neurons (showing both nuclear and cytoplasmic *Arc* RNA distribution) between each tastant group (i.e. Cyx, Cyx vs. Cyx/Cuc) was not statistically different. However, after combining the groups into either animals who received the same bitter stimulus twice (2x Same), or animals who received a different bitter stimulus for each of the two taste stimulations (2x Different), statistical analysis revealed that 2x Same animals (15 %) showed a higher rate of twice-activated neurons compared to 2x Different animals (11 %). This proportion is similar to, albeit lower than, a prior study using the same method to observe *Arc* expression following taste stimulation in the gustatory NTS, which showed that 32 % of *Arc*-expressing neurons were activated by both of two taste stimulations with the same bitter stimulus, compared to 22 % in animals stimulated with two different bitter stimuli (Töle, 2014). The lower percentage of twice-activated neurons in the PbN could be due to a higher number of *Arc*-expressing PbN neurons, which would mean that the same number of neurons in the NTS and PbN would require different percentages of the overall population of *Arc*-expressing neurons. In the gustatory NTS, the higher rate of twice-activated neurons in 2x Same bitter stimulated animals compared to 2x Different bitter stimulated animals was proposed to represent a population of tastant-specific neurons that did not respond to other tastants (Töle, DIfE, 2014), even if they are from the same taste quality (i.e. bitter in this case). In the PbN this would mean that approximately 4 % (extrapolates to ~80 neurons in Cyx stimulated animals) of the bitter-responsive neurons would be tastant-specific, as opposed to 10 % in the gustatory NTS (extrapolates to ~47 neurons in Cyx stimulated animals) that were hypothesised by Töle (DIfE, 2014) to play a role in discrimination between different bitter tastants. The present study is consistent with the NTS results, with a slightly higher number of tastant specific neurons, suggesting that a population of ~47 neurons per bitter tastant in

the NTS and ~80 neurons per bitter tastant in the PbN could allow animals to discriminate between different bitter tastants.

Interpreting this *Arc* expression as a neural-activity marker, the low rate of reactivated neurons would suggest that each taste stimulation event in this paradigm is largely being processed by its own population of neurons, with only a small portion of neurons being activated as a result of both stimulations. Extrapolating this interpretation to other taste stimulation events, this would suggest an exaggerated labelled-line theory where, instead of different neuron populations for each taste quality, there are different neuron populations for every single taste event. However, based on the size of the PbN and electrophysiological studies that show that PbN neurons can be reactivated by the same, or even a different tastant within a short period of time (Lemon & Margolskee, 2009; McCaughey, 2007; Spector & Travers, 2005; Tokita & Boughter, 2016; Wilson & Lemon, 2014); it is unlikely that every single taste event in a mouse's life is processed via a separate population of PbN neurons. This discrepancy in the rate of reactivation in the present study may be due to the difference in method; electrophysiology determines electrical signals resulting from neural activation, whereas IEGs like *Arc* are released following neural activation that results in long-term, structural cellular changes. This consideration further suggests that the *Arc*-expression observed in this study should be considered a marker of cellular plasticity, rather than neural activation *per se*. This would mean that the *Arc* expression seen in the present study represents changes in synaptic strength occurring in response to bitter activation, rather than a map of bitter taste-responsive neurons.

Töle (DIfE, 2014) observed a similarly low rate of reactivation in the NTS and hypothesised that in order to induce *Arc* expression a certain threshold of cellular activity is required, and that not all NTS neurons elicit a strong enough neural response to a single bitter taste stimulation to induce *Arc* expression. Töle further hypothesised that the second population of neurons could be due to some type of neuronal priming elicited by the first taste stimulation: if one of these neurons elicits a low-frequency stimulation to the initial taste stimulation, a second taste stimulation may be able to induce a stronger stimulation frequency due to the neuron being primed and already excited by the first stimulation; resulting in a second population of *Arc*-expressing cells that showed no *Arc*-expression following the initial taste stimulation. Considering Töle's theory in light of the present PbN results and interpreting *Arc* as a synaptic plasticity signal, it is more likely that PbN neurons undergoing plastic changes may require a longer time than the 25 minute inter-

stimulation period used in the stimulation protocol to re-trigger *Arc* release and subsequent additional cellular changes. Although the long-term time-span of plastic states in the NTS and PbN have not been studied, research in the insular cortex has revealed that neurons show enhanced responses to conditioned tastants after CTA learning. Taste-responsive neurons show heightened electrophysiological responses (increased stimulation frequency) to taste stimuli they were conditioned to find aversive and these neurons either show short-term (peaking at 30 minutes) or long-term (peaking at 60 minutes, but remaining enhanced up to 360 minutes after stimulus presentation) plasticity (Yasoshima & Yamamoto, 1998). Although the mice in the present study are naïve, if neurons in the PbN behave in a similar manner to inherent aversions, this would suggest that, in the 30 minute stimulation paradigm in the present study, even neurons showing short-term enhancement profiles would still not have reached the peak of their enhanced activity by the presentation of the second taste stimulus (25 minutes after the first). This may result in a lower rate of neurons expressing a second release of *Arc* RNA in response to the second taste stimulus in the present experiment. Though the authors did not observe the time-span of enhanced activity, Shimura et al. (1997) observed larger electrophysiological responses to a salty taste stimulus after they had been conditioned to find it aversive, though this finding was not consistent at all concentrations or taste stimuli, the authors interpret this result as an increased salience to the now aversive salt solution. This would result in animals drawing stronger associations between the stimulus and relevant post-ingestive effects. It is possible that the bitter-specific increase in *Arc*-expression observed in this experiment may represent an inherent increased salience to bitter tastants compared to other tastants.

5.2.2 Lateral/medial distribution of *Arc*-expressing neurons

The distribution of *Arc* signals throughout the PbN is higher in the lateral PbN compared to the medial PbN. This was true for all taste stimulations, although for some tastants the effect was merely approaching significance (control, sour, and Cuc). This uneven distribution of *Arc* expression was not seen in animals that received no stimulation. Based on early tracing studies, the PbN is often described as being functionally divided, with the lateral PbN processing non-gustatory responses and the medial PbN processing gustatory responses. This distinction is based on the finding that the majority of PbN projections to the gustatory-processing areas of the thalamus originate in the medial PbN and evidence of stronger taste responses occurring in the medial PbN (Norgren & Pfaffmann, 1975). Based on this distinction the increased *Arc*-expression in the lateral PbN

after taste-stimulation would be occurring in the "non-gustatory" portion, and would likely be processing other autonomic responses to the taste experience such as changes in heart rate, respiratory rate, body temperature, etc, or perhaps hedonic value.

A recent electrophysiology study showed a similar distribution of bitter-responsive neurons to the present study; Tokita and Boughter (2016) reported a larger number of salt-best, sour-best, and bitter-best neurons in the lateral PbN compared to the medial PbN, in fact the bitter-best neurons they observed were almost exclusively located in the lateral PbN. However, 33 of the 76 sweet-best neurons they observed were located in the medial PbN, 28 were in the brachium conjunctivum, and 15 were in the lateral PbN. Additionally, other electrophysiological studies have reported higher number of salt-best neurons in the medial PbN (Halsell & Travers, 1997; Ogawa et al., 1987; Shimura et al., 2002; Van Buskirk & Smith, 1981). Although the distribution of bitter-best neurons is in line with results in the present study, differences among other tastants may be due to differences in the methods used, such as categorisation of neurons into "best" stimulus groups, as mentioned previously.

Drawing comparisons between the present study and other IEG studies is more difficult as many of them with focus on only one subnucleus, or they simply publish representative images of the IEG expression with no quantification of the results reported. One study used c-*fos* to observe the general distribution of taste responsive neurons in the PbN (Yamamoto, Shimura, Sakai, et al., 1994); though the rate of activated neurons for the lateral and medial nuclei was not quantified, the representative images from animals stimulated with sweet, salty, sour, and bitter compounds appear to show a higher rate of expression in the lateral PbN. A previous study (Yamamoto & Sawa, 2000) reported a high rate of c-*fos* expression around the external lateral portion of the PbN following intraoral quinine infusion, and a similarly high rate of c-*fos* expression in the dorsal/central lateral areas of the PbN following intraoral sucrose infusion. Although they did not analyse the medial PbN, a representative image shows c-*fos* expression in the medial PbN following intraoral sucrose infusion. They did not report, or show images for bitter-stimulated animals in the lateral PbN. These c-*fos* results show similarities to the high lateral PbN distribution of taste-responsive *Arc* expressing neurons. However further research showing a direct comparison of taste-induced c-*fos* expression in the lateral and medial PbN would provide further insight.

The present study focused on the lateral/medial distinction of the PbN, however the PbN contains approximately ten distinct subnuclei which can be distinguished based on the

size/shape of the neurons, the targets of the neurons, and the neuropeptides found in the neurons (Fulwiler & Saper, 1984). Unfortunately, the method used in this study did not allow the observation of the size/shape of the neurons, as 4',6-Diamidinie-2'-phenylindole dihydrochloride (DAPI) only stains the nuclei of the neurons, so it was not possible to confirm the exact sub-nuclear distribution based on neuronal size or shape. However, estimation based on the general location of the *Arc*-expression would suggest that it is occurring in the external lateral PbN, which is known to be important for the formation of conditioned taste aversion memories (Carter et al., 2015).

It is clear that *Arc*-expression in the PbN and NTS marks a neural response that is unique to bitter taste stimulation compared to other taste qualities. One of the unique characteristics of bitter compounds is the inherent aversive responses to bitter that are conserved across multiple species. Taken together with the evidence that *Arc* is crucial for the development of CTA memories (Plath et al., 2006) it is possible that the bitter-enhanced *Arc* expression may be modulating the animals' inherent aversive-response to bitter stimuli via the external lateral PbN. To investigate this further, a CTA protocol was used to observe how conditioning aversions to umami and Cyx affected taste-response behaviour and *Arc* expression in the PbN.

5.3 Behavioural and neural correlates of conditioned taste aversion

Arc expression was observed in mice that underwent the conditioned taste aversion protocol in which either Umami or Cyx tastants (for details see Table 2.8 in section 2.7 on page 21) were paired with either malaise-inducing LiCl or control NaCl injections. Animals that were conditioned to find umami aversive (Umami-LiCl) showed a significant decrease in the total number of licks of an umami tastant in the lickometre. This decrease in licking during umami trials was not seen in the non-averse control group (Umami-NaCl), nor in animals who were conditioned to find Cyx aversive (Cyx-LiCl) due to the already low rate of licking prior to conditioning. All animals showed a significant decrease in the total number of licks of Cyx in the lickometre, regardless of which tastant they were trained to find aversive, showing that animals will learn to decrease their consumption of aversive tastants. This finding shows that Umami-LiCl animals successfully acquired a conditioned aversion to umami after a single pairing of umami with LiCl injection. However, it appears that the CTA protocol did not produce a stronger behavioural aversion to Cyx than is seen inherently in non-conditioned mice. This suggests that the inherent aversive behaviours elicited by bitter taste presentation are not enhanced by CTA training.

In addition to total number of licks, an effect was also seen in the latency until first lick, showing that Cyx-LiCl animals were waiting significantly longer to initiate licking during Cyx trials after their conditioned taste aversion (CTA) training compared to before CTA. This was also seen in all of the other animal groups, though it was only approaching significance ($p = 0.06$), and Umami-LiCl animals also showed a trend of delayed licking initiation for umami trials. This behaviour suggests that the animals are able to learn to detect tastants by some other method than licking, most likely by smell. Although Cyx is not volatile, mice and rats have been shown to use odour cues to avoid extremely high concentrations of Cyx; Hettinger et al. (2007) postulate that they may be detecting its fragrant dimethylcyclohexanone breakdown product, which itself is not aversive.

5.3.1 *Arc* expression after conditioned taste aversion

When analysing the *Arc* response induced by umami and Cyx in the same conditioned animals, it was observed that Umami-LiCl animals showed a significant increase in *Arc* expression following umami taste stimulation, to a similar rate as was shown previously in bitter-stimulated naïve animals, with the same lateral-medial distribution pattern. Additionally, as was observed in the behavioural results, following Cyx taste stimulation Cyx-LiCl mice did not show an increase in *Arc* expression above a level seen in Cyx-stimulated non-conditioned mice. Taken together with the behavioural results from the lickometre, these results suggest that this umami CTA paradigm results in aversive behavioural responses to umami, and a bitter-like increase in *Arc* expression in the PbN, whereas the Cyx CTA paradigm enhances neither the inherent behavioural aversive responses to Cyx, nor the increased *Arc* expression seen in the PbN. This finding echoes the behavioural results and further supports the idea that inherent aversive neural activation and behaviour elicited by bitter taste presentation is not enhanced by CTA training.

Importantly, this finding suggests that *Arc* expression in the PbN is not bitter-specific, as was previously hypothesised by Töle (DIfE, 2014), and extends the function of *Arc* to include umami in umami-averse mice. Although this *Arc* expression is occurring in a similar distribution throughout the PbN compared to the bitter-stimulated *Arc* expression, this does not necessarily suggest that bitter-aversion and conditioned umami-aversion are both processed via the same population of neurons. Instead, it is more likely that both of these aversive substances result in synaptic changes to mediate subsequent behaviour to inhibit further ingestion of the aversive compounds, and that these synaptic changes require *Arc* expression in both inherent and learned aversions. This would mean that the

similarity in *Arc* expression suggests that taste stimulation with these two aversive compounds result in the same plasticity-inducing cellular mechanisms, rather than result in activation of the same neuron population.

The distribution of the neural response to the umami stimulus after CTA in the lateral PbN in this study is consistent with previous research showing c-*fos* immunofluorescence in the lateral PbN following CTA training in multiple studies (Yamamoto, Shimura, Sakai, et al., 1994; Yamamoto et al., 1992; Yamamoto et al., 1993; Yamamoto, Shimura, Sako, et al., 1994). Although this could suggest that increased *Arc* expression is a neural correlate for the "taste aversion" behaviour, it is unlikely that these *Arc* expressing neurons are encoding general averseness, as the initial experiment in naïve animals included an aversive highly concentrated salt solution which did not result in increased *Arc* expression. Bitter-aversion is believed to be a mechanism to alert animals to toxic compounds and CTA training teaches animals to associate nausea and malaise with a taste solution; it is possible that increased *Arc* expression in the PbN is a way to ensure that animals develop accurate taste-associations with compounds that lead to malaise by strengthening synaptic connections between relevant neurons. However, the absence of increased *Arc* response following administration of an aversive salt concentration suggests that not all types of aversion trigger this enhanced synaptic plasticity. This could be due to the different aversion responses elicited by bitter (aversive even at low concentrations) and salt solutions (dose-dependently avoided). As mice determine whether or not to reject a salt stimulus based on the concentration of the stimulus – one high-concentration salt stimulation would not be sufficient to trigger a learned response in the animal to avoid all salt-taste stimuli, and would therefore not require strengthening of synapses at salt-responsive neurons. This could explain the absence of *Arc*-expressing neurons following aversive-salt taste stimulation.

5.4 Distribution and co-expression of secondary probe RNA

Using the new, extended *Arc* catFISH protocol it was observed that calcitonin and glucagon-like peptide 1 receptor (Glp1r) RNA is expressed at a similar rate throughout the lateral and medial subnuclei of the PbN. Hypocretin receptor 1 (Hcrtr1) RNA and gastrin-releasing peptide (Grp) RNA both showed higher levels of expression in the medial PbN, however this difference is only significant for Hcrtr1. Neurotensin (Nts) was evenly distributed throughout the PbN. These were all consistent with results reported in the Allen

Brain Atlas gene explorer (for reference numbers for each probe see section 3.2 Preparation of the neuropeptide probes on page 29).

The rate of neurons co-expressing *Arc* and secondary probe RNA was then calculated for each of the selected candidate neuropeptides. 16 % of bitter-activated *Arc*-expressing neurons co-expressed mRNA for calcitonin, 17 % co-expressed Glp1r, 17 % co-expressed Hcrtr1, 9 % co-expressed Grp, and 20 % co-expressed neurotensin. Of these markers, only neurotensin showed an uneven distribution throughout the subnuclei, showing a significantly higher rate of co-expressing cells in the lateral PbN compared to the medial PbN.

Taken as individual populations of neurons, this would suggest that these five neuropeptides account for approximately 79 % of the bitter-activated *Arc*-expressing neurons in the PbN. However, this is unlikely, as PbN neurons have been shown to co-express multiple neuropeptides within single neurons, this has notably been observed that substance P-like immunoreactive neurons in the external lateral PbN also contain neurotensin and calcitonin gene-related peptide (Shinohara et al., 1988). Previous tracing studies showed that the majority of Calca neurons in the PbN are innervated by Glp1 neurons originating in the NTS (Richard et al., 2014), it is therefore likely that the 16 % of Calca neurons and the 17 % of Glp1r neurons are the same population of neurons. Consistent with this finding, the present study shows no significant difference between the rate of Calca and Glp1r neurons distributed throughout the lateral and medial PbN. However, there was a noticeable trend in the data which suggested a higher rate of Calca neurons in the lateral PbN and a higher rate of Glp1r neurons in the medial PbN. The overlap of these neurons could be confirmed using a control ISH experiment including both of the marker probes to calculate the rate of co-expression.

5.4.1 Possible functions for bitter-responsive Calca and Glp1r PbN neurons

These rates of co-expressing neurons allow insight into the possible functions and projections of the bitter-responsive neuron population in the PbN. The rate of Calca RNA seen in both the lateral and medial subdivisions in this study is congruent with previous findings showing clusters of calcitonin gene-related peptide (CGRP, coded by the *Calca* gene) in both the external lateral and the external medial subnuclei of the PbN (Yasui et al., 1989). The majority of CGRP neurons in the external medial PbN innervate the parvicellular ventroposterior medial nucleus of the thalamus (VPMpc), which is considered to be the main viscerosensory relay to the insular cortex (Cechetto & Saper, 1987) and

CGRP neurons in the external lateral PbN project to the central nucleus of the amygdala and the Bed Nucleus of the Stria Terminalis (BdNST) (Dobolyi et al., 2005). It has also been shown that both stimulation of Glp1r neurons and CGRP neurons in the lateral PbN result in a reduction of food intake (Richard et al., 2014), and that antagonism of Glp1r neurons in the lateral PbN results in increased food intake (Alhadeff et al., 2014). More recently, Carter et al. (2015) observed that optogenetic activation of calcitonin gene-related peptide (CGRP) neurons in the PbN is sufficient to induce a conditioned taste aversion.

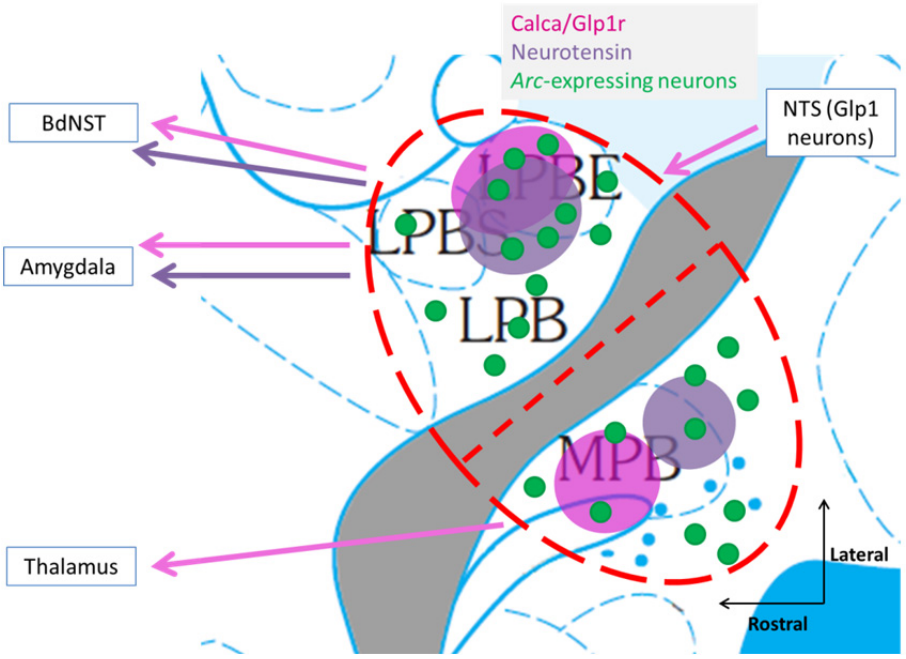

Figure 5.1 Distribution and projections of bitter-responsive *Arc*-expressing neurons co-expressing Calca-, Glp1r-, and Nts RNA.
Clusters of PbN neurons are shown as pink (Calca/Glp1r) and purple (Nts) circles, and their projections are shown with pink and purple arrows.

Taken together, this suggests that 16 – 17 % of bitter-responsive *Arc*-expressing PbN neurons may be processing inherent bitter-aversive responses via CGRP neurons projecting to the amygdala, thalamus, and BdNST, these pathways are known to be involved in physiological and behavioural responses to stress (Davern, 2014; Sink et al., 2011; Yamano et al., 1988) and conditioned taste aversion (Carter et al., 2015; Yamamoto et al., 1990) resulting inhibition of eating behaviours. As the naïve animals included in this study were tasting these bitter compounds for the first time, this suggests that the inherent aversion to bitter compounds may be processed through the same neural pathway that processes LiCl-induced conditioned aversions.

5.4.2 Bitter-activated *Arc*- and Grp-expressing PbN neurons

As in the present study, previous research by Wada et al. (1990) has reported the presence of Grp throughout the lateral PbN, observing the most prominent distribution to occur in the dorsal and internal lateral subnuclei, however the presence or absence of Grp in the medial PbN was not reported. At present the function of Grp specifically within the PbN has not yet been studied, however it has been shown that Grp and closely related peptides reduce food intake either by intracerebroventricular injection (Ladenheim & Ritter, 1988), or intraperitoneal injection (Ladenheim et al., 1996). More specifically, microinjections into the central and basolateral amygdala reduce food intake without altering other behavioural patterns (Vígh, Lénárd, & Fekete, 1999; Vígh, Lénárd, Fekete, et al., 1999). This could mean that the 9 % of bitter-responsive *Arc*- and Grp- expressing neurons observed in this study could be triggering an inhibition of food consumption, this correlates with the classic behavioural responses to bitter compounds which generally elicit avoidance-behaviour. Additionally, though targets of Grp neurons in the PbN have not been studied, based on studies showing that this Grp-induced inhibition of eating involves the amygdala, it is possible that these bitter-responsive *Arc*-/Grp-expressing neurons are innervating the amygdala.

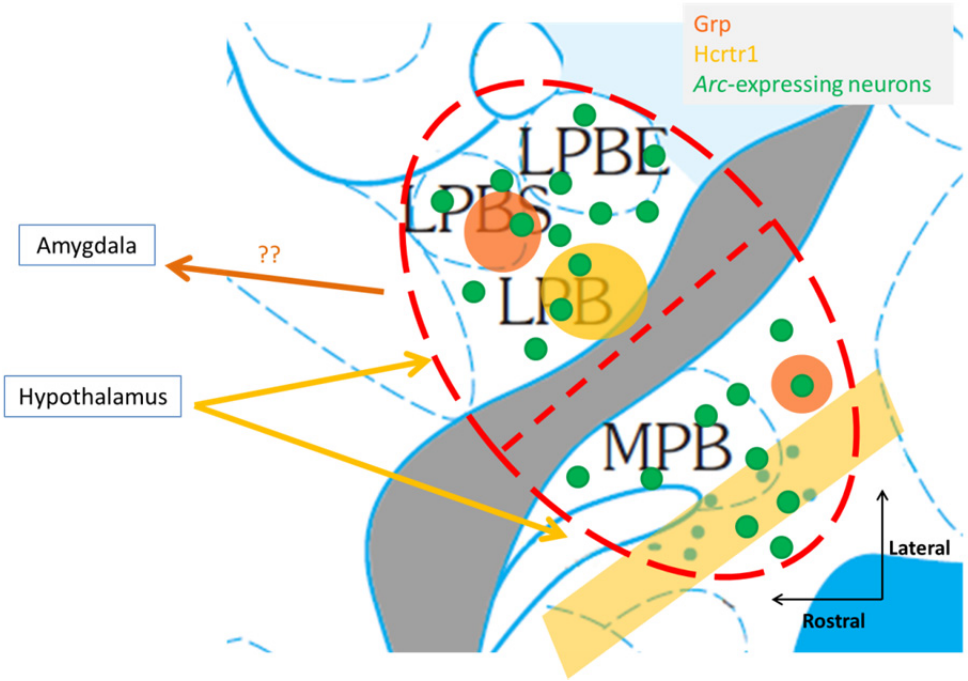

Figure 5.2 Distribution and projections of bitter-responsive *Arc*-expressing neurons co-expressing Grp and Hcrtr1 RNA
Clusters of PbN neurons are shown as orange (Grp neurons) and yellow (Hcrtr1) shapes, and their projections are shown with orange and yellow arrows.

5.4.3 Bitter-activated *Arc*- and Hcrtr1-expressing PbN neurons

Although Hcrtr1 neurons are known to be present in the PbN, possible functions for this population of neurons has not been determined. Peyron et al. (1998) observed a moderate density of hypocretin-immunoreactive fibres in the PbN, however they did not distinguish between the medial and lateral subnuclei. This study expanded on these findings and showed a much larger population of Hcrtr1 neurons in the medial PbN compared to the lateral PbN.

The PbN Hcrtr1 neurons are innervated by hypocretin neurons in the hypothalamus which are involved in multiple autonomic functions including sleep-wakefulness regulation (Adamantidis et al., 2007), food intake (Sakurai et al., 2005), and stress-responses (Bonnavion et al., 2015). Niu et al. (2010) observed that glutamatergic lateral PbN neurons innervate the lateral-most part of the dorsomedial nucleus and dorsal perifornical area. Interestingly, where Niu et al. (2010) showed lateral PbN neurons innervating the hypothalamus, the present study showed a denser population of Hcrtr1 neurons in the medial PbN suggesting that there may be bi-directional modulation of PbN function via the hypocretin system.

Although more Hcrtr1 receptors were observed in the medial PbN, Hcrtr1 cells co-expressing *Arc* RNA were distributed evenly throughout both the lateral and medial subnuclei of the PbN. However, in terms of percentage of *Arc*-expressing neurons, Hcrtr1 RNA was co-expressed in 20 % of medial PbN bitter-activated *Arc*-expressing neurons, representing the largest proportion of bitter-activated neurons in the medial PbN in this study. This suggests that a fifth of bitter-responsive neurons in the "gustatory" medial PbN are modulated via hypothalamic hypocretin neurons. Considering the known functions of hypocretin neurons and behavioural evidence of stress-mediated changes in taste perception has been seen in humans (Al'absi et al., 2012; Ileri-Gurel et al., 2013; Nakagawa et al., 1996), this could suggest that the hypothalamic mediation of neural responses to taste-stimulation may be modulated by stress-/sleep-/nutritional-status via the hypocretin system.

5.4.4 Bitter-activated *Arc*- and neurotensin-expressing PbN neurons

The neuropeptide that showed the highest rate of RNA co-expression with *Arc* was neurotensin, accounting for 20 % of the bitter-activated *Arc*-expressing neurons. Neurotensin-like immunoreactivity has been observed most densely in the NTS, amygdala,

BdNST, and parabrachial nucleus (Jennes et al., 1982; Moga & Gray, 1985; Moga et al., 1989). Athough neurotensin has not been reported in the medial PbN, researchers investigating the lateral PbN, such as Yamano et al. (1988), show representative images which clearly show neurotensin-like immunoreactivity present in the medial PbN. Interestingly, a cluster of neurotensin neurons in the external lateral PbN has been shown to co-express calcitonin gene-related peptide, though this is not true for neurotensin neurons in other subdivisions of the PbN (Shinohara et al., 1988; Yamano et al., 1988). Similarly to CGRP neurons, lateral PbN neurotensin neurons innervate the amygdala and the BdNST (Yamano et al., 1988).

Neurotensin has been implicated in regulating cardiovascular function (Ciriello & Zhang, 1997). This function is of particular interest with regard to the present study, as oral quinine administration triggers increased instantaneous heart rate and skin temperature in human subjects (Rousmans et al., 2000). Therefore it is possible that the neurons co-expressing *Arc* and neurotensin RNA following bitter-taste stimulation could be triggering cardiovascular responses to the bitter compound; however, bitter compounds are not the only tastants that elicit cardiovascular responses. Indeed, humans show a greater increase in heart rate in response to citric acid administration than to bitter compounds (Horio, 2000), whereas naïve animals do not show increased *Arc*-expression following taste stimulation with citric acid (Sour stimulus). This discrepancy could, however, be due to different stimulus concentrations, or different species of subject.

This high rate of co-expression with neurotensin neurons also provides a possible mechanism for *Arc* induction. *Arc* expression in the hippocampus occurs after high-frequency stimulation (Steward et al., 1998), and it is believed that a certain stimulation threshold is required for *Arc* induction to occur, though this threshold has not been determined for PbN neurons. Neurotensin has been shown to dose-dependently, and reversibly enhance several glutamate-mediated neuronal actions in the PbN (such as glutamate-mediated, excitatory post-synaptic currents) (Saleh et al., 1997). This could be one of the mechanisms involved in triggering the increased *Arc* expression following different taste stimulations by enhancing neuronal activation to a frequency that results in *Arc* induction. It is possible that neurotensin in the nucleus of the solitary tract and the PbN are enhancing neural signals along the gustatory pathway, thereby inducing *Arc* expression and triggering enhanced synaptic plasticity following bitter taste stimulation. This would allow animals to form memories relevant to the taste experience to modulate future food-seeking behaviours.

5.5 The function of *Arc*-expressing PbN neurons

The findings in this study suggest that the increased *Arc* expression observed following taste stimulation with bitter stimuli, and umami in umami-averse mice, may represent a state of enhanced neural plasticity. Considering that *Arc* regulates synaptic strength (for review see Bramham et al., 2008; Okuno, 2011; Shepherd & Bear, 2011), this enhanced state of neural plasticity would suggest that these *Arc*-inducing taste events could be resulting in the strengthening of synapses connecting relevant aversive-taste-activated neurons. Strengthening these bitter-activated neural connections would result in a greater salience for tastes associated with potential poisons, making them more prominent, requiring more attention than other stimuli.

In light of the functional role of *Arc* in CTA learning, and as a marker for synaptic plasticity, the theory that this bitter- or aversive-specific increase in *Arc* expression represents an enhanced salience to dangerous stimuli is compelling; however poisonous compounds are not the only taste stimuli that require attention. The inability to recognise rewards appropriately can lead to starvation (Palmiter, 2008), so positive or rewarding food sources also require salience. If this hypothesis that *Arc* expression correlates to compound-salience is true, *Arc* expression in the PbN would change according to the nutritional status of the animal, for example, animals in a state of starvation would require increased salience for high-calorie food sources. If this hypothesis is true, food deprived mice would show a higher rate of *Arc* expressing neurons in the PbN in response to sucrose compared to the mice used in the present study that were being fed ad libitum. This could be explored in further experiments observing *Arc*-expression in animals in a variety of different nutritional states.

The co-expression results presented in this study suggest multiple possible functions for the bitter-responsive *Arc*-expressing neurons in the PbN. The cluster occurring in the most-lateral area of the PbN is likely a cluster of Calca-, Glp1r-, and neurotensin-expressing neurons innervating amygdala and BdNST neurons involved in the neural processing of taste aversions. To confirm these, and any additional targets of bitter-responsive *Arc*-expressing PbN neurons, the *Arc* catFISH method could be adapted to incorporate a tracing study. For example, NTS or PbN neurons could be injected with neural tracers such as wheat germ agglutinin-horseradish peroxidase conjugate or phaseolus vulgaris-leucoagglutinin approximately 2 or 9 days before sacrifice, respectively

(Herbert et al., 1990), to observe how many of these *Arc*-expressing neurons are innervated directly by NTS neurons.

There are also likely to be additional bitter-responsive neurotensin neurons in the lateral and medial PbN, possibly mediating cardiovascular and respiratory responses to stress via the amygdala. Additionally, the co-expression of Hcrtr1 with 17 % of the bitter-activated *Arc*-expressing cells suggests that the function of these neurons is mediated by hypothalamic signalling via the hypocretin circuit. Though this research has shown the involvement of several genes in these bitter-responsive PbN neurons, based on the rate of *Arc* expression and the rate of co-expression of each of these genes, it is clear that there must be additional neuropeptides involved in this neural activation. Future studies could further explore the molecular characteristics of these neurons, in particular, recent evidence of genes from the taste receptor 2 family (Tas2r genes) in the brain (Stolzenburg, 2016; Voigt, Bojahr, et al., 2015; Voigt, Hübner, et al., 2015) raise the possibility of investigating the co-expression of bitter taste receptor Tas2r131 RNA in bitter-responsive *Arc*-expressing neurons, using the double-FISH protocol used in this study.

The present study has shown that *Arc* expression in the PbN following bitter- and aversive umami-taste stimulation appears to represent long-term cellular changes resulting from the taste stimulation event. The observation that this increase in plasticity occurs inherently following bitter taste stimulation, suggests that bitter taste stimulation may improve the ability to associate post-ingestive effects with taste experiences, thus mediating future food-seeking behaviours by inducing synaptic plasticity. This would suggest that food-seeking behaviours and strong food attractions or aversions could be manipulated by inhibiting or inducing synaptic plasticity in the PbN during food intake. Considering the relevance of this research for treating human food-choice behaviours it is important to consider possible species-differences in gustatory processing; the most notable difference between rodents and primates comes from an early study suggesting that gustatory NTS projections bypass the PbN in primates and project directly to the gustatory thalamic NTS targets, suggesting that the primate PbN processes predominantly non-gustatory responses to food or taste stimuli (Beckstead et al., 1980). These non-gustatory processes may be triggering reward circuitry or aversive responses and could play an important role in mediating food-choices. Further exploration of the neuropeptides involved in mediating these behaviours could lead researchers to uncover possible pharmacological targets for manipulating or improving food-choice behaviours that result in metabolic dysfunction or malnutrition.

5.5.1 Summary

The results of these experiments indicate that bitter taste stimulation results in a state of enhanced neural plasticity in the PbN, this can also be induced by taste solutions that have previously been paired with LiCl, subsequently inducing malaise. This could possibly represent an increased salience for taste experiences involving bitter taste stimulation or stimulation with tastes that have previously resulted in malaise, allowing the animals to strengthen relevant neural pathways for responding appropriately to these tastes.

Literature

Adamantidis, A. R., Zhang, F., Aravanis, A. M., Deisseroth, K., & De Lecea, L. (2007). Neural substrates of awakening probed with optogenetic control of hypocretin neurons. *Nature, 450*(7168), 420-424.

Adler, E., Hoon, M. A., Mueller, K. L., Chandrashekar, J., Ryba, N. J., & Zuker, C. S. (2000). A novel family of mammalian taste receptors. *Cell, 100*(6), 693-702.

Al'absi, M., Nakajima, M., Hooker, S., Wittmers, L., & Cragin, T. (2012). Exposure to acute stress is associated with attenuated sweet taste. *Psychophysiology, 49*(1), 96-103.

Alhadeff, A. L., Baird, J. P., Swick, J. C., Hayes, M. R., & Grill, H. J. (2014). Glucagon-like Peptide-1 receptor signaling in the lateral parabrachial nucleus contributes to the control of food intake and motivation to feed. *Neuropsychopharmacology, 39*(9), 2233-2243. doi: 10.1038/npp.2014.74

Barot, S. K., Chung, A., Kim, J. J., & Bernstein, I. L. (2009). Functional imaging of stimulus convergence in amygdalar neurons during Pavlovian fear conditioning. *PLoS One, 4*(7), e6156.

Barretto, R. P., Gillis-Smith, S., Chandrashekar, J., Yarmolinsky, D. A., Schnitzer, M. J., Ryba, N. J., & Zuker, C. S. (2015). The neural representation of taste quality at the periphery. *Nature, 517*(7534), 373-376. doi: 10.1038/nature13873

Beckstead, R. M., Morse, J. R., & Norgren, R. (1980). The nucleus of the solitary tract in the monkey: projections to the thalamus and brain stem nuclei. *Journal of Comparative Neurology, 190*(2), 259-282.

Bonnavion, P., Jackson, A. C., Carter, M. E., & de Lecea, L. (2015). Antagonistic interplay between hypocretin and leptin in the lateral hypothalamus regulates stress responses. *Nature communications, 6*.

Boucher, Y., Simons, C. T., Faurion, A., Azérad, J., & Carstens, E. (2003). Trigeminal modulation of gustatory neurons in the nucleus of the solitary tract. *Brain Research, 973*(2), 265-274.

Bramham, C. R., Worley, P. F., Moore, M. J., & Guzowski, J. F. (2008). The immediate early gene arc/arg3.1: regulation, mechanisms, and function. *J Neurosci, 28*(46), 11760-11767. doi: 10.1523/JNEUROSCI.3864-08.2008

Breslin, P. A., & Spector, A. C. (2008). Mammalian taste perception. *Curr Biol, 18*(4), R148-155. doi: 10.1016/j.cub.2007.12.017

Carpenter-Hyland, E. P., Plummer, T. K., Vazdarjanova, A., & Blake, D. T. (2010). Arc expression and neuroplasticity in primary auditory cortex during initial learning are inversely related to neural activity. *Proceedings of the National Academy of Sciences, 107*(33), 14828-14832.

Carter, M. E., Han, S., & Palmiter, R. D. (2015). Parabrachial calcitonin gene-related Peptide neurons mediate conditioned taste aversion. *J Neurosci, 35*(11), 4582-4586. doi: 10.1523/JNEUROSCI.3729-14.2015

Carter, M. E., Soden, M. E., Zweifel, L. S., & Palmiter, R. D. (2013). Genetic identification of a neural circuit that suppresses appetite. *Nature, 503*(7474), 111-114. doi: 10.1038/nature12596

Cartoni, C., Yasumatsu, K., Ohkuri, T., Shigemura, N., Yoshida, R., Godinot, N., . . . Damak, S. (2010). Taste preference for fatty acids is mediated by GPR40 and GPR120. *J Neurosci, 30*(25), 8376-8382. doi: 10.1523/JNEUROSCI.0496-10.2010

Caterina, M. J., Schumacher, M. A., Tominaga, M., Rosen, T. A., Levine, J. D., & Julius, D. (1997). The capsaicin receptor: a heat-activated ion channel in the pain pathway. *Nature, 389*(6653), 816-824. doi: 10.1038/39807

Cechetto, D. F., & Saper, C. B. (1987). Evidence for a viscerotopic sensory representation in the cortex and thalamus in the rat. *Journal of Comparative Neurology, 262*(1), 27-45. doi: 10.1002/cne.902620104

Chamberlin, N. L., & Saper, C. B. (1994). Topographic organization of respiratory responses to glutamate microstimulation of the parabrachial nucleus in the rat. *J Neurosci, 14*(11 Pt 1), 6500-6510.

Chandrashekar, J., Kuhn, C., Oka, Y., Yarmolinsky, D. A., Hummler, E., Ryba, N. J., & Zuker, C. S. (2010). The cells and peripheral representation of sodium taste in mice. *Nature, 464*(7286), 297-301. doi: 10.1038/nature08783

Chen, X., Gabitto, M., Peng, Y., Ryba, N. J., & Zuker, C. S. (2011). A gustotopic map of taste qualities in the mammalian brain. *Science, 333*(6047), 1262-1266. doi: 10.1126/science.1204076

Chomczynski, P., & Sacchi, N. (1987). Single-step method of RNA isolation by acid guanidinium thiocyanate-phenol-chloroform extraction. *Analytical Biochemistry, 162*(1), 156-159. doi: http://dx.doi.org/10.1016/0003-2697(87)90021-2

Chowdhury, S., Shepherd, J. D., Okuno, H., Lyford, G., Petralia, R. S., Plath, N., . . . Worley, P. F. (2006). Arc/Arg3. 1 interacts with the endocytic machinery to regulate AMPA receptor trafficking. *Neuron, 52*(3), 445-459.

Ciriello, J., & Zhang, T.-X. (1997). Cardiovascular effects of neurotensin microinjections into the nucleus of the solitary tract. *Brain Research, 749*(1), 35-43. doi: http://dx.doi.org/10.1016/S0006-8993(96)01176-6

Conte, C., Ebeling, M., Marcuz, A., Nef, P., & Andres-Barquin, P. J. (2003). Evolutionary relationships of the Tas2r receptor gene families in mouse and human. *Physiological genomics, 14*(1), 73-82.

Contreras, R. J., Beckstead, R. M., & Norgren, R. (1982). The central projections of the trigeminal, facial, glossopharyngeal and vagus nerves: an autoradiographic study in the rat. *J Auton Nerv Syst, 6*(3), 303-322.

Cullinan, W. E., Herman, J. P., Battaglia, D. F., Akil, H., & Watson, S. (1995). Pattern and time course of immediate early gene expression in rat brain following acute stress. *Neuroscience, 64*(2), 477-505.

Dalton, P., Doolittle, N., Nagata, H., & Breslin, P. A. (2000). The merging of the senses: integration of subthreshold taste and smell. *Nat Neurosci, 3*(5), 431-432. doi: 10.1038/74797

Danilova, V., Danilov, Y., Roberts, T., Tinti, J.-M., Nofre, C., & Hellekant, G. (2002). Sense of taste in a new world monkey, the common marmoset: recordings from the chorda tympani and glossopharyngeal nerves. *Journal of Neurophysiology, 88*(2), 579-594.

Danilova, V., & Hellekant, G. (2004). Sense of taste in a New World monkey, the common marmoset. II. Link between behavior and nerve activity. *Journal of Neurophysiology, 92*(2), 1067-1076.

Davern, P. J. (2014). A role for the lateral parabrachial nucleus in cardiovascular function and fluid homeostasis. *Front Physiol, 5*, 436. doi: 10.3389/fphys.2014.00436

De Araujo, I. E., Kringelbach, M. L., Rolls, E. T., & McGlone, F. (2003). Human cortical responses to water in the mouth, and the effects of thirst. *Journal of Neurophysiology, 90*(3), 1865-1876.

Deisseroth, K. (2011). Optogenetics. *Nature methods, 8*(1), 26-29.

Deshpande, D. A., Wang, W. C., McIlmoyle, E. L., Robinett, K. S., Schillinger, R. M., An, S. S., . . . Liggett, S. B. (2010). Bitter taste receptors on airway smooth muscle bronchodilate by localized calcium signaling and reverse obstruction. *Nat Med, 16*(11), 1299-1304. doi: 10.1038/nm.2237

Di Lorenzo, P. M., Chen, J.-Y., & Victor, J. D. (2009). Quality time: representation of a multidimensional sensory domain through temporal coding. *The Journal of Neuroscience, 29*(29), 9227-9238.

Di Lorenzo, P. M., Hallock, R. M., & Kennedy, D. P. (2003). Temporal coding of sensation: mimicking taste quality with electrical stimulation of the brain. *Behavioral Neuroscience, 117*(6), 1423.

Di Lorenzo, P. M., & Victor, J. D. (2003). Taste response variability and temporal coding in the nucleus of the solitary tract of the rat. *J Neurophysiol, 90*(3), 1418-1431. doi: 10.1152/jn.00177.2003

Di Lorenzo, P. M., & Victor, J. D. (2007). Neural coding mechanisms for flow rate in taste-responsive cells in the nucleus of the solitary tract of the rat. *J Neurophysiol, 97*(2), 1857-1861. doi: 10.1152/jn.00910.2006

DiPatrizio, N. V., & Simansky, K. J. (2008). Activating parabrachial cannabinoid CB1 receptors selectively stimulates feeding of palatable foods in rats. *J Neurosci, 28*(39), 9702-9709. doi: 10.1523/JNEUROSCI.1171-08.2008

Dobolyi, A., Irwin, S., Makara, G., Usdin, T. B., & Palkovits, M. (2005). Calcitonin gene-related peptide-containing pathways in the rat forebrain. *Journal of Comparative Neurology, 489*(1), 92-119.

Elias, C. F., Kelly, J. F., Lee, C. E., Ahima, R. S., Drucker, D. J., Saper, C. B., & Elmquist, J. K. (2000). Chemical characterization of leptin-activated neurons in the rat brain. *J Comp Neurol, 423*(2), 261-281. doi: 10.1002/1096-9861(20000724)423:2<261::AID-CNE6>3.0.CO;2-6

Emmers, R., Benjamin, R. M., & Blomquist, A. J. (1962). Thalamic localization of afferents from the tongue in albino rat. *Journal of Comparative Neurology, 118*(1), 43-48.

Erickson, R. P. (2008). A study of the science of taste: On the origins and influence of the core ideas. *Behavioral and Brain Sciences, 31*(01), 59-75.

Farbman, A. I. (1965). Fine Structure of the Taste Bud. *J Ultrastruct Res, 12*(3), 328-350.

Foster, S. R., Blank, K., See Hoe, L. E., Behrens, M., Meyerhof, W., Peart, J. N., & Thomas, W. G. (2014). Bitter taste receptor agonists elicit G-protein-dependent negative inotropy in the murine heart. *FASEB J, 28*(10), 4497-4508. doi: 10.1096/fj.14-256305

Foster, S. R., Porrello, E. R., Purdue, B., Chan, H. W., Voigt, A., Frenzel, S., . . . Thomas, W. G. (2013). Expression, regulation and putative nutrient-sensing function of taste GPCRs in the heart. *PLoS One, 8*(5), e64579. doi: 10.1371/journal.pone.0064579

Fowler, T., Sen, R., & Roy, A. L. (2011). Regulation of primary response genes. *Molecular cell, 44*(3), 348-360.

Frank, M. E. (1991). Taste-responsive neurons of the glossopharyngeal nerve of the rat. *Journal of Neurophysiology, 65*(6), 1452-1463.

Frank, M. E., Bouverat, B. P., MacKinnon, B. I., & Hettinger, T. P. (2004). The distinctiveness of ionic and nonionic bitter stimuli. *Physiol Behav, 80*(4), 421-431.

Franklin, K., & Paxinos, D. (2007). The Mouse Brain Stereotaxic Coordinates. Elsevier Academic Press. *San Diego, CA, USA*.

Fulwiler, C. E., & Saper, C. B. (1984). Subnuclear organization of the efferent connections of the parabrachial nucleus in the rat. *Brain Res, 319*(3), 229-259. doi: http://dx.doi.org/10.1016/0165-0173(84)90012-2

Galindo, M. M., Voigt, N., Stein, J., van Lengerich, J., Raguse, J. D., Hofmann, T., . . . Behrens, M. (2012). G protein-coupled receptors in human fat taste perception. *Chem Senses, 37*(2), 123-139. doi: 10.1093/chemse/bjr069

Garfield, A. S., Shah, B. P., Madara, J. C., Burke, L. K., Patterson, C. M., Flak, J., . . . Heisler, L. K. (2014). A parabrachial-hypothalamic cholecystokinin neurocircuit

controls counterregulatory responses to hypoglycemia. *Cell Metab, 20*(6), 1030-1037. doi: 10.1016/j.cmet.2014.11.006
Geerling, J., Kim, M., Agostinelli, L., & Scammell, T. (2015). Genetic identity of warm and cool thermosensory relay neurons in the mouse parabrachial nucleus. *Faseb Journal, 29*(1 Supplement).
Geerling, J. C., Kim, M. Y., Mahoney, C. E., Abbott, S. B., Agostinelli, L. J., Garfield, A. S., . . . Scammell, T. E. (2015). Genetic identity of thermosensory relay neurons in the lateral parabrachial nucleus. *Am J Physiol Regul Integr Comp Physiol*, ajpregu 00094 02015. doi: 10.1152/ajpregu.00094.2015
Glendinning, J. I. (1993). Preference and aversion for deterrent chemicals in two species of Peromyscus mouse. *Physiol Behav, 54*(1), 141-150.
Glendinning, J. I., Davis, A., & Ramaswamy, S. (2002). Contribution of different taste cells and signaling pathways to the discrimination of "bitter" taste stimuli by an insect. *J Neurosci, 22*(16), 7281-7287. doi: 20026695
Glendinning, J. I., Gresack, J., & Spector, A. C. (2002). A High-throughput Screening Procedure for Identifying Mice with Aberrant Taste and Oromotor Function. *Chemical Senses, 27*(5), 461-474. doi: 10.1093/chemse/27.5.461
Glendinning, J. I., Yiin, Y. M., Ackroff, K., & Sclafani, A. (2008). Intragastric infusion of denatonium conditions flavor aversions and delays gastric emptying in rodents. *Physiol Behav, 93*(4-5), 757-765. doi: 10.1016/j.physbeh.2007.11.029
Go, Y., Satta, Y., Takenaka, O., & Takahata, N. (2005). Lineage-specific loss of function of bitter taste receptor genes in humans and nonhuman primates. *Genetics, 170*(1), 313-326.
Guzowski, J. F., Lyford, G. L., Stevenson, G. D., Houston, F. P., McGaugh, J. L., Worley, P. F., & Barnes, C. A. (2000). Inhibition of activity-dependent arc protein expression in the rat hippocampus impairs the maintenance of long-term potentiation and the consolidation of long-term memory. *The Journal of Neuroscience, 20*(11), 3993-4001.
Guzowski, J. F., McNaughton, B. L., Barnes, C. A., & Worley, P. F. (1999). Environment-specific expression of the immediate-early gene Arc in hippocampal neuronal ensembles. *Nat Neurosci, 2*(12), 1120-1124. doi: 10.1038/16046
Halsell, C. B., & Travers, S. P. (1997). Anterior and posterior oral cavity responsive neurons are differentially distributed among parabrachial subnuclei in rat. *J Neurophysiol, 78*(2), 920-938.
Hamilton, R. B., & Norgren, R. (1984). Central projections of gustatory nerves in the rat. *J Comp Neurol, 222*(4), 560-577. doi: 10.1002/cne.902220408
Han, S., Soleiman, Matthew T., Soden, Marta E., Zweifel, Larry S., & Palmiter, Richard D. (2015). Elucidating an Affective Pain Circuit that Creates a Threat Memory. *Cell, 162*(2), 363-374. doi: http://dx.doi.org/10.1016/j.cell.2015.05.057
Hanamori, T., & Smith, D. V. (1989). Gustatory innervation in the rabbit: central distribution of sensory and motor components of the chorda tympani, glossopharyngeal, and superior laryngeal nerves. *J Comp Neurol, 282*(1), 1-14. doi: 10.1002/cne.902820102
Hellekant, G., Ninomiya, Y., & Danilova, V. (1998). Taste in chimpanzees. III: Labeled-line coding in sweet taste. *Physiology & Behavior, 65*(2), 191-200.
Herbert, H., Moga, M. M., & Saper, C. B. (1990). Connections of the parabrachial nucleus with the nucleus of the solitary tract and the medullary reticular formation in the rat. *J Comp Neurol, 293*(4), 540-580. doi: 10.1002/cne.902930404
Herbert, H., & Saper, C. B. (1990). Cholecystokinin-, galanin-, and corticotropin-releasing factor-like immunoreactive projections from the nucleus of the solitary tract to the

parabrachial nucleus in the rat. *J Comp Neurol, 293*(4), 581-598. doi: 10.1002/cne.902930405
Hettinger, T. P., Formaker, B. K., & Frank, M. E. (2007). Cycloheximide: no ordinary bitter stimulus. *Behavioural Brain Research, 180*(1), 4-17.
Hoffman, G. E., Smith, M. S., & Verbalis, J. G. (1993). c-Fos and related immediate early gene products as markers of activity in neuroendocrine systems. *Frontiers in Neuroendocrinology, 14*(3), 173-213.
Hopkins, D. A., & Holstege, G. (1978). Amygdaloid projections to the mesencephalon, pons and medulla oblongata in the cat. *Exp Brain Res, 32*(4), 529-547.
Horio, T. (2000). Effects of Various Taste Stimuli on Heart Rate in Humans. *Chemical Senses, 25*(2), 149-153. doi: 10.1093/chemse/25.2.149
Huang, A. L., Chen, X., Hoon, M. A., Chandrashekar, J., Guo, W., Trankner, D., . . . Zuker, C. S. (2006). The cells and logic for mammalian sour taste detection. *Nature, 442*(7105), 934-938. doi: 10.1038/nature05084
Ileri-Gurel, E., Pehlivanoglu, B., & Dogan, M. (2013). Effect of acute stress on taste perception: in relation with baseline anxiety level and body weight. *Chemical Senses, 38*(1), 27-34. doi: 10.1093/chemse/bjs075
Inberg, S., Elkobi, A., Edri, E., & Rosenblum, K. (2013). Taste familiarity is inversely correlated with Arc/Arg3. 1 hemispheric lateralization. *The Journal of Neuroscience, 33*(28), 11734-11743.
Jennes, L., Stumpf, W. E., & Kalivas, P. W. (1982). Neurotensin: topographical distribution in rat brain by immunohistochemistry. *Journal of Comparative Neurology, 210*(3), 211-224.
John, S. J. S., Pour, L., & Boughter, J. D. (2005). Phenylthiocarbamide produces conditioned taste aversions in mice. *Chemical Senses, 30*(5), 377-382.
Kelly, M. P., & Deadwyler, S. A. (2002). Acquisition of a novel behavior induces higher levels of arc mRNA than does overtrained performance. *Neuroscience, 110*(4), 617-626. doi: 10.1016/S0306-4522(01)00605-4
Kinnamon, J. C. (1987). Organization and innervation of taste buds. *Neurobiology of taste and smell*, 277-297.
Kosar, E., Grill, H. J., & Norgren, R. (1986a). Gustatory cortex in the rat. I. Physiological properties and cytoarchitecture. *Brain Research, 379*(2), 329-341.
Kosar, E., Grill, H. J., & Norgren, R. (1986b). Gustatory cortex in the rat. II. Thalamocortical projections. *Brain Research, 379*(2), 342-352.
Krimm, R. F., & Hill, D. L. (1998). Quantitative Relationships between Taste Bud Development and Gustatory Ganglion Cellsa. *Annals of the New York Academy of Sciences, 855*(1), 70-75.
Ladenheim, E. E., & Ritter, R. C. (1988). Low-dose fourth ventricular bombesin selectively suppresses food intake. *American Journal of Physiology-Regulatory, Integrative and Comparative Physiology, 255*(6), R988-R993.
Ladenheim, E. E., Wirth, K. E., & Moran, T. H. (1996). Receptor subtype mediation of feeding suppression by bombesin-like peptides. *Pharmacology Biochemistry and Behavior, 54*(4), 705-711.
Lawless, H. T., Schlake, S., Smythe, J., Lim, J., Yang, H., Chapman, K., & Bolton, B. (2004). Metallic taste and retronasal smell. *Chem Senses, 29*(1), 25-33.
Lawless, H. T., Stevens, D. A., Chapman, K. W., & Kurtz, A. (2005). Metallic taste from electrical and chemical stimulation. *Chem Senses, 30*(3), 185-194. doi: 10.1093/chemse/bji014
Lemon, C. H., & Margolskee, R. F. (2009). Contribution of the T1r3 taste receptor to the response properties of central gustatory neurons. *Journal of Neurophysiology, 101*(5), 2459-2471.

Lemon, C. H., & Smith, D. V. (2005). Neural representation of bitter taste in the nucleus of the solitary tract. *Journal of Neurophysiology, 94*(6), 3719-3729.
Lewandowski, B. C., Sukumaran, S. K., Margolskee, R. F., & Bachmanov, A. A. (2016). Amiloride-Insensitive Salt Taste Is Mediated by Two Populations of Type III Taste Cells with Distinct Transduction Mechanisms. *The Journal of Neuroscience, 36*(6), 1942-1953.
Li, F. (2013). Taste perception: from the tongue to the testis. *Mol Hum Reprod, 19*(6), 349-360. doi: 10.1093/molehr/gat009
Li, F., & Zhou, M. (2012). Depletion of bitter taste transduction leads to massive spermatid loss in transgenic mice. *Mol Hum Reprod, 18*(6), 289-297. doi: 10.1093/molehr/gas005
Li, X., Staszewski, L., Xu, H., Durick, K., Zoller, M., & Adler, E. (2002). Human receptors for sweet and umami taste. *Proc Natl Acad Sci U S A, 99*(7), 4692-4696. doi: 10.1073/pnas.072090199
Link, W., Konietzko, U., Kauselmann, G., Krug, M., Schwanke, B., Frey, U., & Kuhl, D. (1995). Somatodendritic expression of an immediate early gene is regulated by synaptic activity. *Proceedings of the National Academy of Sciences, 92*(12), 5734-5738.
Liu, Y., Allen, G. V., & Downie, J. W. (2007). Parabrachial nucleus influences the control of normal urinary bladder function and the response to bladder irritation in rats. *Neuroscience, 144*(2), 731-742. doi: 10.1016/j.neuroscience.2006.09.051
Loewy, A., & Burton, H. (1978). Nuclei of the solitary tract: efferent projections to the lower brain stem and spinal cord of the cat. *Journal of Comparative Neurology, 181*(2), 421-449.
Lyford, G. L., Yamagata, K., Kaufmann, W. E., Barnes, C. A., Sanders, L. K., Copeland, N. G., . . . Worley, P. F. (1995). Arc, a growth factor and activity-regulated gene, encodes a novel cytoskeleton-associated protein that is enriched in neuronal dendrites. *Neuron, 14*(2), 433-445.
McCaughey, S. A. (2007). Taste-evoked responses to sweeteners in the nucleus of the solitary tract differ between C57BL/6ByJ and 129P3/J mice. *The Journal of Neuroscience, 27*(1), 35-45.
McKemy, D. D., Neuhausser, W. M., & Julius, D. (2002). Identification of a cold receptor reveals a general role for TRP channels in thermosensation. *Nature, 416*(6876), 52-58. doi: 10.1038/nature719
Meyerhof, W., Batram, C., Kuhn, C., Brockhoff, A., Chudoba, E., Bufe, B., . . . Behrens, M. (2010). The molecular receptive ranges of human TAS2R bitter taste receptors. *Chemical Senses, 35*(2), 157-170.
Miller, I. J., & Smith, D. V. (1984). Quantitative taste bud distribution in the hamster. *Physiology & Behavior, 32*(2), 275-285.
Miller, I. J., & Spangler, K. M. (1982). Taste bud distribution and innervation on the palate of the rat. *Chemical Senses, 7*(1), 99-108.
Mistretta, C. M. (1984). Aging Effects on Anatomy and Neurophysiology of Taste and Smell1. *Gerodontology, 3*(2), 131-136.
Moga, M. M., & Gray, T. S. (1985). Evidence for corticotropin-releasing factor, neurotensin, and somatostatin in the neural pathway from the central nucleus of the amygdala to the parabrachial nucleus. *Journal of Comparative Neurology, 241*(3), 275-284.
Moga, M. M., Saper, C. B., & Gray, T. S. (1989). Bed nucleus of the stria terminalis: cytoarchitecture, immunohistochemistry, and projection to the parabrachial nucleus in the rat. *J Comp Neurol, 283*(3), 315-332. doi: 10.1002/cne.902830302

Montag-Sallaz, M., Welzl, H., Kuhl, D., Montag, D., & Schachner, M. (1999). Novelty-induced increased expression of immediate-early genes c-fos and arg 3.1 in the mouse brain. *Journal of neurobiology, 38*(2), 234.

Myers, K. P., & Sclafani, A. (2003). Conditioned acceptance and preference but not altered taste reactivity responses to bitter and sour flavors paired with intragastric glucose infusion. *Physiology & Behavior, 78*(2), 173-183.

Nakagawa, M., Mizuma, K., & Inui, T. (1996). Changes in taste perception following mental or physical stress. *Chemical Senses, 21*(2), 195-200.

Ninomiya, Y. (1998). Reinnervation of cross-regenerated gustatory nerve fibers into amiloride-sensitive and amiloride-insensitive taste receptor cells. *Proc Natl Acad Sci U S A, 95*(9), 5347-5350.

Niu, J. G., Yokota, S., Tsumori, T., Qin, Y., & Yasui, Y. (2010). Glutamatergic lateral parabrachial neurons innervate orexin-containing hypothalamic neurons in the rat. *Brain Res, 1358*, 110-122. doi: 10.1016/j.brainres.2010.08.056

Norgren, R., & Leonard, C. M. (1973). Ascending central gustatory pathways. *Journal of Comparative Neurology, 150*(2), 217-237.

Norgren, R., & Pfaffmann, C. (1975). The pontine taste area in the rat. *Brain Res, 91*(1), 99-117.

Ogawa, H., Hayama, T., & Ito, S. (1987). Response properties of the parabrachio-thalamic taste and mechanoreceptive neurons in rats. *Experimental Brain Research, 68*(3), 449-457. doi: 10.1007/BF00249789

Okuno, H. (2011). Regulation and function of immediate-early genes in the brain: beyond neuronal activity markers. *Neuroscience Research, 69*(3), 175-186.

Palmiter, R. D. (2008). Dopamine signaling in the dorsal striatum is essential for motivated behaviors. *Annals of the New York Academy of Sciences, 1129*(1), 35-46.

Paran, N., Mattern, C. F., & Henkin, R. I. (1975). Ultrastructure of the taste bud of the human fungiform papilla. *Cell Tissue Res, 161*(1), 1-10.

Paues, J., Engblom, D., Mackerlova, L., Ericsson-Dahlstrand, A., & Blomqvist, A. (2001). Feeding-related immune responsive brain stem neurons: association with CGRP. *Neuroreport, 12*(11), 2399-2403.

Paues, J., Mackerlova, L., & Blomqvist, A. (2006). Expression of melanocortin-4 receptor by rat parabrachial neurons responsive to immune and aversive stimuli. *Neuroscience, 141*(1), 287-297.

Peng, Y., Gillis-Smith, S., Jin, H., Trankner, D., Ryba, N. J., & Zuker, C. S. (2015). Sweet and bitter taste in the brain of awake behaving animals. *Nature, 527*(7579), 512-515. doi: 10.1038/nature15763

Pérez-Cadahía, B., Drobic, B., & Davie, J. (2011). Activation and function of immediate-early genes in the nervous system. *Biochemistry and cell biology= Biochimie et biologie cellulaire, 89*(1), 61-73.

Peyron, C., Tighe, D. K., Van Den Pol, A. N., De Lecea, L., Heller, H. C., Sutcliffe, J. G., & Kilduff, T. S. (1998). Neurons containing hypocretin (orexin) project to multiple neuronal systems. *The Journal of Neuroscience, 18*(23), 9996-10015.

Pfaffmann, C. (1941). Gustatory afferent impulses. *Journal of Cellular and Comparative Physiology, 17*(2), 243-258.

Pfaffmann, C. (1959). The afferent code for sensory quality. *American Psychologist, 14*(5), 226.

Plath, N., Ohana, O., Dammermann, B., Errington, M. L., Schmitz, D., Gross, C., . . . Kuhl, D. (2006). Arc/Arg3.1 is essential for the consolidation of synaptic plasticity and memories. *Neuron, 52*(3), 437-444. doi: 10.1016/j.neuron.2006.08.024

Prandi, S., Bromke, M., Hubner, S., Voigt, A., Boehm, U., Meyerhof, W., & Behrens, M. (2013). A subset of mouse colonic goblet cells expresses the bitter taste receptor Tas2r131. *PLoS One, 8*(12), e82820. doi: 10.1371/journal.pone.0082820

Richard, J. E., Farkas, I., Anesten, F., Anderberg, R. H., Dickson, S. L., Gribble, F. M., . . . Skibicka, K. P. (2014). GLP-1 receptor stimulation of the lateral parabrachial nucleus reduces food intake: neuroanatomical, electrophysiological, and behavioral evidence. *Endocrinology, 155*(11), 4356-4367. doi: 10.1210/en.2014-1248

Richard, S., Engblom, D., Paues, J., Mackerlova, L., & Blomqvist, A. (2005). Activation of the parabrachio-amygdaloid pathway by immune challenge or spinal nociceptive input: A quantitative study in the rat using Fos immunohistochemistry and retrograde tract tracing. *Journal of Comparative Neurology, 481*(2), 210-219.

Roper, S. D. (2013). *Taste buds as peripheral chemosensory processors.* Paper presented at the Seminars in cell & developmental biology.

Rosen, A. M., Roussin, A. T., & Di Lorenzo, P. M. (2010). Water as an independent taste modality. *Front Neurosci, 4*, 175. doi: 10.3389/fnins.2010.00175

Rosen, A. M., Victor, J. D., & Di Lorenzo, P. M. (2011). Temporal coding of taste in the parabrachial nucleus of the pons of the rat. *J Neurophysiol, 105*(4), 1889-1896. doi: 10.1152/jn.00836.2010

Rousmans, S., Robin, O., Dittmar, A., & Vernet-Maury, E. (2000). Autonomic Nervous System Responses Associated with Primary Tastes. *Chemical Senses, 25*(6), 709-718. doi: 10.1093/chemse/25.6.709

Sakai, N., & Yamamoto, T. (1997). Conditioned taste aversion and c-fos expression in the rat brainstem after administration of various USs. *Neuroreport, 8*(9-10), 2215-2220. doi: Doi 10.1097/00001756-199707070-00025

Sakai, N., & Yamamoto, T. (1998). Role of the medial and lateral parabrachial nucleus in acquisition and retention of conditioned taste aversion in rats. *Behavioural Brain Research, 93*(1–2), 63-70. doi: http://dx.doi.org/10.1016/S0166-4328(97)00133-2

Sakurai, T., Nagata, R., Yamanaka, A., Kawamura, H., Tsujino, N., Muraki, Y., . . . Goto, K. (2005). Input of orexin/hypocretin neurons revealed by a genetically encoded tracer in mice. *Neuron, 46*(2), 297-308.

Saleh, T. M., Kombian, S. B., Zidichouski, J. A., & Pittman, Q. J. (1997). Cholecystokinin and neurotensin inversely modulate excitatory synaptic transmission in the parabrachial nucleus in vitro. *Neuroscience, 77*(1), 23-35.

Sammons, J. D., Weiss, M. S., Escanilla, O. D., Fooden, A. F., Victor, J. D., & Di Lorenzo, P. M. (2016). Spontaneous Changes in Taste Sensitivity of Single Units Recorded over Consecutive Days in the Brainstem of the Awake Rat. *PLoS One, 11*(8), e0160143.

Saper, C., Swanson, L., & Cowan, W. (1976). The efferent connections of the ventromedial nucleus of the hypothalamus of the rat. *Journal of Comparative Neurology, 169*(4), 409-442.

Saper, C., Swanson, L., & Cowan, W. (1979). An autoradiographic study of the efferent connections of the lateral hypothalamic area in the rat. *Journal of Comparative Neurology, 183*(4), 689-706.

Saper, C. B., & Loewy, A. D. (1980). Efferent connections of the parabrachial nucleus in the rat. *Brain Res, 197*(2), 291-317. doi: http://dx.doi.org/10.1016/0006-8993(80)91117-8

Schwaber, J. S., Sternini, C., Brecha, N. C., Rogers, W. T., & Card, J. P. (1988). Neurons containing calcitonin gene-related peptide in the parabrachial nucleus project to the central nucleus of the amygdala. *J Comp Neurol, 270*(3), 416-426. doi: 10.1002/cne.902700310

Sclafani, A. (2004). The sixth taste? *Appetite, 43*(1), 1-3. doi: 10.1016/j.appet.2004.03.007

Scott, T. R., Yaxley, S., Sienkiewicz, Z. J., & Rolls, E. T. (1986). Gustatory responses in the nucleus tractus solitarius of the alert cynomolgus monkey. *Journal of Neurophysiology, 55*(1), 182-200.

Shah, A. S., Ben-Shahar, Y., Moninger, T. O., Kline, J. N., & Welsh, M. J. (2009). Motile cilia of human airway epithelia are chemosensory. *Science, 325*(5944), 1131-1134. doi: 10.1126/science.1173869

Sheng, M., & Greenberg, M. E. (1990). The regulation and function of c-fos and other immediate early genes in the nervous system. *Neuron, 4*(4), 477-485.

Shepherd, J. D., & Bear, M. F. (2011). New views of Arc, a master regulator of synaptic plasticity. *Nat Neurosci, 14*(3), 279-284. doi: 10.1038/nn.2708

Shepherd, J. D., Rumbaugh, G., Wu, J., Chowdhury, S., Plath, N., Kuhl, D., . . . Worley, P. F. (2006). Arc/Arg3. 1 mediates homeostatic synaptic scaling of AMPA receptors. *Neuron, 52*(3), 475-484.

Shi, P., Zhang, J., Yang, H., & Zhang, Y.-p. (2003). Adaptive diversification of bitter taste receptor genes in mammalian evolution. *Molecular biology and evolution, 20*(5), 805-814.

Shimura, T., Tanaka, H., & Yamamoto, T. (1997). Salient responsiveness of parabrachial neurons to the conditioned stimulus after the acquisition of taste aversion learning in rats. *Neuroscience, 81*(1), 239-247.

Shimura, T., Tokita, K. i., & Yamamoto, T. (2002). Parabrachial unit activities after the acquisition of conditioned taste aversion to a non-preferred HCl solution in rats. *Chemical Senses, 27*(2), 153-158.

Shinohara, Y., Yamano, M., Matsuzaki, T., & Tohyama, M. (1988). Evidences for the coexistence of substance P, neurotensin and calcitonin gene-related peptide in single neurons of the external subdivision of the lateral parabrachial nucleus of the rat. *Brain Research Bulletin, 20*(2), 257-260.

Singh, N., Vrontakis, M., Parkinson, F., & Chelikani, P. (2011). Functional bitter taste receptors are expressed in brain cells. *Biochem Biophys Res Commun, 406*(1), 146-151. doi: 10.1016/j.bbrc.2011.02.016

Sink, K. S., Walker, D. L., Yang, Y., & Davis, M. (2011). Calcitonin gene-related peptide in the bed nucleus of the stria terminalis produces an anxiety-like pattern of behavior and increases neural activation in anxiety-related structures. *J Neurosci, 31*(5), 1802-1810. doi: 10.1523/JNEUROSCI.5274-10.2011

Smith, D. V., & Frank, M. (1972). Cross adaptation between salts in the chorda tympani nerve of the rat. *Physiology & Behavior, 8*(2), 213-220.

Smith, D. V., & St John, S. J. (1999). Neural coding of gustatory information. *Current Opinion in Neurobiology, 9*(4), 427-435.

Smith, D. V., Travers, J. B., & Van Buskirk, R. L. (1979). Brainstem correlates of gustatory similarity in the hamster. *Brain Research Bulletin, 4*(3), 359-372.

Spector, A. C., & Kopka, S. L. (2002). Rats fail to discriminate quinine from denatonium: implications for the neural coding of bitter-tasting compounds. *J Neurosci, 22*(5), 1937-1941.

Spector, A. C., & Travers, S. P. (2005). The representation of taste quality in the mammalian nervous system. *Behavioral and Cognitive Neuroscience Reviews, 4*(3), 143-191.

Steward, O., Farris, S., Pirbhoy, P. S., Darnell, J., & Driesche, S. J. V. (2015). Localization and local translation of Arc/Arg3. 1 mRNA at synapses: some observations and paradoxes. *Frontiers in Molecular Neuroscience, 7*, 101.

Steward, O., Wallace, C. S., Lyford, G. L., & Worley, P. F. (1998). Synaptic activation causes the mRNA for the IEG Arc to localize selectively near activated postsynaptic sites on dendrites. *Neuron, 21*(4), 741-751.

Steward, O., & Worley, P. F. (2001). Selective targeting of newly synthesized Arc mRNA to active synapses requires NMDA receptor activation. *Neuron, 30*(1), 227-240.

Stolzenburg, A. (2016). Bittergeschmacksrezeptoren des peripheren und zentralen Nervensystems.

Tizzano, M., Gulbransen, B. D., Vandenbeuch, A., Clapp, T. R., Herman, J. P., Sibhatu, H. M., . . . Finger, T. E. (2010). Nasal chemosensory cells use bitter taste signaling to detect irritants and bacterial signals. *Proc Natl Acad Sci U S A, 107*(7), 3210-3215. doi: 10.1073/pnas.0911934107

Tkacs, N. C., & Li, J. (1999). Immune stimulation induces Fos expression in brainstem amygdala afferents. *Brain Res Bull, 48*(2), 223-231.

Tokita, K., & Boughter, J. (2016). Topographic organizations of taste-responsive neurons in the parabrachial nucleus of C57BL/6J mice: An electrophysiological mapping study. *Neuroscience, 316*, 151-166.

Töle, J. C. (2014). Über die Arc-catFISH-Methode als neues Werkzeug zur Charakterisierung der Geschmacksverarbeitung im Hirnstamm der Maus.

Tordoff, M. G., Alarcon, L. K., & Lawler, M. P. (2008). Preferences of 14 rat strains for 17 taste compounds. *Physiol Behav, 95*(3), 308-332. doi: 10.1016/j.physbeh.2008.06.010

Travers, S. P., Pfaffmann, C., & Norgren, R. (1986). Convergence of lingual and palatal gustatory neural activity in the nucleus of the solitary tract. *Brain Research, 365*(2), 305-320.

Van Buskirk, R. L., & Erickson, R. P. (1977). Responses in the rostral medulla to electrical stimulation of an intranasal trigeminal nerve: Convergence of oral and nasal inputs. *Neuroscience Letters, 5*(6), 321-326.

Van Buskirk, R. L., & Smith, D. V. (1981). Taste sensitivity of hamster parabrachial pontine neurons. *Journal of Neurophysiology, 45*(1), 144-171.

Vígh, J., Lénárd, L., & Fekete, E. (1999). Bombesin microinjection into the basolateral amygdala influences feeding behavior in the rat. *Brain Research, 847*(2), 253-261.

Vígh, J., Lénárd, L., Fekete, É., & Hernádi, I. (1999). Bombesin injection into the central amygdala influences feeding behavior in the rat. *Peptides, 20*(4), 437-444.

Voigt, A., Bojahr, J., Narukawa, M., Hübner, S., Boehm, U., & Meyerhof, W. (2015). Transsynaptic tracing from taste receptor cells reveals local taste receptor gene expression in gustatory ganglia and brain. *The Journal of Neuroscience, 35*(26), 9717-9729.

Voigt, A., Hübner, S., Döring, L., Perlach, N., Hermans-Borgmeyer, I., Boehm, U., & Meyerhof, W. (2015). Cre-Mediated Recombination in Tas2r131 Cells—A Unique Way to Explore Bitter Taste Receptor Function Inside and Outside of the Taste System. *Chemical Senses*, bjv049.

Voigt, A., Hubner, S., Lossow, K., Hermans-Borgmeyer, I., Boehm, U., & Meyerhof, W. (2012). Genetic labeling of Tas1r1 and Tas2r131 taste receptor cells in mice. *Chem Senses, 37*(9), 897-911. doi: 10.1093/chemse/bjs082

Voigt, N., Stein, J., Galindo, M. M., Dunkel, A., Raguse, J. D., Meyerhof, W., . . . Behrens, M. (2014). The role of lipolysis in human orosensory fat perception. *J Lipid Res, 55*(5), 870-882. doi: 10.1194/jlr.M046029

Wada, E., Way, J., Lebacq-Verheyden, A. M., & Battey, J. (1990). Neuromedin B and gastrin-releasing peptide mRNAs are differentially distributed in the rat nervous system. *The Journal of Neuroscience, 10*(9), 2917-2930.

Whitehead, M. C., Ganchrow, J. R., Ganchrow, D., & Yao, B. (1999). Organization of geniculate and trigeminal ganglion cells innervating single fungiform taste papillae: a study with tetramethylrhodamine dextran amine labeling. *Neuroscience, 93*(3), 931-941.

Whiteside, B. (1927). Nerve overlap in the gustatory apparatus of the rat. *Journal of Comparative Neurology, 44*(2), 363-377.
Wiener, A., Shudler, M., Levit, A., & Niv, M. Y. (2012). BitterDB: a database of bitter compounds. *Nucleic acids research, 40*(D1), D413-D419.
Wilfinger, W., Mackey, K., & Chomczynski, P. (1997). Effect of pH and ionic strength on the spectrophotometric assessment of nucleic acid purity. *BioTechniques, 22*(3), 474-476, 478-481.
Wilson, D. M., & Lemon, C. H. (2014). Temperature systematically modifies neural activity for sweet taste. *Journal of Neurophysiology, 112*(7), 1667-1677.
Wilson, J. D., Nicklous, D. M., Aloyo, V. J., & Simansky, K. J. (2003). An orexigenic role for μ-opioid receptors in the lateral parabrachial nucleus. *American Journal of Physiology - Regulatory, Integrative and Comparative Physiology, 285*(5), R1055-R1065. doi: 10.1152/ajpregu.00108.2003
Wu, A., Dvoryanchikov, G., Pereira, E., Chaudhari, N., & Roper, S. D. (2015). Breadth of tuning in taste afferent neurons varies with stimulus strength. *Nat Commun, 6*, 8171. doi: 10.1038/ncomms9171
Xu, J., Cao, J., Iguchi, N., Riethmacher, D., & Huang, L. (2013). Functional characterization of bitter-taste receptors expressed in mammalian testis. *Mol Hum Reprod, 19*(1), 17-28. doi: 10.1093/molehr/gas040
Yamamoto, T. (2006). Neural substrates for the processing of cognitive and affective aspects of taste in the brain. *Archives of histology and cytology, 69*(4), 243-255.
Yamamoto, T., Fujimoto, Y., Shimura, T., & Sakai, N. (1995). Conditioned taste aversion in rats with excitotoxic brain lesions. *Neurosci Res, 22*(1), 31-49.
Yamamoto, T., Matsuo, R., Ichikawa, H., Wakisaka, S., Akai, M., Imai, Y., . . . Inoki, R. (1990). Aversive taste stimuli increase CGRP levels in the gustatory insular cortex of the rat. *Neurosci Lett, 112*(2-3), 167-172.
Yamamoto, T., & Sawa, K. (2000). Comparison of c-fos-like immunoreactivity in the brainstem following intraoral and intragastric infusions of chemical solutions in rats. *Brain Research, 866*(1), 144-151.
Yamamoto, T., Shimura, T., Sakai, N., & Ozaki, N. (1994). Representation of hedonics and quality of taste stimuli in the parabrachial nucleus of the rat. *Physiology & Behavior, 56*(6), 1197-1202. doi: http://dx.doi.org/10.1016/0031-9384(94)90366-2
Yamamoto, T., Shimura, T., Sako, N., Azuma, S., Bai, W. Z., & Wakisaka, S. (1992). C-fos expression in the rat brain after intraperitoneal injection of lithium chloride. *Neuroreport, 3*(12), 1049-1052.
Yamamoto, T., Shimura, T., Sako, N., Sakai, N., Tanimizu, T., & Wakisaka, S. (1993). c-Fos expression in the parabrachial nucleus after ingestion of sodium chloride in the rat. *Neuroreport, 4*(11), 1223-1226.
Yamamoto, T., Shimura, T., Sako, N., Yasoshima, Y., & Sakai, N. (1994). Neural substrates for conditioned taste aversion in the rat. *Behavioural Brain Research, 65*(2), 123-137.
Yamamoto, T., Takemura, M., Inui, T., Torii, K., Maeda, N., Ohmoto, M., . . . Abe, K. (2009). Functional Organization of the Rodent Parabrachial Nucleus. *Annals of the New York Academy of Sciences, 1170*(1), 378-382. doi: 10.1111/j.1749-6632.2009.03883.x
Yamano, M., Hillyard, C., Girgis, S., Emson, P., MacIntyre, I., & Tohyama, M. (1988). Projection of neurotensin-like immunoreactive neurons from the lateral parabrachial area to the central amygdaloid nucleus of the rat with reference to the coexistence with calcitonin gene-related peptide. *Experimental Brain Research, 71*(3), 603-610.

Yasoshima, Y., & Yamamoto, T. (1998). Short-term and long-term excitability changes of the insular cortical neurons after the acquisition of taste aversion learning in behaving rats. *Neuroscience, 84*(1), 1-5.

Yasui, Y., Saper, C. B., & Cechetto, D. F. (1989). Calcitonin gene-related peptide immunoreactivity in the visceral sensory cortex, thalamus, and related pathways in the rat. *Journal of Comparative Neurology, 290*(4), 487-501.

Zaidi, F. N., & Whitehead, M. C. (2006). Discrete innervation of murine taste buds by peripheral taste neurons. *J Neurosci, 26*(32), 8243-8253. doi: 10.1523/JNEUROSCI.5142-05.2006

Zeigler, H. P., Jacquin, M. F., & Miller, M. G. (1984). Trigeminal sensorimotor mechanisms and ingestive behavior. *Neurosci Biobehav Rev, 8*(3), 415-423.

A Appendix

A.1 Program for fixation and acetylation with an automatic staining machine

Table A.1: Sequence of fixation and acetylation protocol

Reagents	Time
4 % PFA in PBS	10 min
0.9 % NaCl	2 min
0.9 % NaCl	2 min
Manual Acetylation	
PBS	2 min
0.9 % NaCl	2 min
30 % Ethanol	2 min
50 % Ethanol	2 min
70 % Ethanol	2 min
80 % Ethanol	2 min
95 % Ethanol	2 min
100 % Ethanol	2 min
100 % Ethanol	2 min

The instructions for preparing these solutions can be found in section 2.8.2 Solutions for pre-treatment on page 22.

A.2 The arrangement of the working surface of the pipetting robot

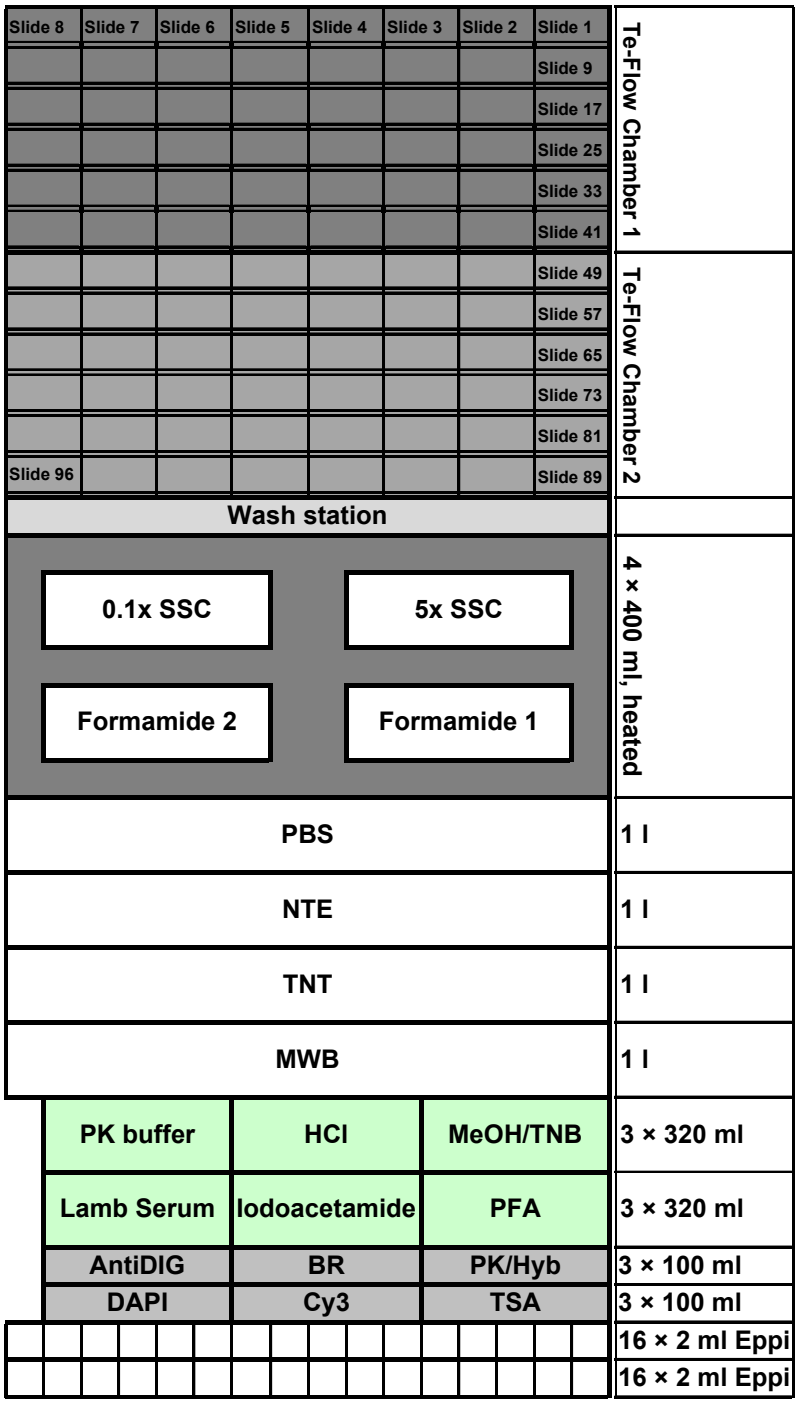

Figure A.1 Arrangement of the workspace of the pipetting robot I
(see Table A.2 for protocol). Formamide 1: 2× SSC, 50 % Formamide; Formamide 2: 1× SSC, 50 % Formamide; BR: Blocking reagent in MWB; MeOH: 0.6 % H2O2 in Methanol; Anti-Dig: Anti-Dig-POD in TNB; PK: Proteinase K in PK-Buffer; Hyb: Hybridisation Buffer; Cy3: Avidin-Cy3 in TN; TSA: Tyramide-Biotin in Amplification Diluent.

A.3 The program for the automated *in situ* hybridisation

Table A.2: The sequence of the *in situ* hybridisation protocol

Volume in µl	Reagents	Number of cycles	Time per cycle	Temp.
300	0.6 % H_2O_2 in Methanol	5	5 min	25 ˚C
300	PBS	7	5 min	25 ˚C
300	0.2 M HCl	2	5 min	25 ˚C
300	PBS	4	5 min	25 ˚C
400	PK-Buffer	1	5 min	25 ˚C
300	Proteinase K in PK Buffer	2	10 min	25 ˚C
300	PBS	7	5 min	25 ˚C
300	4 % PFA in PBS	2	5 min	25 ˚C
300	PBS	7	5 min	25 ˚C
300	Hybridisation Buffer	2	15 min	25 ˚C
	Heat to 64 ˚C			
300	RNA Probe in Hybridisation Buffer	2	180 min	64 ˚C
300	5× SSC	5	5 min	62 ˚C
350	2× SSC, 50 % Formamide	5	10 min	62 ˚C
350	1× SSC, 50 % Formamide	5	12 min	62 ˚C
300	0.1× SSC	4	8 min	62 ˚C
	Cool to 24 ˚C			
300	NTE	4	5 min	24 ˚C
300	20 mM Iodoacetamide in NTE	6	5 min	24 ˚C
300	NTE	4	5 min	24 ˚C
300	TN	2	5 min	24 ˚C
300	4 % Lamb serum in TN	6	5 min	24 ˚C
200	TN	4	5 min	24 ˚C
300	TNB	2	10 min	24 ˚C
200	TN	2	5 min	24 ˚C
300	MWB	2	5 min	24 ˚C
350	Blocking reagent in MWB	2	10 min	24 ˚C
300	MWB	2	5 min	24 ˚C
200	TN	4	5 min	24 ˚C
300	TNB	4	10 min	24 ˚C
350	Anti-Dig-POD 1:500 in TNB	2	30 min	24 ˚C
200	TN	6	5 min	24 ˚C
250	Tyramide-Biotin in Amplification Diluent	1	30 min	24 ˚C
200	TN	4	5 min	24 ˚C
300	Avidin-Cy3 1:1000 in TN	2	30 min	24 ˚C
200	TN	4	5 min	24 ˚C
300	0.3 µM DAPI in TN	2	5 min	24 ˚C
200	TN	4	5 min	24 ˚C
400	Deionised water	3	5 min	24 ˚C

The instructions for preparing these solutions can be found in section 2.8.3 Solutions for *in situ* hybridisation on page 22.

A.4 The arrangement of the working surface of the pipetting robot for the automated double-FISH protocol

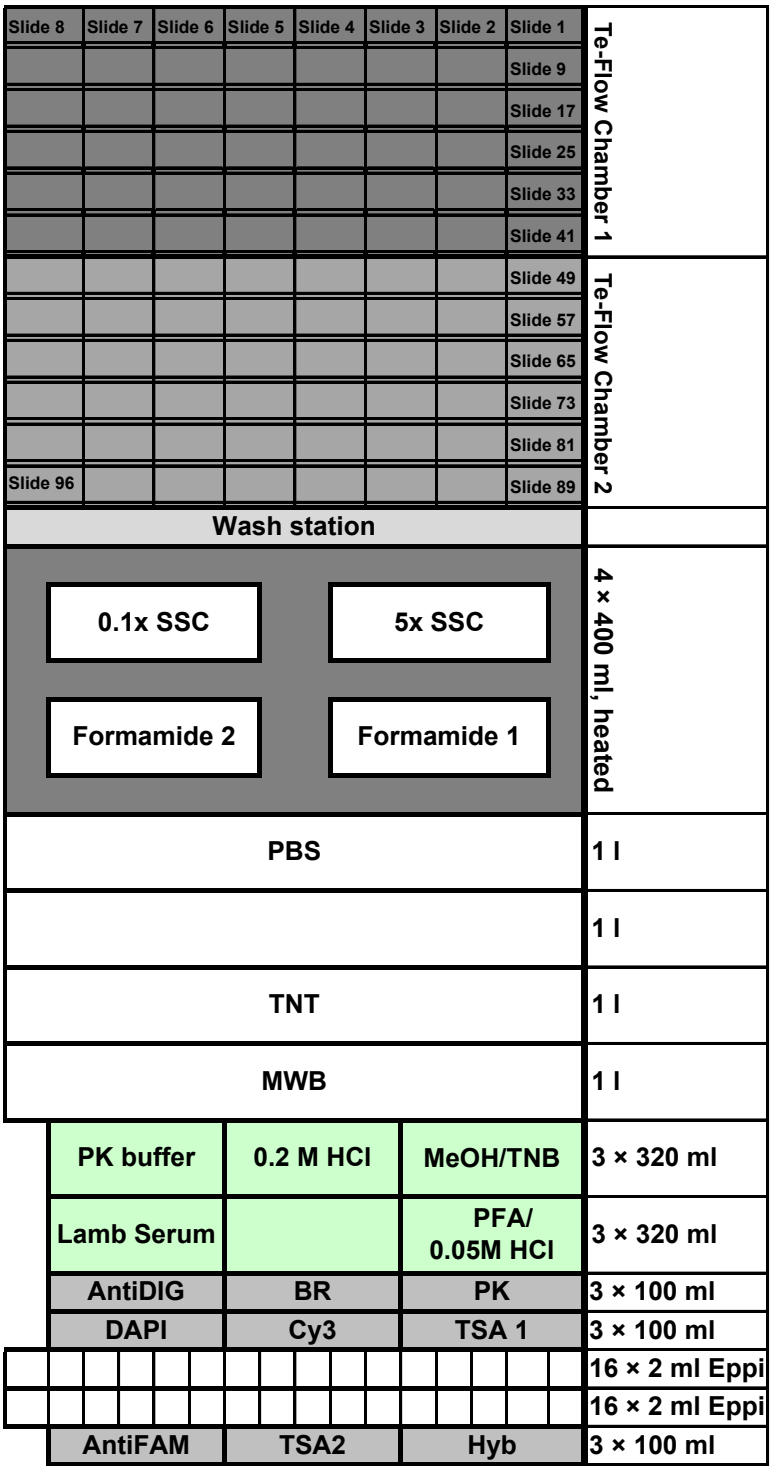

Figure A.2 Arrangement of the workspace of the pipetting robot II
(see Table A.2 for protocol). Formamide 1: 2× SSC, 50 % Formamide; Formamide 2: 1× SSC, 50 % Formamide; BR: Blocking reagent in MWB; MeOH: 0.6 % H2O2 in Methanol; Anti-Dig: Anti-Dig-POD in TNB; Anti-FAM: Anti-FAM-POD in TNB; PK: Proteinase K in PK-Buffer; Hyb: Hybridisation Buffer; Cy3: Avidin-Cy3 in TN; TSA(1&2): Tyramide-Biotin in Amplification Diluent (2 = fluorescein kit).

A.5 The double-FISH protocol

Table A.3 The sequence of the double *in situ* hybridisation protocol

Volume in µl	Reagents	Number of cycles	Time per cycle	Temp.
300	0.6 % H_2O_2 in Methanol	5	5 min	25 ˚C
300	PBS	7	5 min	25 ˚C
300	0.2 M HCl	2	5 min	25 ˚C
300	PBS	4	5 min	25 ˚C
400	PK-Buffer	1	5 min	25 ˚C
300	Proteinase K in PK Buffer	2	10 min	25 ˚C
300	PBS	7	5 min	25 ˚C
300	4 % PFA in PBS	2	5 min	25 ˚C
300	PBS	7	5 min	25 ˚C
300	Hybridisation Buffer	2	15 min	25 ˚C
	Heat to 64 ˚C			
300	RNA Probe in Hybridisation Buffer	2	180 min	64 ˚C
300	5× SSC	5	5 min	62 ˚C
350	2× SSC, 50 % Formamide	5	10 min	62 ˚C
350	1× SSC, 50 % Formamide	5	12 min	62 ˚C
300	0.1× SSC	4	8 min	62 ˚C
	Cool to 24 ˚C			
300	TN	2	5 min	24 ˚C
300	4 % Lamb serum in TN	6	5 min	24 ˚C
200	TN	4	5 min	24 ˚C
300	TNB	2	10 min	24 ˚C
200	TN	2	5 min	24 ˚C
300	MWB	2	5 min	24 ˚C
350	Blocking reagent in MWB	2	10 min	24 ˚C
300	MWB	2	5 min	24 ˚C
200	TN	4	5 min	24 ˚C
300	TNB	4	10 min	24 ˚C
350	Anti-Dig-POD 1:500 in TNB	2	30 min	24 ˚C
200	TN	6	5 min	24 ˚C
250	Tyramide-Biotin in Amplification Diluent #1	1	30 min	24 ˚C
200	TN	4	5 min	24 ˚C
200	0.05 M HCl	4	5 min	24 ˚C
200	TN	4	5 min	24 ˚C
300	TNB	4	10 min	24 ˚C
350	Anti-FAM-POD 1:500 in TNB	2	30 min	24 ˚C
200	TN	4	5 min	24 ˚C
250	Tyramide-Biotin in Amplification Diluent #2 (fluorescein)	1	30 min	24 ˚C
200	TN	4	5 min	24 ˚C
300	Avidin-Cy3 1:1000 in TN	2	10 min	24 ˚C
200	TN	4	5 min	24 ˚C
300	0.3 µM DAPI in TN	2	5 min	24 ˚C
200	TN	4	5 min	24 ˚C
400	Deionised water	3	5 min	24 ˚C

A.6 Raw data

Table A.4 Raw data – single stimulation in naïve animals

Stimulus	Stimulation time-point	n	Analysed sections	Area in mm^2	*Arc* -expressing cells			
					Total	N	C	N+C
No Stim	-	3	21	30.7	339	204	129	6
Control	– 5 min	3	24	33.3	561	333	181	47
	– 30 min	3	22	27.8	346	85	244	17
Sweet	– 5 min	2	16	24.2	326	287	36	3
	– 30 min	2	10	17.3	270	87	171	12
Sour	– 5 min	2	23	30.2	427	371	51	5
	– 30 min	2	14	23.4	342	63	271	8
Salty	– 5 min	2	12	18.4	247	199	41	7
	– 30 min	2	10	15.4	223	39	174	10
Umami	– 5 min	2	8	13.8	172	140	30	2
	– 30 min	2	16	20.9	285	52	231	2
Cyx	– 5 min	3	24	22.6	731	636	80	15
	– 30 min	2	16	14.5	455	87	326	42
Qui	– 5 min	2	12	20.9	690	502	118	70
	– 30 min	3	29	41.7	1467	393	1029	45
Cuc	– 5 min	2	26	42.5	1189	1012	139	38
	– 30 min	2	32	43.9	1671	518	1112	41
Sum		39	315	441.8	9741			

Table A. 5 Raw data – double stimulation in naïve animals

Stimulus	n	Analysed sections	Area in mm^2	*Arc* -expressing cells			
				Total	N	C	N+C
ctrl., ctrl.	6	46	71.6	1520	738	617	165
Cyx, Cyx	6	61	77.1	4438	2011	1639	788
Qui, Qui	10	111	151.3	7795	3029	3939	827
Cuc, Cuc	7	68	116.6	5722	2219	2665	838
Cyx, Qui	3	8	15.8	962	470	343	149
Qui, Cyx	4	32	60.5	3462	1712	1304	446
Cyx, Cuc	3	20	32.4	1975	947	718	310
Cuc, Cyx	4	29	49.7	2335	1114	918	303
Qui, Cuc	4	43	71.9	3636	1774	1552	310
Cuc, Qui	4	22	37.6	2200	855	1058	287
Sum	51	440	684.455	34045			

Table A.6 Mean data – distribution of *Arc*-expressing cells after single stimulation in naive animals

Stimulus	Stimulation time-point	n	*Arc* -expressing cells					
			Whole	SE	Lateral	SE	Medial	SE
No Stim	-	3	5.64	± 2.62	5.38	± 3.09	5.96	± 1.83
Control	─ 5 min	3	11.32	± 0.72	12.65	± 0.53	8.78	± 1.45
	─ 30 min	3	9.23	± 4.37	13.56	± 6.75	4.53	± 2.33
	All	6	10.28	± 2.03	13.11	± 3.04	6.65	± 1.55
Sweet	─ 5 min	2	11.69	± 1.86	14.28	± 2.46	7.36	± 1.24
	─ 30 min	2	11.38	± 3.04	13.86	± 2.26	8.02	± 3.47
	All	4	11.53	± 1.46	14.07	± 1.37	7.69	± 1.52
Sour	─ 5 min	2	12.46	± 0.31	15.33	± 0.17	8.21	± 0.36
	─ 30 min	2	11.86	± 1.89	12.28	± 1.28	11.09	± 3.04
	All	4	12.16	± 0.80	13.81	± 1.03	9.65	± 1.50
Salty	─ 5 min	2	11.50	± 0.93	13.83	± 1.11	8.62	± 0.87
	─ 30 min	2	12.82	± 1.60	16.28	± 0.98	7.71	± 3.29
	All	4	12.16	± 0.85	15.06	± 0.93	8.17	± 1.42
Umami	─ 5 min	2	10.04	± 2.11	18.08	± 3.32	3.20	± 2.22
	─ 30 min	2	10.51	± 2.09	12.14	± 3.15	7.44	± 0.25
	All	4	10.27	± 1.22	15.11	± 2.53	5.32	± 1.53
Cyx	─ 5 min	3	28.27	± 2.64	34.77	± 4.10	19.02	± 1.44
	─ 30 min	2	24.91	± 2.67	31.19	± 6.47	15.45	± 0.86
	All	5	26.59	± 1.87	32.98	± 3.16	17.23	± 1.21
Qui	─ 5 min	2	26.31	± 6.59	30.70	± 6.01	21.61	± 5.60
	─ 30 min	3	23.66	± 3.79	28.28	± 5.26	16.50	± 2.11
	All	5	24.99	± 3.01	29.49	± 3.50	19.06	± 2.46
Cuc	─ 5 min	2	24.19	± 2.20	28.27	± 2.28	17.72	± 1.66
	─ 30 min	2	25.09	± 7.64	30.52	± 9.18	19.74	± 6.01
	All	4	24.64	± 3.26	29.39	± 3.91	18.73	± 2.61

Table A.7 Proportion of candidate gene-expressing PbN cells co-expressing *Arc*

Probe			Whole		Lateral		Medial	
	Stimulus	n	Mean	SE	Mean	SE	Mean	SE
Calca	2x Control	3	2%	± 0%	3%	± 1%	1%	± 1%
	2x Bitter	4	13%	± 1%	13%	± 1%	12%	± 2%
Glp1r	2x Control	3	3%	± 1%	3%	± 1%	2%	± 1%
	2x Bitter	4	16%	± 2%	18%	± 3%	11%	± 2%
Hcrtr1	2x Control	3	1%	± 0%	1%	± 0%	1%	± 0%
	2x Bitter	4	14%	± 3%	19%	± 3%	10%	± 2%
Grp	2x Control	3	0%	± 0%	0%	± 0%	0%	± 0%
	2x Bitter	4	8%	± 2%	9%	± 3%	7%	± 1%
Nts	2x Control	2	2%	± 2%	2%	± 2%	1%	± 1%
	2x Bitter	4	20%	± 3%	26%	± 4%	13%	± 3%

Publications

Former collaborations:

Tyree, S. M., Munn, R. G., & McNaughton, N. (2016). Anxiolytic-like effects of leptin on fixed interval responding. *Pharmacology Biochemistry and Behavior*, *148*, 15-20.

Munn, R. G., **Tyree, S. M.**, McNaughton, N., & Bilkey, D. K. (2015). The frequency of hippocampal theta rhythm is modulated on a circadian period and is entrained by food availability. *Frontiers in behavioral neuroscience*, *9*.

Master's thesis:

Tyree, S. M. (2012). *Food, Leptin, and the Hippocampus: The Anxiolytic Potential of Eating: a Thesis Submitted for the Degree of Master of Science at the University of Otago, Dunedin, New Zealand* (Dissertation, University of Otago.).

Acknowledgements

Thanks are due to my supervisor Professor Wolfgang Meyerhof, thank you for giving me the opportunity to work in your laboratory and also for your guidance throughout my studies. Your assistance with the design and analysis of this work and editing of this thesis has been substantial. To my supervisor from the Department of Psychology, Professor Petra Warschburger, thank you for your assistance throughout this research project and also for reviewing this thesis.

Many thanks also to my colleagues for their support and guidance, especially to Dr. Jonas Töle for helping me to settle into Germany, into the institute, and also into molecular genetics. I'd also like to thank all of my colleagues from the MOGE department, particularly Dr. Antje Stolzenburg, Dr. Kristina Loßow, Steffi Demgensky, Dr. Anja Voigt, and Josefine Würfel for their help and support throughout my Ph.D. tenure. To my desk-neighbours Kristina Blank and Dr. Alessandro Marchiori, thank you for the welcomed distractions that were sometimes necessary, and sometimes less necessary. Also thanks to Elke Thom and the staff at the DIfE animal facility for their time and assistance with my experiments.

To the members of the Psychophysiology of Food Perception lab – Dr. Kathrin Ohla, Sherlley Amsellem, Richard Höchenberger, et al., thank you for your interesting conversations which helped to ensure that I didn't stray too far into molecular biology and forget my roots in psychology.

Thank you to my family for encouraging me to fly half a world away to pursue my dream, and more importantly for reminding me why I did it when I later needed reminding. Expat life can be isolating at times, but you guys managed to make me feel like I wasn't really all that far away.

I would also like to acknowledge the unwavering support of Dr. Robert G. K. Munn. Living on opposite sides of the planet for three years was a big ask – bigger than we probably realised in the beginning – so I can't thank you enough for sticking with me through it all.

Lastly, for the mice that made this work possible, thank you little guys.

Declarations

This Ph.D. thesis is the result of my own work and has not been submitted for any degree or Ph.D. at any other University.

This dissertation has been prepared independently, without unauthorised support, and complies with the rules of good scientific practice.

Erklärung

Hiermit erkläre ich, dass ich die vorliegende Arbeit selbständig verfasst habe und keine anderen als die von mir angegebenen Hilfsmittel und Quellen benutzt habe. Die Arbeit wurde noch an keiner anderen Hochschule zur Begutachtung eingereicht.

Hiermit erkläre ich, dass die Arbeit selbständig, ohne Hilfe Dritter verfasst wurde, und bei der Abfassung alle Regelungen guter wissenschaftlicher Standards eingehalten wurden.

Potsdam, 16. September 2016

Susan M. Tyree